Photovoltaic MPPT Charge Controller

Amber Scheurer
Ersuel Ago
Juan Sebastian Hidalgo
Steven Kobosko

Group 10
Senior Design 2
Spring 2012

Mentor
Alan Shaffer
Lakeland Electric

Sponsored by Workforce Central Florida

Table of Contents

1. Executive Summary 1
2. Project Description 2
2.1 Motivation 2
2.2 Objectives 3
2.2.1 Efficient 3
2.2.2 User Friendly 3
2.2.3 Low-Cost 4
2.2.4 Wireless Data Acquisition 4
2.2.5 Solar Panel 4
2.2.6 Microcontroller 4
2.2.7 LCD 5
2.2.8 Sensors 5
2.2.9 Wireless Transceivers 6
2.2.10 Batteries 6
2.2.11 Inverter 7
2.3 Specifications 7
3. Research 10
3.1 Related Projects 10
3.2 Solar Energy 10
3.2.1 Advantages and Limitations 10
3.2.2 Harvesting Solar Energy 11
3.2.3 Solar Cells and Manufacturing Technology 12
3.2.3.1 Mono-crystalline Silicon Panel 13
3.2.3.2 Polycrystalline Silicon Panel 14
3.2.3.3 Amorphous Silicon and Thin Film Panel 14
3.2.3.4 Copper Indium Gallium (de)Selenide CIGS Thin Film Panel 15
3.2.3.5 Cadmium Telluride CdTe Thin Film Panel 16
3.2.3.6 Gallium Arsenide GaAs Thin Film Panel 16
3.2.4 Photovoltaic Effect in Solar Cells 16
3.2.5 Photovoltaic Panel Performance 17
3.2.6 Solar Radiation 19
3.3 Charge Controllers 20
3.4 DC-DC Regulators 21

3.4.1 Buck Converter 21
3.4.2 Boost Converter 23
3.4.3 Inverting Buck-Boost Converter 23
3.4.4 Non-Inverting Buck-Boost Converter 24
3.4.5 Half-Bridge and Full-Bridge Drivers 26
3.4.6 Circuit Power Supply 28
3.5 Microcontroller 29
3.5.1 ATmega328P 29
3.5.2 Arduino 30
3.6 MPPT Algorithms 30
3.6.1 Perturb and Observe Method 31
3.6.2 Incremental Conductance Method 32
3.6.3 Constant Voltage Method 34
3.7 LCD 35
3.7.1 Segmented LCD (Alphanumeric) 35
3.7.2 Character LCD (Dot Matrix) 35
3.7.3 Graphical LCD 36
3.7.3.1 Backlighting 36
3.7.3.2 Color vs. Monochrome 36
3.7.3.3 Touchscreen 37
3.8 Wireless Transceivers 37
3.8.1 XBee 37
3.8.2 Wi-Fi Module 40
3.9 Sensors 41
3.9.1 Temperature Sensors 42
3.9.1.1 Thermocouple 42
3.9.1.2 Thermistors 43
3.9.1.3 LM35 44
3.9.1.4 DS1624 Digital Thermometer 44
3.9.2 Voltage Sensor 46
3.9.3 Current Sensor 46
3.9.3.1 ACS712 Current Sensor 46
3.9.3.2 Current Shunt Monitor 47
3.9.4 Irradiance Sensor 48
3.10 Batteries 50

3.10.1 Lead-Acid Batteries 51
3.10.2 Lithium-ion Batteries 52
3.11 Battery Charging Algorithms 52
3.11.1 Lead-Acid Charging 53
3.11.2 Lithium-Ion Charging 55
3.12 Inverter and Power Distribution 56
3.12.1 Why an Inverter 56
3.12.2 Features of an Inverter 57
3.12.2.1 Brand Comparison 58
3.12.2.2 Inverter Interface 58
3.12.3 Batteries to Inverter 61
3.12.4 Fuses and Fuse Holder 62
4. Design 64
4.1 Solar Panel 64
4.1.1 Mounting 64
4.2 Microcontroller 67
4.3 Electrical Configuration 69
4.4 LCD 71
4.5 Sensor Implementation 73
4.5.1 Voltage Sensor 73
4.5.2 Current Sensor 75
4.5.3 Temperature Sensor 76
4.5.4 Irradiance Sensor 77
4.6 Wireless Transceiver 78
4.7 Wireless Methodology 80
4.7.1 User Interface 81
4.8 Algorithm Implementation 82
4.9 PCB Design 85
4.9.1 PCB Software 86
4.10 Battery Bank 88
4.11 Inverter 90
4.11.1 Power Cables 91
4.11.2 Mounting 91
4.12 Packaging 91
4.13 Equipment Protection 92

5. Design Summary 95
6. Testing 106
6.1 Solar Testing 106
6.2 Battery Testing 107
6.3 Sensor Testing 108
6.4 Software Testing 109
6.5 Wireless Testing 110
6.6 Safety Procedures 110
6.6.1 Batteries 110
6.6.2 Power Cables Precaution 111
6.6.3 Power Inverter 112
6.6.3.1 General Installation Precautions 112
6.6.3.2 Mounting Precautions 113
6.6.3.3 Operating Limits 113
7. Operators Manual 114
8. Administrative Content 116
8.1 Budget 116
8.2 Industry Mentor 117
8.3 Milestones 118
9. Conclusion 123
9.1 Changes to Design 123
9.2 Future Work 124
9.3 Industrial Scaling 125

List of Figures

Figure 1 - Model of maximum efficiencies based on materials. [1] 2
Figure 2 - Renewable Energy Consumption in the Nation's Energy Supply, 2008. 11
Figure 3 - Market share of the different PV technologies. 13
Figure 4 - Photovoltaic solar radiation map of the US. 19
Figure 5 - Buck Converter Circuit ON-State. 22
Figure 6 - Buck Converter Circuit OFF-State. 22
Figure 7 - Boost Converter Circuit. 23
Figure 8 - Inverting Buck-Boost Converter Circuit. 24
Figure 9 - Non-Inverting Buck-Boost Converter Circuit. 25
Figure 10 – IRS2104 Half-Bridge Driver. 27
Figure 11 - Buck Converter and Boost Converter LT Spice Simulation. 28
Figure 12 - LT3500 2A Buck Regulator LT Spice Simulation. 29
Figure 13 - The Perturb-and-Observe Method for MPPT. 32
Figure 14 - The Incremental Conductance Method for MPPT. 33
Figure 15 - The Constant Voltage Method for MPPT. 34
Figure 16 - XBee modules with two antenna types. 38
Figure 17 - ZigBee Mesh Network. 39
Figure 18 - DigiMesh Network. 39
Figure 19 - Thermocouple schematic. [38] 42
Figure 20 - Diagram of a Thermistor. [39] 43
Figure 21 - LM35 Integrated Current Sensor. [40] 44
Figure 22 - DS1624 Digital Thermometer Pinout. [41] 45
Figure 23 - ACS712 Current Sensor. 47
Figure 24 - AD8215 Current Shunt Monitor. [42] 48
Figure 25 - Output Frequency vs. Irradiance Graph. 49
Figure 26 - Charging diagram for a typical lead-acid battery. 54
Figure 27 - Lithium-Ion Charging Diagram. 56
Figure 28 - Power Bright PW 1500 Inverter. 59
Figure 29 - Cobra CPI 800 Watt Power Inverter. 60
Figure 30 – Connecting batteries to inverter. 62
Figure 31 - 10 A Fuse and Fuse Holder. 63
Figure 32 - Pivot Mounts and Caster Wheels for Solar Panels. 67
Figure 33 - PMCC Microcontroller Interfacing with Peripherals. 70
Figure 34 - Serial Enabled Black on Green LCD. 72
Figure 35 - Voltage Sensor Flow Chart. 73
Figure 36 - Voltage Sensor Circuit. 75
Figure 37 - Current Sensor Flow Chart. 76
Figure 38 - Light to frequency converter. [45] 78
Figure 39 - Wireless Subsystem Setup. 80
Figure 40 - Xbee to microcontroller configuration. [35] 81
Figure 41 – Excel spreadsheet for data recording and plotting. 82
Figure 42 - Block Diagram of Perturb and Observe Method. 83
Figure 43 - Buck-Boost Circuit Diagram for MPPT. 84
Figure 44 - BYV42E Rectifier Diode Connection, Configuration and Symbol. [60] 94
Figure 45 - Overall System Block Diagram. 96
Figure 46 - PMCC Microcontroller Interfacing with Peripherals. [25] 97

Figure 47 - Wireless Subsystem Setup. 100
Figure 48 - Block Diagram of Perturb and Observe Method. 101
Figure 49 - Buck-Boost Circuit Design for MPPT. 102
Figure 50 - Cobra CPI 880 Power Inverter. 104
Figure 51 – Overall PCB Schematic. 104
Figure 52 – Final packaging of the PMCC system. 105
Figure 53 - Siemens SP75 IV Characteristics. [61] 106
Figure 54 – Input (Panel) Side and Toggle Switch. 114

List of Tables

Table 1 - Power Generation Specifications. 7
Table 2 - Charge Controller Specifications. 8
Table 3 - Power Storage and Delivery Specifications. 9
Table 4 - Comparison of ZigBee Mesh and DigiMesh. [36] 40
Table 5 - SunWize SW-Series Panel Comparison. [53] 64
Table 6 - Vertical Mounting Angle for Solar Panels in Orlando. [54] 65
Table 7 - Required functions for LCD programming. [56] 73
Table 8 - Temperature Chip Detailed Pin Description. 77
Table 9 - Comparison of Xbee and Wifly Modules. [35] 78
Table 10 - Lead-acid vs. Li-ion Batteries. [47] 88
Table 11 - Sun Xtender PVX-420T AGM Battery Specifications. [59] 90
Table 12 - List of Specifications of Chosen XBee Module. [35] 99
Table 13 - Sun Xtender PVX-420T AGM Battery Specifications. [59] 103
Table 14 - Battery Testing Plan. 107
Table 15 – Voltage Sensor Testing Plan. 108
Table 16 – Current Sensor Testing Plan. 108
Table 17 – Temperature Sensor Testing Plan. 109
Table 18 – Irradiance Sensor Testing Plan. 109
Table 19 - Software Testing Plan. 110
Table 20 - Wireless Testing Plan. 110
Table 21 - Budget. 116
Table 22 - Gantt Chart depicting research timeline. 118
Table 23 - Gantt Chart depicting design timeline. 119
Table 24 - Gantt Chart depicting parts acquisition timeline. 120
Table 25 - Gantt Chart depicting prototyping timeline. 121
Table 26 - Gantt Chart depicting testing timeline. 122

1. Executive Summary

In a world of increasing energy demand, it is imperative to come up with innovative solutions to reduce and conserve energy use. There is a significant interest in creating an environmentally friendly system that will save money on electricity and maximize the cost return on investment for solar panels. The photovoltaic industry continues to strive to create efficient and inexpensive systems that can be competitive with other energy sources.

The goal of the project was to create a stand-alone off-the-grid photovoltaic (PV) system that utilizes maximum power point tracking (MPPT) to obtain the most efficiency. Due to the inherent losses that occur in photovoltaic systems, it was essential that the maximum power was extracted. The intent was to create an extremely efficient charge controller that would be able to monitor the power generated by the photovoltaic array and deliver the maximum amount to the battery bank during varying atmospheric conditions.

While it seemed instinctive to incorporate several solar panels in order to harvest more energy, this proof of concept project demonstrated that a single panel integrated with a charge controller has the potential to be scaled for industrial use. The majority of the design took place in the charge controller module of the system but was integrated with the other parts to demonstrate a fully functional stand-alone system. The overall system consisted of a solar panel, MPPT charge controller, battery bank, and a distribution system to deliver usable power to the end user. The plan was to construct a product that would be portable, easy to use, efficient, and inexpensive.

In order to implement maximum power point tracking, data from several different sensors were fed into a microcontroller. Here the MPPT algorithms interprets the incoming current and voltage from the PV panel as well as the battery and calculates what amount of power should be used to charge the battery. The microcontroller then physically changes the voltage by driving the buck and boost DC-DC converters in the circuitry.

Within the charge controller, several features were added to increase the ease of use and allow for more thorough testing. In order to quickly view the status of the system, an LCD screen was attached to the charge controller to display several values such as current, voltage, and temperature. In addition, this information was transmitted wirelessly to a separate wireless transceiver that was connected to a computer. Along with the previously mentioned sensor quantities, the ambient irradiance on the solar panel was measured and recorded to give further insight into how the system performed in varying atmospheric conditions.

2. Project Description

2.1 Motivation

A general interest in power electronics and power systems was a significant motivation behind the decision to develop a photovoltaic project. The group members were interested in investigating the methods and hardware involved in building a fully functional solar setup. Furthermore, as the population of the world increases and other natural resources continue to be used up, research in to renewable energy sources becomes increasingly relevant.

There are many stages of production and integration in the photovoltaic energy harvesting process where losses occur. One of the very first levels or stages in this process that can be analyzed is the actual material that makes up the solar cells themselves. Although many different semiconductor materials and combinations have been investigated, each of these choices can only operate over a small region of the spectral range that they are exposed to. As Figure 1 demonstrates, certain materials are more efficient than others, but none of the ones shown are even 40% efficient. This is because each combination of materials has a certain band gap that corresponds to certain wavelengths of light. Consequently there is a range of spectral energy that is not high enough to stimulate these materials and is ultimately wasted. [1]

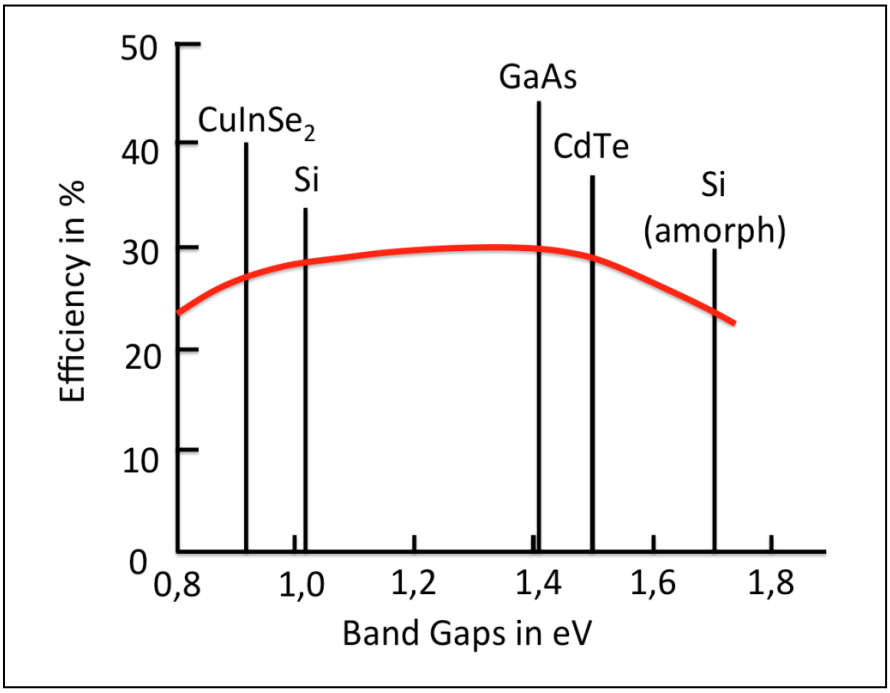

Figure 1 - Model of maximum efficiencies based on materials. [1]

In addition, other loss mechanisms include material defects and contamination, the loss of energy that is dissipated as heat, optical losses due to the glass or other materials used to encase the solar cells, and resistance in the cables and connections of the array. [1] Since the photovoltaic system encompassed these losses, it was absolutely necessary to look for ways to offset them. The charge controller and its methodology were identified as an area that can supply up to 30% gains in efficiency based on the use of maximum power point tracking. [2,3] The group agreed that this was an area of design that could make a significant impact in the overall PV system and was therefore chosen for investigation.

2.2 Objectives

The overall objective of this project was to design an efficient charge controller. This meant implementing the microcontroller, sensors, and electronics necessary to monitor and adjust the power while consuming as little of the power as possible.

2.2.1 Efficient

The main objective of the software is the implementation of the maximum power point tracking embedded algorithm. There are several algorithms and ways to achieve maximum power point tracking that were be discussed. A specific one was programmed on the microcontroller and it adjusted the current and voltage of the system to achieve maximum efficiency.

Efficiency was also an objective in component selection for the charge controller circuit. This resulted in an overall low powered charge controller system, which meant that more of the solar panel energy was transferred to the battery.

2.2.2 User Friendly

The system was designed to be Plug-and-Play and implemented a user-friendly setup. Size and portability were primary objectives, which made the system very easy to setup in an outdoor environment such as a remote location without any access to electricity. The charge controller connections were kept to a minimum and were clearly marked for a quick setup and a safe experience. In addition, the charge controller incorporates a LCD screen which constantly allows the user to monitor important operational variables such as input voltage, output voltage, input current, output current, battery and panel temperature.

2.2.3 Low-Cost

Production cost was an important objective in design and implementation. Limiting the number of circuit components allows for a simpler circuit, which in turn reduces the PCB size, design and production cost. Since a smaller casing was needed, due to circuit size, the packaging cost was subsequently lowered.

2.2.4 Wireless Data Acquisition

The Photovoltaic MPPT Charge Controller (PMCC) was able to wirelessly transmit data from the charge controller, located with the solar panels and battery bank, to a computer where the data was processed and displayed in an easy-to-read format. The wireless transceivers provide remote monitoring and data logging functionality. This was incredibly useful when a user is not physically at the system itself and wanted to be able to know the performance and whether any anomalies occur.

2.2.5 Solar Panel

The solar panel was the most expensive part needed to test and implement the project. Therefore finding an inexpensive module with an optimal power rating was going to be imperative to the entire project's performance and cost. Solar panel efficiency and power output needs to surpass the battery charging requirements during normal operating conditions, in order for the charge controller system to be fully tested. The panel should also be powerful enough to provide a quick charge, in order to shorten the battery charging time in various operational states and weather conditions. Power output depends on panel efficiency, so efficiency is the main objective in selecting a PV panel.

2.2.6 Microcontroller

The microcontroller is responsible for all input and output processing of the entire photovoltaic system. The tasks included reading sensor values, controlling battery-charging circuitry, monitoring system performance and anomalies, along with transmitting data wirelessly and outputting data to an LCD. The microcontroller needed to be low-power, small form factor, and contain enough programming space for all project objectives. The device needs to run at a relatively fast processor clock speed in order to be able to multitask between the various peripheral devices and provide useful data in a short amount of time. The chip should have adequate digital I/O and analog input pins to be able to handle all peripherals used in PMCC. Additionally, multiple TTL serial ports are desirable, as well as Inter-Integrated Circuit (I^2C) communication in order to interface with the devices that use these digital communication protocols. A robust programming language and programming software (IDE) associated with the microcontroller are preferred.

2.2.7 LCD

The incorporated LCD screen should allow the user to quickly and easily view the current and voltage supplied by the solar panel, the battery level, the temperature of both of these components as determined by the temperature sensors, and any status indicators. Additionally, the LCD should be backlit so that the status of the system can be read in any lighting situation. Ideally this LCD provides a balance between ease of use/image quality and power consumption. Ultimately, the charge controller and associated hardware should use as little power as possible in order to maintain efficiency and charge the battery quickly.

Also, another key aspect of the chosen LCD was it capability to easily interface with the microcontroller being used. It was important that the drivers and established code libraries were intended for use with the chosen brand and type of microcontroller. The software should be able to display the necessary values quickly and easily so that the user can interpret the status of the system. Depending on the size of the display and the state of the system, it was programmed to scroll through several values.

2.2.8 Sensors

The implementation of sensors in the PMCC was essential in order to achieve the desired functionality of the system. The sensors in the PMCC are the devices that are going to be in charge of monitoring and communicating everything that was happening in the system to the microcontroller. Two of the sensors that were going to be needed in the design were a voltage and current sensor. Both of these sensors played a significant role in one of the main goals of the project which was achieving maximum power point tracking. As its name implies, these sensors keep the microcontroller updated with the voltage and current values being provided by the panel so that it can react to it accordingly. Aside from keeping track of the solar panel's energy output, these sensors also take part in determining the status of the batteries.

In addition to these sensors, a temperature and irradiance sensor are also incorporated in the system. A temperature sensor helps keep track of the temperature in the solar panel as well as in the batteries. The irradiance sensor helps keep track of the light intensity the PV panels are receiving. These sensors don't actually play a role in the performance of the design itself, but instead, they provide the user with extremely valuable information about the temperature and light intensity in system, and it can later be used in correlation with the power output of the design to determine the efficiency.

It is important that these sensors are efficient and that they provide the user with an accurate reading of what is going on in the system because the data gathered does not only effect the performance of the system but also future solar energy research.

2.2.9 Wireless Transceivers

The wireless transceivers are responsible for communicating the sensor and performance values to a remote computer over RF. These devices should be able to provide a long enough range for a typical homeowner to be able to receive wireless data from a photovoltaic system located near the house. The transceivers should be low power, high throughput, and run at either 3.3 or 5V, which will be the logic voltages used for the electrical components. The modules should also feature TTL serial communication (for compatibility with the microcontroller) and point-to-point communication protocol. The transceivers should have a small form factor and built-in antenna to allow for PMCC to be as compact as possible.

2.2.10 Batteries

The batteries used in PMCC served as a way to store energy so that devices can be powered in the event that the sun is not shining and when more power is needed than can be provided by the solar arrays at a given time. The battery bank should provide a large energy capacity, run at 12V, and provide a large output current to handle high power loads. The weight of the batteries is an issue, but cost should take precedence as long as the whole system is not too heavy. The battery bank should have a long lifetime and be as low cost as possible.

There are four possible states that the battery can be in that will determine what charging mechanism is going to be used. The quantitative value of each of the thresholds was determined by the battery and solar array that was ultimately implemented, but the software was able to check and react to the following conditions:

- Off State: When there is little or no power coming from the solar panel, the device should go into an off state to protect the battery from leaking back into the solar panel.
- On State: When there is minimal power coming from the solar panel, enough to power the system but not enough to move to the next state, the system turns on and attempts to deliver all of the power.
- Bulk State: This is the main charging state where the MPPT algorithms were most relevant. Here the maximum power point was determined and the battery was charged accordingly.
- Float State: Once the battery reached a high enough voltage and was close to fully charged, the controller then moved into the float state. In this state, the goal was to maintain the voltage level and compensate for self-discharge [2,4].

2.2.11 Inverter

The inverter is the final stage of the system. It is through the inverter that the user has the opportunity to access the power stored in the batteries that was originally generated in the solar panel. The main functionality of the inverter is to take the DC voltage stored in the batteries and transform it into AC voltage that can be used by small household appliances. The inverter that is desired in the system should also have incorporated a USB port that allows small gadgets such as cell phones, iPods, and PDAs to be powered as well.

It is important that the inverter can deliver a decent amount of power so that multiple devices can be powered simultaneously and the user is not stuck powering a single device. It is also important that the inverter has a user interface that is easy to use and that no extensive knowledge of the equipment is needed to operate it safely. Finally, the unit should be power efficient so that the energy generated in the system is utilized to the fullest in the most efficient way possible.

2.3 Specifications

The specifications of this project are divided up into three main sections that include power generation, charge controller, and power storage and delivery. The specifications of each section are dependent on one another as they are all tied together and many are specific to the amount of power that is moving through the system. Table 1 shows the specifications needed for the power generation aspect, which consists of the solar panel.

Solar Panel	
Output Power	> 50 W
Open Circuit Output Voltage	> 15 V
Short Circuit Output Current	> 4 A
Weight	< 30 lbs

Table 1 - Power Generation Specifications.

The next stage of the project is the charge controller as shown in **Error! Reference source not found.**. This was the aspect of the system that constitutes the majority of the design and was implemented using a custom ordered printed circuit board (PCB).

Microcontroller	
Clock Speed	16 MHz
Number of Serial Ports	At least 2
Communication Protocol	I2C, Serial
Programming Memory	32 KB
Analog Pins	4
Digital input/output Pins	9
PWM Output Pins	2
Cost of Software	Free
Cost of Hardware	< $10
Current Draw	< 50 mA
Voltage	3.3 or 5 V
LCD	
Current Draw	< 100 mA
Voltage	3.3 or 5 V
Lines needed	4
Cost	< $50
Wireless	
Range	30 m
Frequency Band	2.4 GHz
Communication Interface	TTL Serial
Communication Style	Point-to-point
Form Factor	Small, < 2 sq. in.
Baud Rate	9600

Table 2 - Charge Controller Specifications.

Power storage and delivery consists of the battery bank and the inverter as described in Table 3. This allowed for the end user to power small devices using either AC or DC power.

Battery Bank	
Voltage	12 V
Capacity	80 Ah
CCA	50 A (600W)
Deep Charge Cycles	500-1000
Weight	< 80 lbs
Cost	< $400
Inverter	
Continuous Max Power	1500 W
Surge Power	3000 W
Wave Output	Moderate Sine
Inverter Input Voltage	12 V
Output Voltage	110-120 VAC
Types of Outlets	AC & DC
Display	Yes

Table 3 - Power Storage and Delivery Specifications.

3. Research

3.1 Related Projects

There have been numerous implementations of MPPT charge controllers from many different sources in industry and academia. Of the similar projects that were researched, there were not any that incorporated wireless data transfer into their design. This was believed to be a significant value added to this project in terms of testing and data capture.

A previous senior design project conducted by students at the University of Central Florida in the Fall of 2010 provided insight into a solar project that fulfilled the requirements of a UCF senior design. The Universal Charging Friend (UCF) project incorporated a small solar panel design and was referenced for documentation style. [5]

Another similar project was conducted by Bryan Buckley of the University of Alabama. This student built a maximum power point tracking system that used a 40 W solar panel. This documentation provided significant insight into the process and features needed to design a stand-alone charge controller. [6]

While many other sites and papers are referenced in the documentation, this project encompasses unique features and has been designed to comply with the specific requirements of the products being incorporated.

3.2 Solar Energy

3.2.1 Advantages and Limitations

Traveling at the speed of light, it takes sunlight eight minutes and twenty seconds to reach Earth's surface. Solar energy, in the form of irradiance or sunlight and thermal energy or heat, is one of the most abundant and cleanest energies used on planet Earth. [7] Solar energy is considered a renewable source. As shown in Figure 2, renewable energy makes up 7% of consumption in United States' energy supply for year 2008. Solar energy was accountable for less than 0.1 percent of electricity consumption in the United States in that same year. [8] The solar energy market is projected to double by 2020, even though today this type of energy is not as commonly used to produce electricity as other renewable sources of energy available, like hydroelectric, geothermal, or wind. [9]

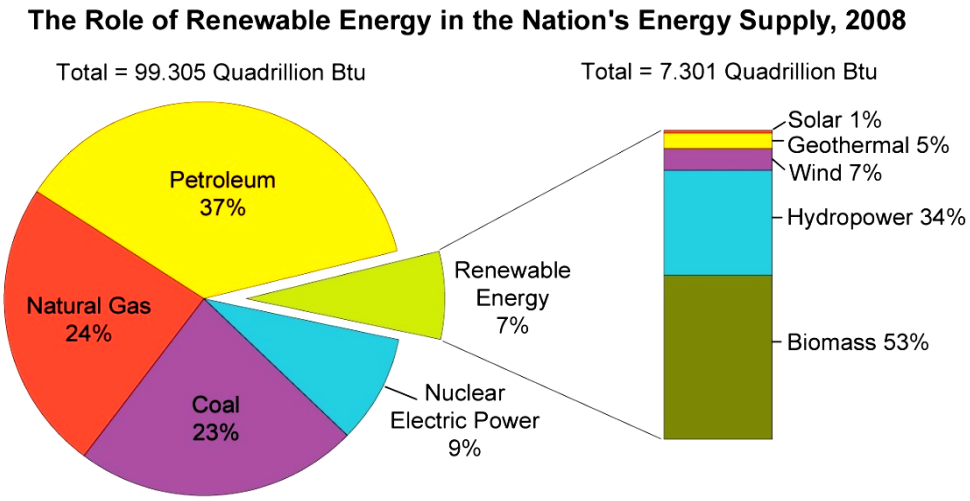

Figure 2 - Renewable Energy Consumption in the Nation's Energy Supply, 2008. Available in public domain by U.S. Energy Information Administration.

The fact that solar energy is renewable and also cleaner than any other energy produced from fossil fuels makes this resource of sustainable energy very important for the planets future. Solar energy is virtually available everywhere in the world. In conclusion, the advantages of solar energy are its abundance and the “zero emission” factor. On the other hand, its main limitation is the fact that this kind of energy is not constant even during the daytime. Due to Earth’s atmosphere and its atmospheric conditions, it is approximated that only half of the solar energy that is directed to the planet reaches its surface. Another disadvantage of solar energy is the limitation that the current available technologies place on the efficiency at which this energy is harvested and utilized. Even though there are numerous solar panel and solar cell technologies available, the highest efficiency at which these devices convert solar energy to electricity is lower than 30%. This last factor is another reason why harvesting solar energy is still not the most popular way of producing energy.

3.2.2 Harvesting Solar Energy

Solar energy can be harvested in two different ways, directly using photovoltaic systems or indirectly using Concentrated Solar Power (CSP). The photovoltaic effect is used in the conversion of light or photons to electric current or electrons. [10] Solar or photovoltaic cells are primarily made of crystalline silicon and are connected in series to attain a desired voltage or in parallel to attain a desired current. These interconnected cells form a solar panel that traditionally produces a DC potential.

The panels are built of aluminum for durability. The cells are usually places behind tempered glass for safety, durability and protection of cells against weather conditions. A clear resin is used to insulate the back of the solar cells

and also keep them in place against the top panel glass. The CSP process involves the use of mirrors and lenses to intensify sunlight and its thermal energy is used to heat up water and produce steam. Steam is then used to drive steam turbines which produce electricity.

This project made use of solar panels, which were first used in space projects to power orbiting satellites. A brief discussion and research on different types of panels and their efficiency is required in order to select the best solar panels to use for this project. Panel placement and panel temperature are also important in increasing the efficiency at which solar panels capture solar energy.

3.2.3 Solar Cells and Manufacturing Technology

There are many different types of solar cells and various materials used to make them, but the two most popular technologies used in today's solar energy market are silicon, which is consider a first-generation technology and thin film which is considered a second-generation technology. Both technologies mentioned above divide in two separate groups: mono-crystalline and polycrystalline. Mono-crystalline thin-film solar cells include Gallium Arsenide (GaAs). Polycrystalline thin-films include solar cells like: amorphous silicon (TF-Si), Copper Indium Gallium deSelenide (CIGS), and Cadmium Telluride (CdTe).

Thin film solar panels are made by placing thin layers of semiconductor material onto various surfaces, usually on glass. The term thin film refers to the amount of semiconductor material used. It is applied in a thin film to a surface structure, such as a sheet of glass. Contrary to popular belief, most thin film panels are not flexible. Overall, thin film solar panels offer the lowest manufacturing costs, and are becoming more prevalent in the industry. A third generation technology used today which is also the latest in the thin film category is the organic solar panel technology. In this fabrication process the solar panels are built by placing a conductive organic polymer, usually plastic, layer between two conductive plates. These organic panels are not widely used and harder to purchase. They are very inefficient and therefore a lot of them are needed in order for this project to work.

Space is one of the major factors to consider in implementing this project, therefore organic solar panels are not going to be used. The annual market share of different solar panels according to different materials used in their manufacturing is shown in Figure 3. [11] For the main purpose of finding the most efficient and cost effective panel for the project, a quick review of the different types of panels is needed. Efficiency is more important than cost since in this MPPT charge controller project, the batteries need to be charged in the fastest manner possible. A solar panel that will do the best job at converting solar power into electricity (higher efficiency) is a major requirement, considering that sunlight is at its full potential for only half of the daytime hours.

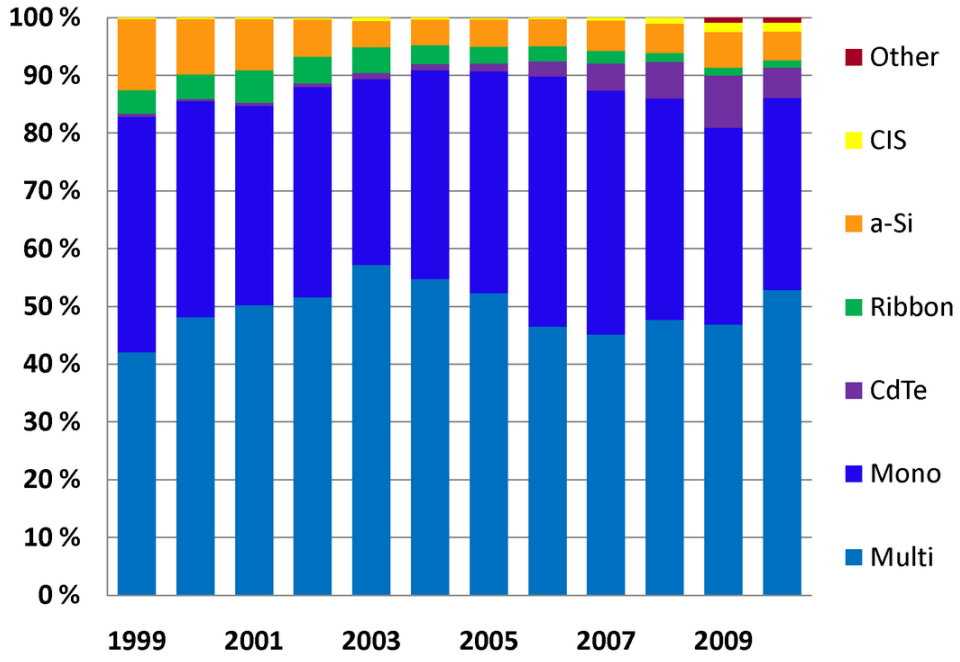

Figure 3 - Market share of the different PV technologies.
Reproduced with Permission under the Creative Commons License Attribution 3.0.

3.2.3.1 Mono-crystalline Silicon Panel

The first type of crystalline silicon used in solar panels is mono-crystalline. Even though not the most commonly used, this technology is one of the oldest and most proven in comparison to the rest. As the name implies this type of solar cells are made from the same silicon crystal, which is very pure and has less irregularities and imperfections than polycrystalline solar cells. This type of silicon is produced using the Czochralski process where seed crystal silicon is dipped into molten silicon and withdrawn very slowly. This process produces a two meter long cylindrical single-crystal ingot as the molten silicon crystallizes around the seed. [12] The silicone can be intrinsic or doped with impurities depending on its future use. The ingot is then sliced into thin wafers. These same wafers are also used for semiconductor device fabrication.

Considering the square shape of a solar cell, a lot of silicone material is wasted in the process; hence the main drawback of this type of solar cell is its price point. This manufacturing process is also more complicated and more silicon is used to make mono-crystalline solar cells. These last facts contribute to a high price per panel compared to the rest of the solar panels in this review. However, due to the lack of imperfections and cell structure this type of solar panel is the most efficient, with percentages averaging around 11% - 16%. [13] Efficiency is the factor at which absorbed light is converted to electricity.

Because of the higher efficiency level these panels perform better and have been proven to last longer than the rest of the silicon technology panels. These panels

are estimated to last at least 25 years. And some have been proven to last up to 50 years, so the higher price is justified by the returned energy cost that these panels produce during their long life. [12] Another positive factor about these panels is the fact that the user will get the most watts per square foot of panel used, since these panels are so efficient. As a result these panels are a good choice when limited space is an issue. Mono-crystalline solar panels are very fragile, and care must be given during the shipping and installation processes. These panels were used to implement this project. Most online solar panel retailers have recently dropped the prices for these panels to competitive levels with the prices of the polycrystalline panels, making this panel a functional choice for this project.

3.2.3.2 Polycrystalline Silicon Panel

Next in the silicon solar cell category is polycrystalline silicon. Polycrystalline solar panels are the most common type of solar panel in home installations today, due to their low cost and average power efficiency. In this fabrication process molten silicon is usually casted and then cooled in a rectangular shape for a more profitable outcome. The block is then sliced similarly to the mono-crystalline ingot to create the thin solar cells. As the name implies the ingot is made of multiple crystals resembling pieces of shattered glass due to the manufacturing process. This process is a faster and a lot easier to implement. As a result, these types of silicon cells are cheaper and therefore cost less to produce in comparison to mono-crystalline cells. The lower grade semiconductor used in fabrication and the imperfections drop the solar cell performance. Efficiency is the main disadvantage of polycrystalline solar panels. They convert only 10%-14% of the solar energy that hits their surface. [13] Efficiency for these solar panels drops in comparison to their mono-crystalline counterpart because of the energy loss at the separation or fusion points between two adjacent crystals. Polycrystalline panels like mono-crystalline panels perform poorly in shade or low light conditions. These panels account for most of the market shares in the solar panel manufacturing industry in the past decade.

3.2.3.3 Amorphous Silicon and Thin Film Panel

Thin film technology is newer than the crystal silicon technology discussed previously. Amorphous silicon or other non-silicon semiconductors are used, instead of crystal silicon. The semiconductor is placed between flexible laminate, glass or steel plates. The flexible laminate is most commonly used to produce these panels. Thin film solar panels are cheaper and faster to produce since the entire panel is considered a solar cell, unlike traditional panels constructed of numerous solar cells. The manufacturing process makes these panels the most readily available solar panel on the market.

The flexible laminate makes these panels bendable and therefore easier to mount on uneven surfaces and also more durable to extreme weather condition

like a hailstorm. This factor is extremely important for thin film technology, considering that these panels are often laid on house roofs to replace traditional roofing materials. In case of damage the thin films panels with continue to work at a lesser rate, while crystalline silicon panels stop working altogether if a single cells is damaged. Another advantage of thin film panels is their weight. Thin film panels weigh less than crystalline silicon panels, making them easier to mount and work with for residential use. Another advantage that thin film panels have is their performance in hotter climates. Thin film semiconductors used today like Copper Indium Gallium Selenide do not lose as much efficiency as their temperature increases. Because of this ability to withstand hotter temperatures thin film systems have an added advantage over the crystalline rivals in hot climates like the southeast. This also makes it easier to design solar panel systems as the solar panels perform closer their manufactures rating without factoring high temperature as much. Thin film panels perform better than the competition in shade or low light conditions. So in conclusion the main advantages of thin film panels are: cost, weight, durability, flexibility, high heat and shade performance.

However, as with all the solar panels in this review, thin film panels have their disadvantages. The most significant disadvantage is their efficiency, which is also the main reason why this new technology has not replaced older silicon technology. Thin film technology efficiency ranges between 4% - 7%. [13] This means that in order to produce the same amount of electricity twice as many thin film panels are needed in comparison with polycrystalline panels and almost three times as many when compared to mono-crystalline. Last of all disadvantages of thin film technology is longevity. Because the technology is fairly new, it is unknown how these panels perform over time.

3.2.3.4 Copper Indium Gallium (de)Selenide CIGS Thin Film Panel

Another type of panel to be reviewed is the CIGS panel in the thin film family. The semiconductor in this type of panel is composed of copper, indium, gallium and selenium. Like in other thin film panels the CIGS compound is layered on a glass back plate. This compound has a high optical absorption coefficient, therefore very little is needed to produce the panels. As a result CIGS panels are very light in comparison to crystalline silicon panels. Another advantage is their unmatched performance in higher temperatures. Unlike silicon, CIGS efficiency is not affected as much as the panel temperature increases, making CIGS panels appropriate for hotter climates like here in Central Florida. CIGS panel efficiency ranges from 10% - 15% with a record of 19.9% achieved by National Renewable Energy Laboratory with minor modifications. [14] Due to the moderate efficiency associated with these panels their production is projected to increase rapidly in the future. However these panels are usually very expensive and hard to find due to their vacuum based fabrication process, so they were considered for this project.

3.2.3.5 Cadmium Telluride CdTe Thin Film Panel

CdTe was one of the first semiconductors that was used in thin film technology to improve the low efficiency experienced with amorphous silicon. CdTe panels are manufactured on glass substrate like CIGS. They are the most common type of thin film solar panel on the market and the most cost-effective to manufacture. CdTe panels perform significantly better in high temperatures and in low-light conditions similarly to CIGS panels. However CdTe thin film panels have maxed out at 16.5% efficiency and range between 7% - 12% on average. [15] The limited supply of Tellurium and toxicity of Cadmium make these panels expensive and dangerous for the environment.

3.2.3.6 Gallium Arsenide GaAs Thin Film Panel

The last type of solar panels reviewed in the mono-crystalline thin film group is GaAs panel. The semiconductor compound used to make these panels is Gallium Arsenide, a mixture of Gallium and Arsenic. GaAs in a single crystal form is very expensive. It is important to note that Gallium is a rare material and Arsenic is very poisonous, making these panels expensive and dangerous if damaged to the point that the semiconductor is exposed. The main benefit of GaAs panels is their efficiency. GaAs efficiency can range between 20% - 25%, with a record near the 30% mark. [16] This high efficiency is mainly due to the nearly ideal GaAs band gap. The role of the semiconductor material band gap will be discussed in the next section. GaAs panels are very useful in space applications because of its resistance to radiation damage and insensitivity to heat. So CdTe and GaAs photovoltaic modules have similar advantages in heat tolerance and high temperature performance.

3.2.4 Photovoltaic Effect in Solar Cells

In order to fully understand the photovoltaic effect and make a better decision on the most expensive part of this project, a brief review is needed to show how solar panels convert solar energy to usable electricity for the end user. The photovoltaic cell is usually constructed of some light absorbing material, which is usually silicon or some other type of semiconductor. All semiconductors are associated with a specific band gap. [17] The potential difference between the lowest energy level on the conduction band E_c and the highest energy level on the valence band E_v is called band gap energy or E_g. Electrons with enough input energy can jump this band gap from their usual steady state spot on the valence band to an excited state on the conduction band. These electrons are responsible for the direct current that the solar cells produce. Solar energy packets or photons that contain different amounts of energy correspond to different wavelengths of the solar spectrum. When the photon energy matches

that of the semiconductor band gap, the semiconductor material absorbs these photons. Consequently photons with higher energy levels than E_g are also absorbed but their excess energy is reflected or dissipated in the form of heat (wasted energy) and photons with lower energy levels than E_g are not able to get absorbed at all.

Ultimately the goal of a solar cell designer is to choose a semiconductor material with optimal band gap energy near the middle of the energy spectrum for solar radiation. No single semiconductor has a band gap that can respond to sunlight's full range, from the low-energy infrared through the visible light to the high-energy ultraviolet. Full-spectrum solar cells have already been invented, but not at a suitable consumer price. Scientists at the Solar Energy Materials Research Group in the Materials Sciences Division (MSD) at the U.S. Department of Energy's Lawrence Berkley National Laboratory have tested and produced a GaNAs solar cell that responds to almost the entire solar spectrum. The main objective in this new technology is to produce a solar cell that stacks three different semiconductors with different energy band gaps. These semiconductors are usually connected in series. [18]

A solar cell can be compared to a diode because of the p-type and n-type semiconductor materials used to fabricate them. As in all diodes there are two metal contacts attached to each side of this p-n junction. When the electron-hole pair is formed across the p-n junction, a forward voltage or photo voltage is created between the two photovoltaic cell terminals. Traditional photovoltaic cells are usually protected from the outside elements with a protecting layer such as glass or clear plastic cover. A clear encapsulant is used to attach the rest of the cell to the glass. Then an antireflection coat covers the top or front contact (n-type terminal), which is connected to the n-type silicon. Below the n-type silicon layer is the p-type layer needed to form the p-n junction in-between them. The p-type terminal or bottom contact lies beneath all the above-mentioned layers.

3.2.5 Photovoltaic Panel Performance

From the previous part of this review it is quite clear the solar panels in all the various makes and models are not very efficient at converting solar energy. So panel performance and means to increase it were very important to this project. All solar panels suffer from naturally inherited issues such as temperature effect, electron-hole recombination rate, and light absorption efficiency. Electron hole recombination is the main reason why mono-crystalline cells perform better than polycrystalline ones. The impurity concentration and structure abnormality associated with multiple crystal silicon increases electron-hole recombination rate, which in turn, decreases panel efficiency.

Temperature is another negative factor that affects solar panel performance. As mentioned earlier, crystalline silicon panels suffer the most when their cell temperature rises. The main reason why researchers use non-silicon

semiconductor materials on thin film panels is to reduce panel sensitivity to temperature. Ironically, solar panels perform at their best on a cold and sunny day. Unfortunately those days are very few and far in between in hot and sunny Central Florida. Therefore this project had to take great consideration of temperature effects on the selected solar panel. As the semiconductor temperature goes up so does its conductivity. Higher conductivity reduces the electric field at the silicon p-n junction, which in turn reduces the voltage across a solar cell. [19] A smaller cell voltage translates to a smaller power output, which also means lower efficiency. Solar panels will usually have a temperature coefficient, which is usually the rate of power reduction for every degree the above normal operating temperature of 25 degrees Celsius.

Every solar panel has an I-V curve or I-V characteristics associated with it. The area under the I-V curve is approximately the maximum power that that a panel would produce if it would operate at maximum voltage or open-circuit voltage and maximum current or short-circuit current. The area under the I-V curve (total cell power) shrinks as the solar cell voltage drops due to the higher cell temperature.

In order to increase or maintain an optimal efficiency the solar panel temperature needs to stay low and close to room temperature range. There is a lot of research being done in cooling methods used to lower panel temperature. There are active and passive-cooling methods suggested in maintaining a lower panel temperature. Pumping a coolant or some type of refrigerant through the backside of the panels is an active method. Attaching a heat sink or cooling fins is a passive way of dissipating heat from the panels. Usually these methods are not very cost effective in comparison to the gained efficiency or power from the panels.

The last inefficiency associated with solar panels is their ability to absorb light. It is a well-known fact that solar panels cannot make use of the entire light spectrum. Some light is lost due to reflection, which is why antireflection coating is used on top of every solar cell. As mentioned earlier the semiconductor will absorb only the amount of light that has matching or higher wavelength energy to the semiconductor band gap. This makes more than half of the spectrum of light available useless to the solar panels. Band gap engineering is one of the methods used to increase the light absorption efficiencies. The design engineer can maximize power by maximizing photocurrent or photo voltage individually. To maximize photocurrent, it is desirable to capture as many photons from the spectrum of solar radiation as possible. A small band gap may then be selected so that even photons with lower radiation energies can excite electrons into the conduction band. However, the small band gap results in a lower photo voltage. Additionally, the photons with higher energies will have much of their energy wasted as heat, instead of conversion into electrical energy. Alternatively, the designer can choose a higher band gap, but then will not capture any photon energy less than that band gap, resulting in a lower photocurrent and, in turn, reducing the output current of the device. In designing conventional single-junction solar cells, these two competing issues are balanced by choosing

optimal band gaps near the middle of the energy spectrum for solar radiation. Conveniently, high-quality wafers of silicon, with a band gap of 1.1 eV, and GaAs, with a band gap of about 1.4 eV, are readily available and have nearly the optimal band gap for solar energy conversion in a conventional single-junction solar cell. [17]

3.2.6 Solar Radiation

The intensity of solar radiation or irradiance is the main reason which explains why solar panels perform better in the middle of the day versus in the morning or in the evening. Solar radiation is the electromagnetic (EM) radiation emitted from the sun. Insolation is expressed by the amount of energy received on a given surface in a given time. It is expressed by watts per square meter (W/m^2) or kilowatt-hours per square meter per day ($kW \cdot h/(m^2 \cdot day)$). Considering Earth's distance from the Sun, the amount of insolation from the Sun on Earth's surface averages at 1368 W/m^2. Figure 4 shows the annual average solar radiation map of the United States. [20] According to this map Central Florida averages close to 5 $kW \cdot h/(m^2 \cdot day)$. The southwestern United States would be the best area to design and test this project since the average solar radiation there is close to or above 6 $kW \cdot h/(m^2 \cdot day)$.

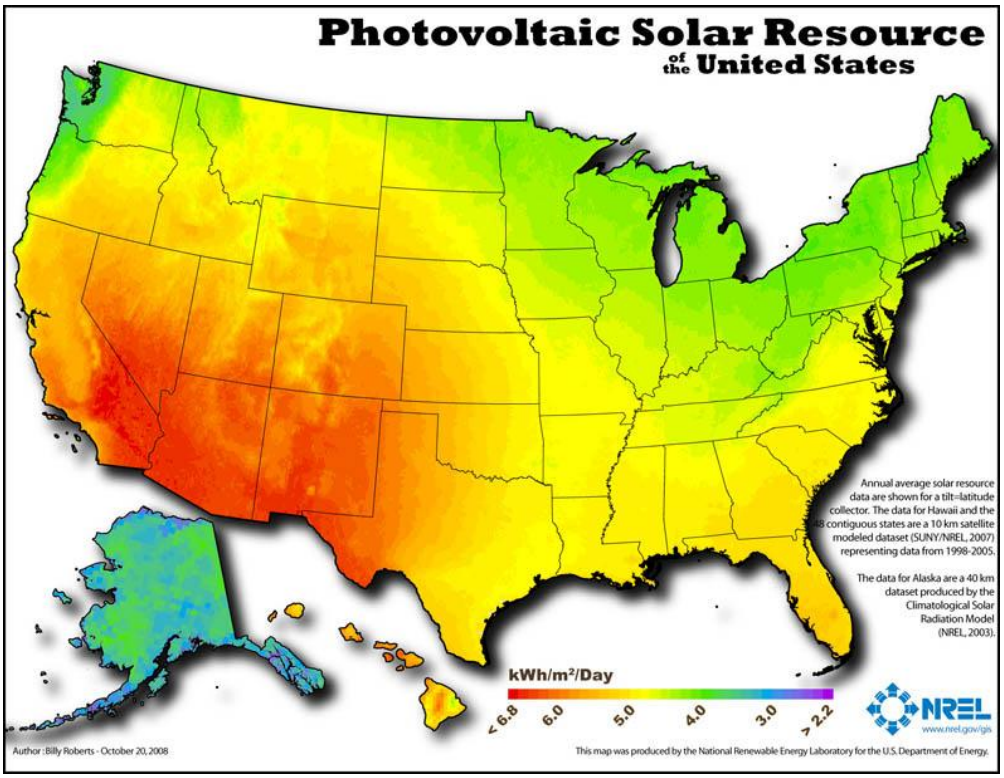

Figure 4 - Photovoltaic solar radiation map of the US.
This map was created by the NREL for the Department of Energy.

There are a few methods to increase solar panel performance to make up for lower levels of solar irradiance. They would include direct methods like solar tracking and light concentration or indirect method such as the one covered in this project, which considers the use of an MPPT charge controller. Solar tracking is used to minimize the angle of incidence between the sunlight and the panels. In other words, this method ensures that the solar panels face the sun at any given point of the day. This is achieved by mounting the solar panels on a single or double axis mounting mechanism that is controlled by the intensity of the sunlight. Light concentration is achieved with the use of mirrors or lenses above or around the solar panel in order to intensify the amount of sunlight that hits the panel.

MPPT is an indirect method of maximizing the efficiency at which the solar panels deliver electricity to an on-grid or off-grid scenario like charging a bank of batteries. MPPT charge controllers optimize the output voltage of the panel to match the required-state voltage level of the batteries. This is achieved by maintaining the panel's power level and therefore changing the panel's output current accordingly. So for example, if the batteries require a lesser voltage from the panel the MPPT charge controller will reduce the PV output voltage and increase the output current in order to maintain the same level of power.

3.3 Charge Controllers

Charge controllers are designed to maximize the output efficiency of a solar panel or solar array. Usually used in an off-grid scenario, charge controllers are used to monitor and regulate the solar array output voltage to the batteries, which store the energy generated. Output voltage regulation is very important in battery charging because batteries require a specific charging method with various voltage and current levels for each specific stage. These charging methods are needed to prolong battery life and performance. This is where the charge controller does most of the work.

Depending on the type of controller, the input voltage is regulated to match the battery required voltage at the output. This can be done by using standard or MPPT charge controllers. Standard charge controllers are typically used in a situation where the input voltage from the solar panel is higher than the voltage from the battery. In this case the voltage is reduced by the controller while the current that the panel is outputting stays the same. This last factor results in power loss from the total power generated from the panels. MPPT charge controller use smart technologies, such as microcontrollers, to compute the highest possible power output at any given time. In this scenario the voltage is monitored and regulated without power loss. Therefore in the same conditions as above, where the input voltage is higher than the output voltage, the MPPT charge controller lowers the voltage and simultaneously increases the current to the batteries. This results in higher power transfer efficiencies, which means less solar power is lost during the storage process.

3.4 DC-DC Regulators

The DC voltage from the panel varies depending on the light intensity, which varies based on the time of day and solar panel temperature. On the battery side of the system, the battery voltage varies depending on the load connected to it. In order to maintain optimal battery charging, it is extremely important that the panel voltage and current matches the required battery charging stage at that particular moment.

A DC-to-DC regulator is needed to increase or decrease the input panel voltage to the required battery level. These regulators are also known as switching regulators where a power switch, an inductor, a capacitor and a diode are used to transfer power from input to output. These components can be arranged to form different types of DC-to-DC regulators. The switches are either passive or active. Passive switches usually consist of a diode, while the active switches are usually some type of a MOSFET transistor. MOSFET transistors are an efficient and fast way to allow a pulse width modulation (PWM) signal to control the frequency and duty cycle of the ON and OFF time of the “switch”. The higher the duty cycle the more power is transferred from input to output. One of the advantages of the PWM is that the signal remains digital from the source, in this case from the microcontroller to the MOSFET’s, reducing or even eliminating the need for any analog-to-digital signal conversion. Digital signals are not affected as much from outside noise, unless the noise is sufficient to change the signal from one to zero or vice versa.

There are many DC-to-DC converter topologies used today, such as Buck, Boost, Buck/Boost, CUK, and Sepic. These regulators do not produce power. In fact these regulators consume some of the input power according to their efficiency. Therefore the adjusted voltage level affects the current level, ideally maintaining the same power level. Since current and voltage are both directly proportional to power, it is intuitive that in buck mode the voltage is lowered as the current increases. While in boost mode the voltage is increased as the current decreases. There are three main types of DC-to-DC converters presented in this research: Buck Converters, Boost Converters, and Inverting and Non-inverting Buck-Boost Converters.

3.4.1 Buck Converter

A buck converter or voltage regulator is also called a step down regulator since the output voltage is lower than the input voltage. In a simple example of a buck converter, a diode is connected in parallel with the input voltage source, a capacitor, and the load, which represents output voltage. A switch is connected between the input voltage source and the diode and an inductor is connected between the diode and the capacitor. A pulse width modulation controller controls the switch. In this project the microcontroller served as a pulse width modulation source.

There are two states in a buck converter topology. The first state is demonstrated Figure 5. When the switch is closed the inductor absorbs power as its current increases. Due to this power absorption the output voltage is higher than the input voltage. The capacitor current can point in either direction depending on the difference between the inductor current and load current. In Figure 5 the capacitor is charging on the left and discharging on the right. Equations (1) and (2) govern the operation of the circuit in the first state. [21]

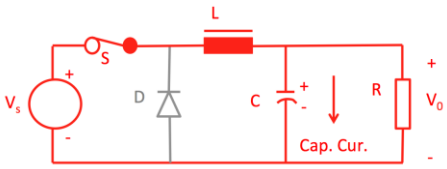

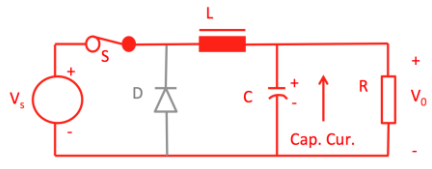

$$\frac{di_L}{dt} = \frac{v_S - v_0}{L} \quad (1)$$

$$\frac{dv_0}{dt} = \frac{i_L - \frac{v_0}{R}}{C} \quad (2)$$

Figure 5 - Buck Converter Circuit ON-State.

In the next state, Figure 6, the switch is open and the diode is turned on. In this state the inductor is the power supplier to the output side of the circuit. As the energy stored in the inductor decreases so does its current. The capacitor current can point in either direction depending on how the inductor current compares to the load current. As the energy stored in the inductor is used up, the inductor current becomes zero and the inductor current tends to reverse. The reversal is stopped by the diode. During this time the inductor and the diode part of the circuit are at rest. The capacitor is now the power supply for the load as it discharges its energy. Equations (3) and (4) govern the operation of the circuit in the third state. [21]

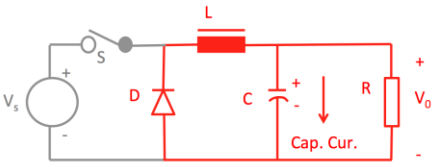

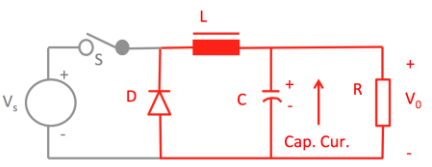

$$\frac{di_L}{dt} = \frac{-v_0}{L} \quad (3)$$

$$\frac{dv_0}{dt} = \frac{i_L - \frac{v_0}{R}}{C} \quad (4)$$

Figure 6 - Buck Converter Circuit OFF-State.

When the circuit switch receives a PWM signal, the response of the circuit becomes periodic. In this case it is assumed that the source voltage remains constant with no ripple, and the frequency of operation is kept fixed with a fixed duty cycle. If the RC time constant due to the load resistor and the filter capacitor is very large compared to the cycle period of the switching frequency, the output voltage is more or less constant, with no noticeable ripple. When both the input voltage and the output voltage are constant, the current through the inductor rises linearly when the switch is closed and it falls linearly when the switch is open. Under this condition, the current through the capacitor also varies linearly when it is being charged or discharged. [21]

3.4.2 Boost Converter

As with the buck converter, the boost or step-up converter circuit consists of a switch, a diode, an inductor and a capacitor. Their positions in the circuit vary in comparison to the buck converter. In this case the switch is in parallel with the input voltage source, the capacitor and the load. The inductor is placed between the input voltage source and the switch and the diode is placed in-between the switch and the capacitor. A simple boost circuit with the components mentioned above is pictured in Figure 7. The switch is pictured as a transistor.

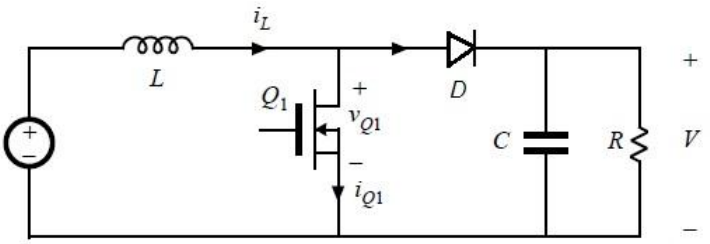

Figure 7 - Boost Converter Circuit.

Just like in the buck converter case there are two separate states in this boost converter topology. When the switch is on or closed the input voltage is used to increase the inductor current as energy is stored in the inductor. The switch acts as short circuit path to disable the RC part of the circuit on the right side of the diode. The diode prevents the capacitor from discharging the output voltage to ground. The second state is encountered when the switch is opened or off. The inductor's tendency to resist changes in current enables the boost in voltage. When the inductor is charging it acts as a load and stores energy. In this state the inductor acts as an energy source and the output voltage produced during its discharge is related to the current's rate of change, not the input voltage, therefore allowing a difference between the two voltages. The inductor current is used to charge the capacitor and in turn boost the output voltage. As the output voltage increases the current decreases.

3.4.3 Inverting Buck-Boost Converter

The last and most important type of switching regulator is the buck-boost converter. In this converter, the buck and boost topologies covered earlier are combined into one. A buck-boost converter is also built using the same components used in the converters covered before. The inductor in this case is placed in parallel with the input voltage and the load capacitor. The switch or transistor is placed between the input and the inductor, while the diode is placed between the inductor and the load capacitor in a reverse direction, shown in Figure 8. This means that the diode regulates current flow from the output or right side of the circuit to the input side or the left side of the circuit. During the ON time of the switch the circuit behaves similarly to a boost converter, where the

input voltage source is used to increase the current through the inductor and in turn increase the energy stored in it. The diode during this time with not let current reach the load side of the circuit because it is in reverse bias. In this state the capacitor is used to power the load.

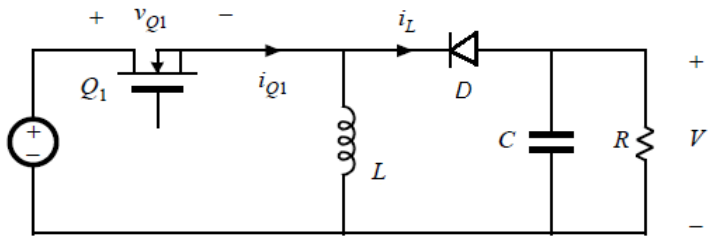

Figure 8 - Inverting Buck-Boost Converter Circuit.

In the OFF state of the circuit the inductor is used to supply energy to the RC load circuit. The inductor current that the load capacitor sees is in the reverse polarity to that of the input voltage. Therefore the name of this converter describes one of the main features of this converter, which is the reversal of the polarities between input and output voltages. For this reason, extreme attention should be paid in designing a circuit that uses this type of converter. This converter can be used when the output polarity is not important to the load. One of the main advantages of this converter is the low number of parts needed to implement the topology. Therefore losses in the circuitry are low. The main disadvantage to this topology is the fact that it operates in buck-boost mode only. So if buck-only mode or boost-only mode is needed this converter is not going to be able to meet the requirements.

3.4.4 Non-Inverting Buck-Boost Converter

As the name implies, this converter does not invert the polarities of the output voltage in relation to the polarities of the input. This converter requires the use of four active switches or transistors and is designed by combining a buck converter and boost converter design in the same topology. Due to this design this converter can work as Buck-only, Boost-only or Buck/Boost converter. The input voltage source is connected in parallel with switch Q2, Q3 and load capacitor as indicated in Figure 9. Switch Q1 is connected between the input voltage source and switch Q2. The inductor is connected between Q2 and Q3, while Q4 is connected between switch Q3 and the output or load capacitor.

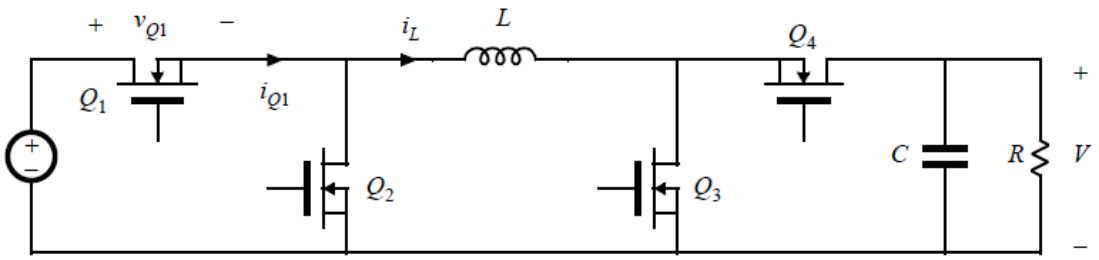

Figure 9 - Non-Inverting Buck-Boost Converter Circuit.

In buck-only mode, Q1 is used as a switching transistor, while Q2 acts as the diode described previously in the buck converter. Q3 is turned OFF and Q4 is always ON. Q1 and Q2 form the buck switching leg. In boost-only mode Q3 is used as a switching MOSFET and Q4 acts as the diode in the boost regulator. Q1 is always ON and Q2 is turned OFF. Q3 and Q4 form the boost switching leg. In buck-boost mode the Q1 and Q3 are simultaneously ON during the switching cycle or ON time, while Q2 and Q4 are simultaneously ON during the opposite switching cycle or OFF time. This means that when Q1 and Q3 are turned ON, the inductor is getting charged, so Q2 and Q4 are turned OFF. Vice versa when Q2, Q4 are ON, the inductor is charging the load capacitor, so Q1 and Q3 are turned OFF. [22]

A 4-channel MOSFET Driver will be needed to convert the PWM signal from the microcontroller to the switches, in order to operate this full-bridge (H-Bridge) power converter in buck-boost mode. This topology is very advantageous for this project because it combines all possible converting topologies into one DC to DC converter circuit. The main disadvantage to this circuit is the greater amount of components used in comparison with the other converters. This fact should be looked into when the production cost of the circuit board and components is considered.

Another disadvantage related with the high amount of switches used in this circuit is the switching losses of the buck-boost mode are twice as large as the switching losses of the buck-only or boost-only mode. This happens because in either the buck or boost topology only two switches are cycling ON and OFF, while in buck-boost topology four switches are cycling ON and OFF. The output to input voltage ration is given by D/(D-1) where D is the duty cycle of the PWM signal. As a result, if the duty cycle is set to half or 50%, the output voltage is equal to the input voltage. In this case the inductor current is twice as large as the load current, which means that the resistive losses are four times that of a Buck or low duty cycle Boost converter. The physical size of the inductor must also be larger to accommodate this extra current without saturating. Furthermore, as the output capacitor must carry the full output current during the PWM ON-time (D), and the charge current during the PWM OFF-time, the output capacitor must have low equivalent series resistance (ESR).

To diminish these disadvantages, it is better to have a four-switch DC-DC converter that changes its mode of operation depending on the input and output voltages. The microcontroller is programmed in such order that it changes modes to make the H-bridge operate like a buck converter for Vin greater than Vout and switch to a boost converter for Vout greater than Vin. This solution introduces a buck-boost mode for Vin~Vout, where the direct connection of input to output via the inductor is maximized. The direct connection ensures a more continuous DC current, as opposed to the high peak current experienced in a classic four-switch buck-boost. It also minimizes stress on both input and output capacitors and reduces ripple voltage. [23]

3.4.5 Half-Bridge and Full-Bridge Drivers

These integrated circuits are needed in order to operate a DC-to-DC regulator as a non-inverting buck-boost converter. They drive the PWM signal from the microcontroller to turn the (Q1, Q2, Q3 and Q4) N-channel MOSFET transistors ON, OFF or switch them at a certain frequency (f) and duty cycle (D). This can be achieved by using a full-bridge driver, which controls up to four different switching MOSFETs according to four separate and independent inputs. In lack of a full-bridge driver, two identical half-bridge drivers can be used to control a pair of switching MOSFETs independently. Half-bridge drivers are easier to find in today's market. These drivers are also available in high voltage, which means that they are able to drive a high voltage switching MOSFET.

An example of a high voltage half-bridge driver is the LM5102 by National Semiconductor, LT1160 by Linear Technology, and IRS2104 by International Rectifier. These drivers amplify a PWM signal with frequencies up to 100 kHz, to a higher voltage, which in turn is capable of switching the required MOSFETs by charging their gates. The driver with the most interest for this project is the IRS2104, which allows one synchronous PWM input in pin 2 and a shutdown digital input on pin 3. The MOSFETs are controlled through pins 5 and 7. This IC is powered at pins 1 and 8 from a source voltage between 10 and 20 Volts, and it can handle input voltage up to 600 Volts. Figure 10 shows a typical way to connect this half-bridge driver. Two of these will be needed in order to form a full bridge buck and boost converter. LT1162 includes two IRS2104s in the same IC. Therefore LT1162 is considered a full-bridge driver that might work well in this scenario. [24]

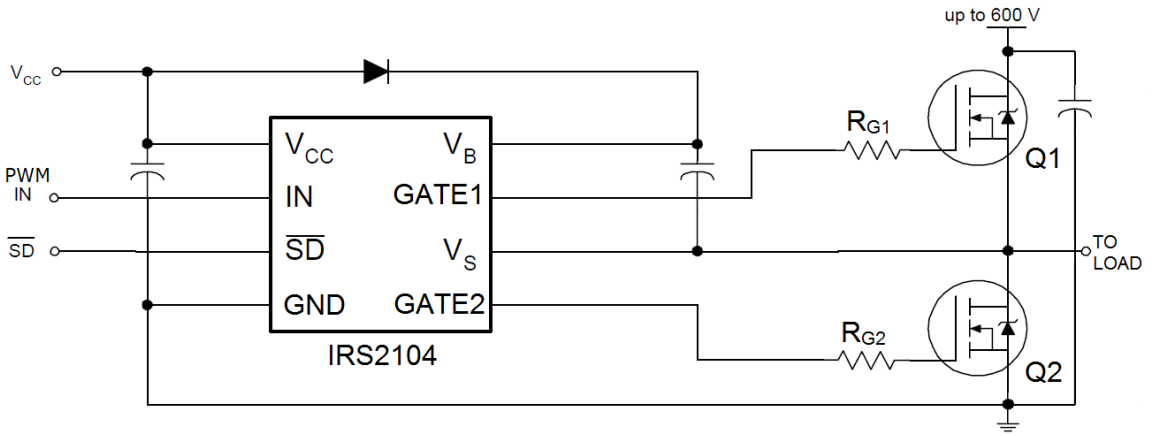

Figure 10 – IRS2104 Half-Bridge Driver.

Another type of type of half-bridge driver that can be used to build a buck-only or a boost-only converter is the Linear Technology LTC4449 MOSFET Driver. With a single PWM input from the microcontroller, similar to the IRS2104, this IC can drive two separate MOSFETs simultaneously. When the input is set to HIGH the top gate-driving pin turns ON while the bottom one stays OFF. When the pulse is LOW the top-driving pin turns OFF and the bottom one is turned ON. These drivers are ideal because of their low participation and high switching times. A simulation in LT-Spice, Linear Technology's own simulation program, is shown Figure 11, in order to demonstrate the functionality of these particular drivers in buck-only and boost-only topologies. Both converters use the same 12V input from voltage source V3 for a better demonstration. As in the buck converter circuit MOSFET Q1 acts as the switch. And Q2 replaces the diode. Similarly in the boost converter circuit on the right Q3 replaces the diode while Q4 is the switch. The buck output is plotted in blue while the boost output is plotted in red. V2 and V5 serve as PWM simulators with a 50% duty cycle and 500 kHz frequency. Within 300 microseconds the boosted output reaches 18V and the bucked output approaches 6V. As we increase the duty cycle of the buck PWM source V2 the bucked voltage output approaches the input voltage. As we increased the duty cycle of the boost PWM source V5 the boosted output voltage started to approach the input voltage as well. In conclusion, as long as the microcontroller is able to change the duty cycles of the PWM outputs, it should be able to operate either buck or boost converters.

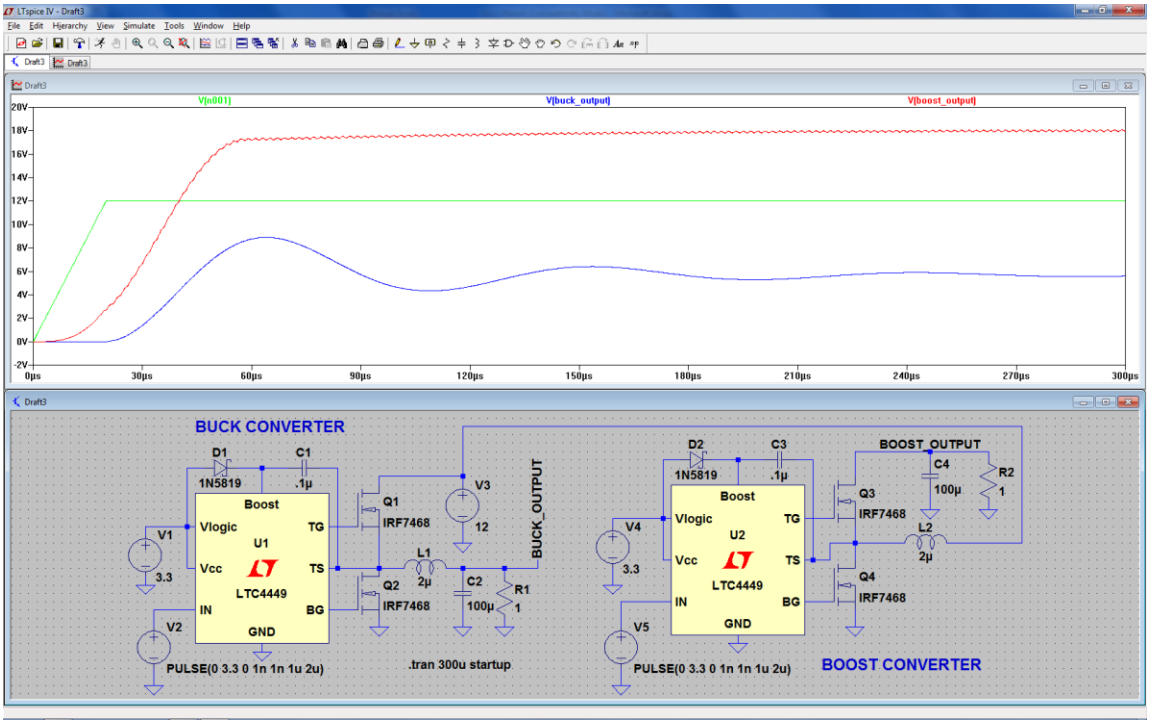

Figure 11 - Buck Converter and Boost Converter LT Spice Simulation.

3.4.6 Circuit Power Supply

Power from the panels is needed to power the current, voltage and temperature sensing circuit. Power is also needed to power the MOSFET gate drivers, LCD, wireless transmitters and microcontroller. In order to achieve this, a simple step-down or switching regulator was connected to the input voltage from the panel. An IC version of this converter was sufficient, since the load connected to it did not draw a significant amount of currents. The voltages needed to power the internal circuits of the charge controller were 5V and 3.3V. These voltages should be a deciding point on picking the right type of Buck converter. The LT3500 is a linear technology product that is capable of outputting both DC voltage levels simultaneously, at a 1A load current rating for each of the outputs. Figure 12 shows an example simulation of a LT3500 IC and supporting circuitry, where a 24V input (green trace) is reduced to a 5V (blue trace) and a 3.3V (red trace) output voltages. The 1A rating on both these rails will ensure constant power delivery to the charge controller's circuit board and its peripherals. This IC chip requires special attention during circuit board design. It has an exposed metal pad underneath. When this part is mounted on the circuit board, the metal pad is design to make full contact with the ground copper-conducting pad. This mounting method ensures proper heat transfer from the chip onto the ground circuit pad, which results in better performance and longer product life. The LM2675-5V and LM2675-3.3V were the switching regulator used for this project.

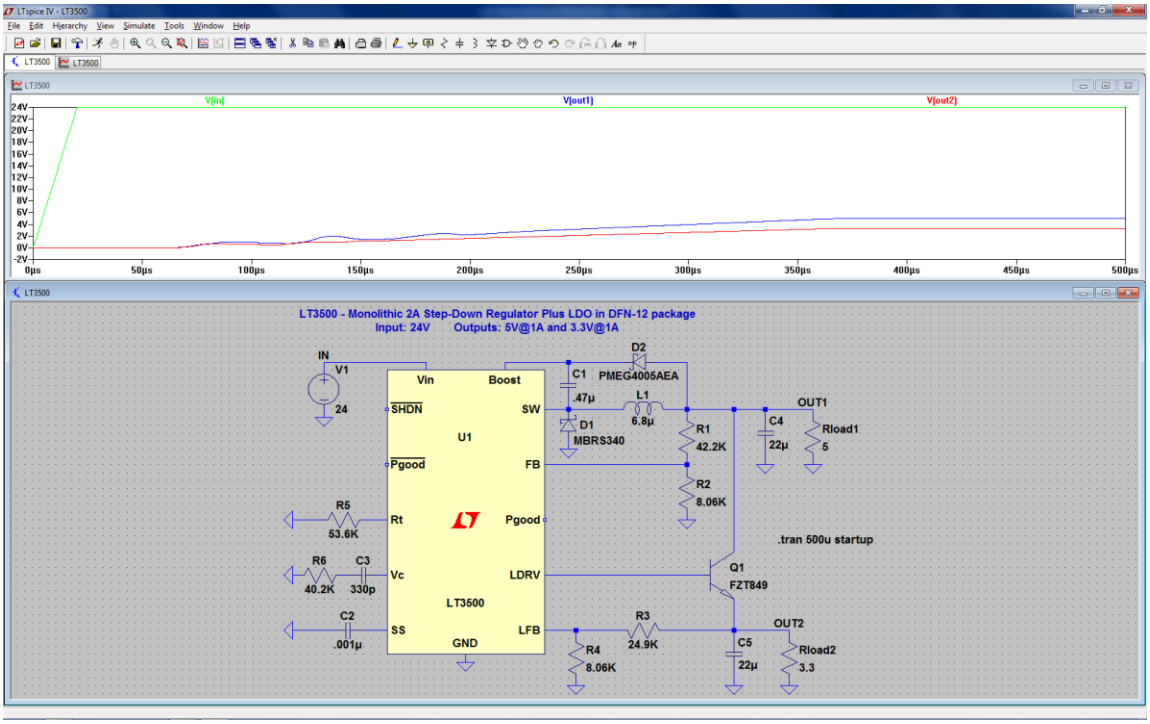

Figure 12 - LT3500 2A Buck Regulator LT Spice Simulation.

3.5 Microcontroller

The microcontroller is a key component of PMCC and it needs to perform monitoring tasks, MPPT and other charging algorithms, and be capable of transmitting and receiving wireless data. It is responsible for reading numerous sensors and controlling the circuitry used to track the maximum power. The microcontroller must possess ample input and output pins and must be compatible with all sensors chosen. The programming language of the microcontroller should be both robust and easy to use. Other desirable specifications would be low-cost, low-power, small footprint, and fast clock speed.

3.5.1 ATmega328P

The Atmel ATmega328P is a low cost, mid-range performance microcontroller. It features a 20 MHz clock, 32 KB flash memory for programming, 2 KB SRAM, and 1 KB of non-volatile EEPROM. The chip runs at 5V DC and contains 14 general digital input/output pins, of which 6 can be used for PWM outputs, and 6 analog input pins. The microcontroller contains one hardware USART serial port, Serial Peripheral Interface Bus (SPI) and Two-Wire Interface (TWI) communication. This microcontroller can be programmed using Atmel's AVR Studio software. The Integrated Development Environment (IDE) allows programming in either C/C++ or assembly code. The ATmega328P requires an external programmer to implement new code. This requires (in the case of a

Dual-Inline Package) that the chip be physically removed from a circuit and inserted into the programmer to load a new program into the flash memory. [25]

3.5.2 Arduino

Arduino is a single-board microcontroller, consisting of an Atmel ATmega328P along with various other components that allow for easy programming and access to various digital and analog pins. The Atmega328P microcontroller is pre-loaded with the Arduino bootloader, allowing this chip to be programmed in the Arduino programming language and eliminating the need for an external programmer.

The Arduino Uno is powered either through USB (5V) or an external DC power source (7V – 12V). The board breaks out the 14 digital input/output pins, of which 6 can be used as PWM outputs, and 6 analog input pins. In addition, there is a 16 MHz crystal oscillator, USB connector, and reset button. The Uno incorporates an ATmega8U2 onboard to mediate between the USB and TTL serial communications, allowing programming through USB. The board also provides 5V and 3.3V regulated DC output to power sensors or other low-power systems. The Uno contains 32 KB (0.5 KB is used for the bootloader) of flash memory to which the program is written, 2 KB SRAM, and 1KB EEPROM (non-volatile storage). The Uno contains one set of hardware UART for serial communication, Serial Peripheral Interface Bus (SPI) communication, and Two-Wire Interface (TWI), also known as Inter-Integrated Circuit (I^2C) communication.

By way of the Arduino bootloader, the ATmega328 can be programmed in the Arduino programming language instead of either AVR's C-like language or its assembly language. The Arduino language is based on the Wiring programming language, and the development environment is based on the Processing IDE. All of these languages and IDE's are free and open source.

The Arduino programming language consists of functions, variables, and mathematical operations that allow the user to interface with sensors and other peripherals through the digital and analog pins utilizing the numerous communication protocols. In addition, many libraries have been written by the Arduino community to interface with various sensors, user interfaces, communications, data logging, and other peripherals. [26]

3.6 MPPT Algorithms

While research on solar power has been conducted for decades, for many applications the implementation of solar panels is not efficient enough to be considered cost effective. There are many different stages in the process of harvesting solar energy where losses occur. Advancements in solar cell materials and integration can make the overall system more effective but there are other aspects that can provide significant savings.

This project is addressing the efficiency that can be achieved through the optimal use of the charge controller, specifically by implementing what is known as Maximum Power Point Tracking (MPPT). Under constant conditions, a photovoltaic array demonstrates a constant current-voltage (IV) graph. The power can be calculated from this IV curve and the specific point where the maximum power is achieved can be located.

There are many factors that play a role in whether or not the PV array is operating optimally and effect the determination of the maximum power point. Due to fluctuations in environmental conditions, predominantly the ambient temperature of the panels and the irradiance level, the IV curve changes and therefore the maximum power point is at a different location. This is why the MPPT algorithm must not be static and should be constantly tracking the power point. [27]

In order to extract the most power from the cells, although sometimes attenuated by the temperature, dirt, irradiance and other conditions, the system cannot simply operate at a constant voltage. [28] Maximum power point tracking has been shown to increase the efficiency of the system by approximately 30% over charge controllers that do not implement MPPT. [2,3] In addition, as the battery charges the voltage changes as it passes through several charging states which would create further inefficiencies in the absence of a charge controller. [29] In this project, the charge controller is be able to monitor voltages from both the photovoltaic array and the battery in order to determine these charging states and maintain maximum efficiency.

To illustrate a potential scenario, consider if the goal of the system is to charge a 12 V battery but the maximum power point occurred at a panel voltage of 15 V. If the panel were connected directly to the battery, it would pull the panel voltage down to 12 V, which the IV graph would clearly show is inefficient and operating below the maximum power point. Rather than allow this energy to be wasted, the charge controller allows the panel to continue to operate at the MPP but uses DC-to-DC converters to compensate for the difference in voltage needed. This prevents significant losses and allows the system to take advantage of the valuable power that is produced in the solar array. [2]

There are several common methods that are used to implement maximum power point tracking. These iterative approaches imply varying levels of complexity based on the type of tracking that they utilize. The most common methods of MPPT are the Perturb and Observe Method, Incremental Conductance Method, and the Fixed Voltage Method.

3.6.1 Perturb and Observe Method

This method of power point tracking follows the procedure of constantly checking the voltage (or current in some systems) and continuing to increase the voltage as long as the power continues to increase. After passing over the maximum

power point the power begins to decrease which the algorithm interprets as having gone too far and starts decreasing the voltage to compensate. This process continues to iterate until the maximum power point has been reached. Figure 13 provides a graphical representation of this algorithm in operation.

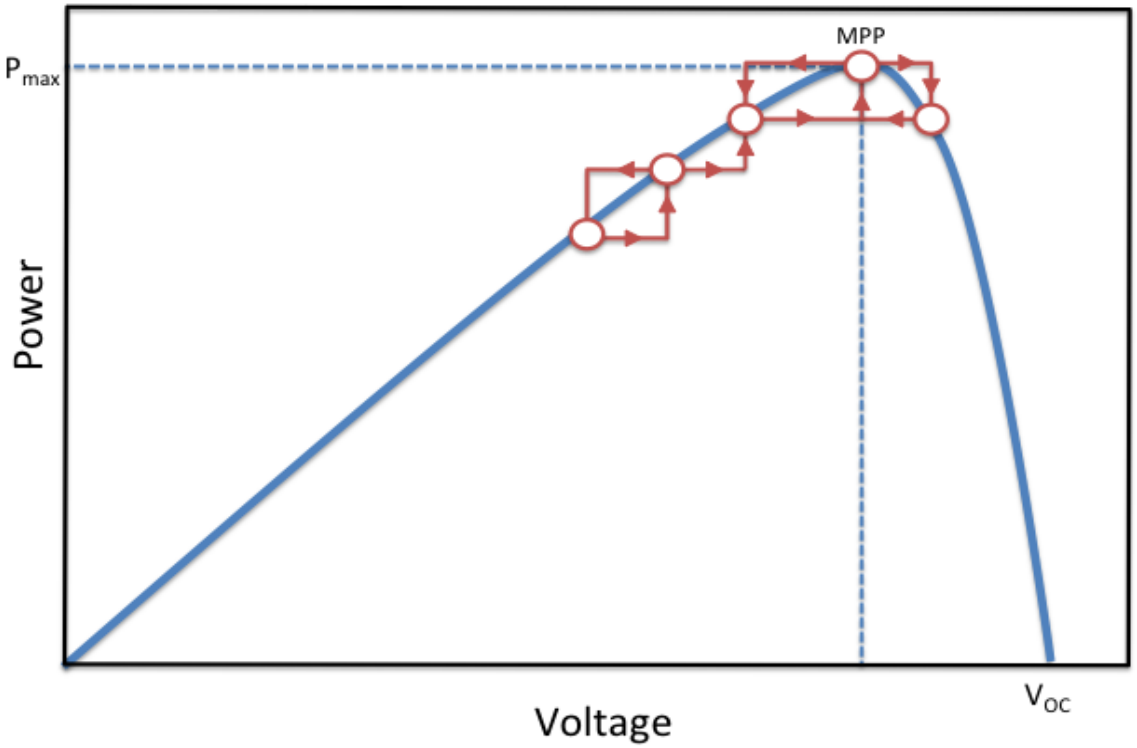

Figure 13 - The Perturb-and-Observe Method for MPPT.

One of the disadvantages of the perturb-and-observe method is that based on the algorithm, the system continues to oscillate around the maximum power point. This can lead to inefficiencies, especially in situations when the irradiance is low and the power-voltage curve begins to flatten out. When this occurs, the perturb-and-observe method can sometimes have difficulty determining when it has actually reached the maximum power point. In addition sometimes this algorithm performs several iterations in the wrong direction if it is affected by rapidly changing conditions. [30] However, the perturb-and-observe method is widely recognized as the most common method for maximum power point tracking because of its simple design.

3.6.2 Incremental Conductance Method

A more complex but typically more accurate procedure is known as the incremental conductance method. The underlying idea behind this method is to compare the differentiation of the power with respect to voltage to zero and determine if it is more or less, as depicted in Figure 14.

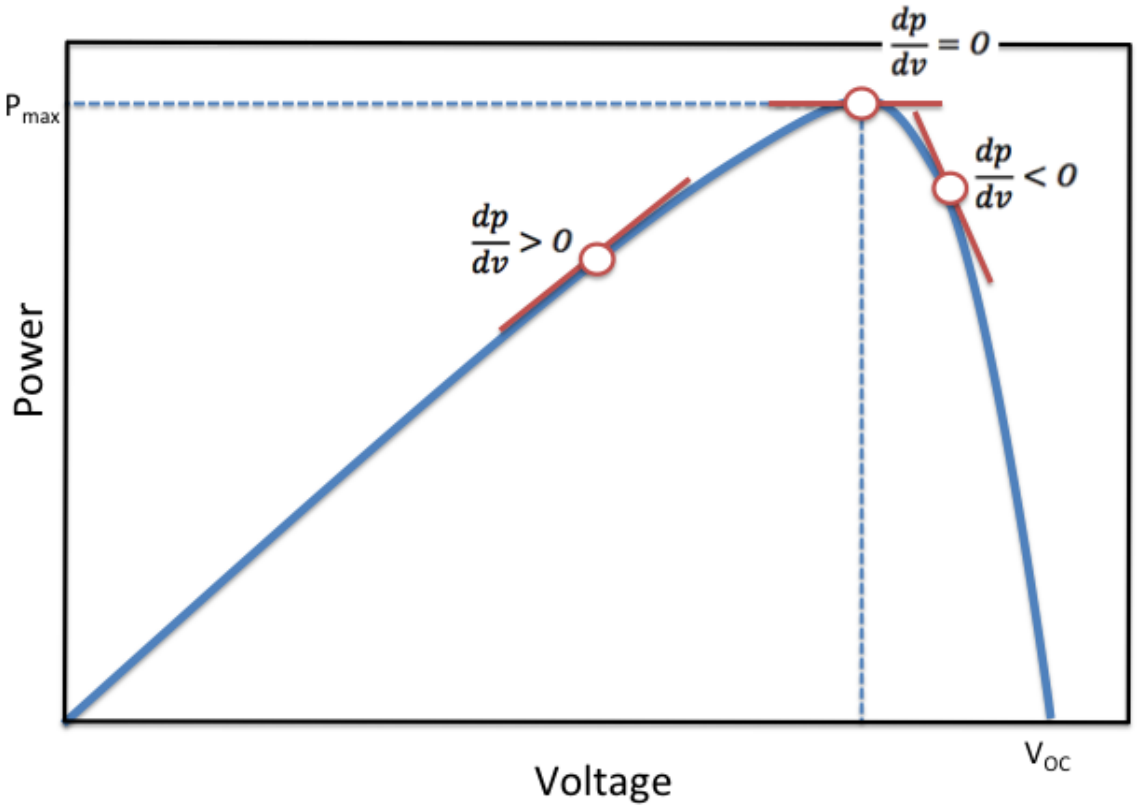

Figure 14 - The Incremental Conductance Method for MPPT.

The differentiation of the power equal to zero can be rewritten in terms of the conductance. In this form, the instantaneous conductance is equal to the incremental conductance but with the opposite sign.

$$-\frac{I}{V} = \frac{dI}{dV}$$

This equation (and each of the two inequalities that could arise) corresponds to the three regions referenced in Figure 14, one of which being the point where $dP/dV = 0$. If the incremental conductance is greater than the instantaneous conductance the algorithm continues to increase the voltage until the maximum power point is determined. Unlike the perturb and observe method, using incremental conductance a discreet value for the maximum power point can be obtained and the system remains at this point until it undergoes a change in the environmental conditions affecting the power. The other important advantage of the incremental conductance method is that by calculating the derivative and creating the inequality, the algorithm knows which direction to move along the curve in order to reach the maximum power point. [30]

3.6.3 Constant Voltage Method

The simplest of the widely recognized MPPT algorithms is the constant voltage method. As the name implies this algorithm operates as a constant voltage value based off of the open circuit voltage. Literature reports a range of accepted approximations for the operating voltage, usually between 73-80%. [30] In Figure 15, the constant voltage is assumed to be at 76% of V_{OC}.

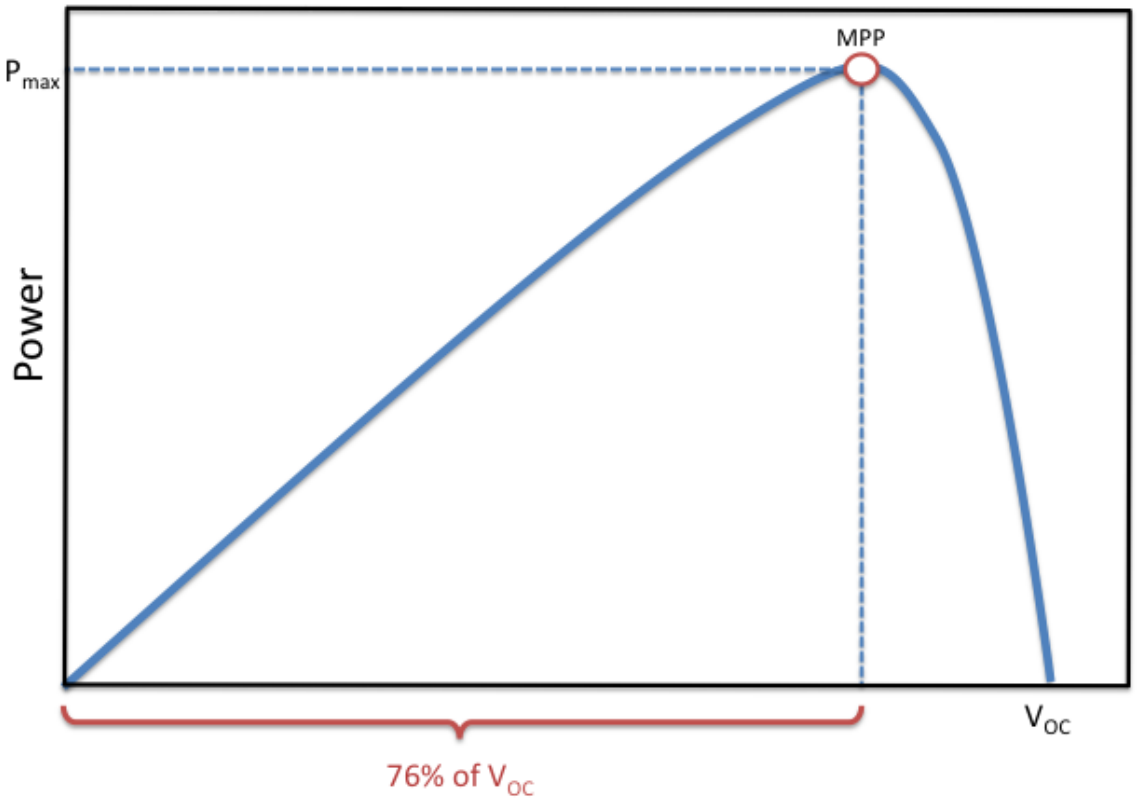

Figure 15 - The Constant Voltage Method for MPPT.

The system temporarily sets the PV current to zero in order to determine the open circuit voltage. Once it has this value it can calculate, based on the specified ratio, what the operating voltage should be and the system can begin moving to that point. There is a specific amount of time, which can be programmed into the system, to wait before isolating the source and repeating the calculation. This method is inherently much less efficient than either the perturb-and-observe method or the incremental conductance algorithm. Significant losses in efficiency occur when the current is set to zero to determine V_{OC} because of the wasted energy. In addition the maximum power point is not always at 76% and it is difficult to accurately approximate where it is going to be. The primary advantage of this technique is that it requires much less

computational time and is a much simpler algorithm than the previous methods. [31]

3.7 LCD

To improve the user interactivity with the system and make it easier to use, a Liquid Crystal Display (LCD) was implemented into the design to show several numerical values. This screen displays the current and voltage coming through the charge controller, as well as the temperature at several locations in the system. It also allows the user to see the battery charging status as well as any system warnings or messages.

Liquid Crystal Displays are extremely common in battery-powered electronics because they consume relatively low power. In addition, they are reasonably priced and there is a wide range of types to choose from. The LCD is made up of a given number of pixels that are generally arranged in front of the light source. These pixels are turned on and off based on an applied electric field. [32] The LCD used in this design will be programmed to interface with the microcontroller.

There are several different types of LCD screens readily available. Choices range from very minimal characters to full color displays with touch screen functionality. The balance between the ability to read relevant information quickly and the amount of power consumption determined which type was incorporated into the design.

3.7.1 Segmented LCD (Alphanumeric)

Segmented LCD screens are sometimes referred to as alphanumeric displays. They are denoted as such because of the 14 segments in a segmented display that can be programmed to create numerous alphanumeric characters. One of the advantages of an alphanumeric LCD screen is the low power consumption. Another benefit is the ease of control and simplicity of programming. The clear disadvantage is that there is very little flexibility and a limited number of characters that can be displayed. [33]

3.7.2 Character LCD (Dot Matrix)

Character LCDs, or Dot Matrix, have the ability to construct individual alphanumeric characters using an array of pixels in the displays. This type of LCD is commonly denoted by the number of characters it can display, often in terms of the dimensions of the rows. For example, a 16 x 2 LCD can display 16 characters per row and consists of 2 rows.

Each character is generally made up of a 5 x 7 array of pixels providing more flexibility in the types of symbols that can be generated. Dot Matrix displays have the capability to create numbers, letters in multiple languages, and several other

symbols. Character LCDs are a good choice if one needed to display characters outside of the limitations of the segmented LCD. Similar to the segmented displays, character LCDs are relatively easy to program and do not consume much power, especially when compared to graphical displays. They are also less expensive than other larger, color displays. Disadvantages include being confined to only text and not being able to include images, icons, or other interfaces, including graphical menus. [33]

3.7.3 Graphical LCD

In the same way that character LCDs operate on a grid of pixels, a graphical display utilizes an array as well, but the grouping of pixels spans the entire screen and each pixel is accessible individually. This allows the user to program any type of graphic or text that they wish, and place it in any area of the screen.

Advantages of incorporating graphical LCDs are the flexibility in design, allowing for more text as well as pictures and logos, as well as a larger interface. Because of the increase in size, this LCD also consumes more power. Another disadvantage is that the controller circuits are more difficult to design, while most are supplemented by preexisting controller chips. In addition, the programming required is also more complex. [33]

3.7.3.1 Backlighting

When considering an LCD the designer must decide if their system requires a screen that is backlit or if internal illumination is not necessary. For certain outdoor (daytime) applications, a given product may not to have a backlight. These types of LCDs use considerably less power than those that require lighting. However in many cases, non-backlit LCD screens are difficult to read, even in moderate lighting conditions. Therefore, while backlighting requires more power, it makes the product more versatile and able to operate in a wider range of situations.

3.7.3.2 Color vs. Monochrome

Another option to consider when choosing an LCD is whether to incorporate a color or monochrome screen. Monochrome LCDs are typically passive-matrix, and color screens can be either passive or active-matrix (TFT screens are active-matrix). The matrix type influences the speed at which the transistors can switch and change the pixels. Both are relatively low power, and can display graphics using the array of pixels. The main difference between the two choices is cost. Color LCD screens cost more than monochrome ones and this difference can be amplified when choosing larger screen sizes. [34]

3.7.3.3 Touchscreen

Advantages of including touchscreen capability are the increased appeal in user interaction. The user would be able to quickly and easily choose the data that they would like to display on the screen. When compared to a smaller character LCD that may need to scroll through values, this is usually viewed as a significant advantage, but when compared to a larger graphical screen that displays all the values without the need to scroll or incorporate touch capability it is not as necessary. Furthermore, a touch screen eliminates the need for any buttons or control devices that causes additional difficulty when packaging.

Oppositely, touchscreen operability incurs extra costs and programming time. There is a significant increase in the complexity of the programming and the software organization. This also results in using more memory and more power when incorporated into the system. In addition, a touchscreen device is much more costly to implement than the other types of displays.

3.8 Wireless Transceivers

3.8.1 XBee

XBee radio frequency (RF) modules were used to wirelessly transmit and receive data in the system. There was need to transmit data such as voltage, current, and temperature from the charge controller to a computer which then processed, logged, and displayed the data in a useable form. Two modules were required: one transmitting at the charge controller and another receiving at a data acquisition computer.

XBee modules act as a virtual UART serial port, what one modules sends to the transmit pin shows up on the receive pin of the other. The modules run on 3.3 V logic, have a wireless data rate up to 250 Kbps and have 128-bit AES encryption for security. These devices are addressed by network ID, channel, and a 64-bit address unique to each device. Either 12 or 16 of the 16 total channels available in the 2.4 GHz frequency band can be utilized, depending on the model.

Many types of XBee modules are available with varying range, antenna type, protocol, transmitting power, form factor, and data rate. Figure 16 compares two XBee modules with similar functionalities such as data rate and range, but use two different antenna types. There are four types of antennas available in an XBee module: chip, wire whip, U.FL, and RPSMA. U.FL and RPSMA connectors both require external antennas and though they allow for increased range, the smaller footprint of the chip or wire whip antennas is more desirable. The whip antenna has a higher gain than does the chip antenna and thus the whip antenna has a greater range than the chip antenna.

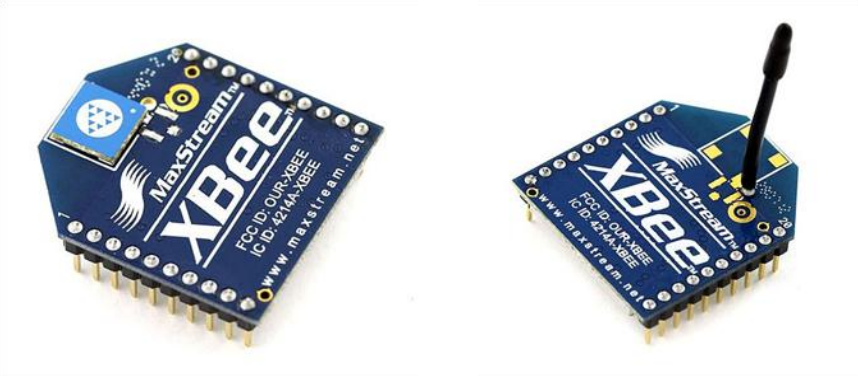

Figure 16 - XBee modules with two antenna types.
Reproduced with permission from Sparkfun Electronics.

In addition to the antenna type, the module for a desired range can be chosen. The modules come in two versions: XBee and XBee-Pro. The Pro versions have an increased range, but as a tradeoff the transmitting power is significantly higher. The ordinary XBee has an indoor range of 30 m and an outdoor range (line-of-sight range) of 90 m. In contrast, the XBee-Pro has an indoor range of 90 m and outdoor range of 1.6 km. The transmitting power is 1 mW and 63 mW respectively. [35]

XBee modules have one of two varieties of communication protocols: ZigBee and DigiMesh. ZigBee is a global standard that operates on the IEEE 802.15.4 physcal radio specification and in the 2.4 GHz and 900 MHz bands. It is designed for low-power applications such as sensor monitoring and controlling. Digi (previously MaxStream) designs and manufactures the XBee modules. In addition, they have created another wireless protocol: DigiMesh. This protocol is similar to ZigBee in that it uses the IEEE 802.15.4 and the same frequency bands, but sets up its mesh network in a different way.

The ZigBee mesh protocol utilizes three node types: coordinator, router, and end device nodes. Figure 17 shows a sample set-up of a ZigBee mesh network. The Coordinator nodes act as the central hub where information can be stored and managed. The Router nodes act as relays to End Devices. The ends of the mesh network are populated with End Devices. These are the low-power sensors and/or controllers of the network where the useful data is acquired.

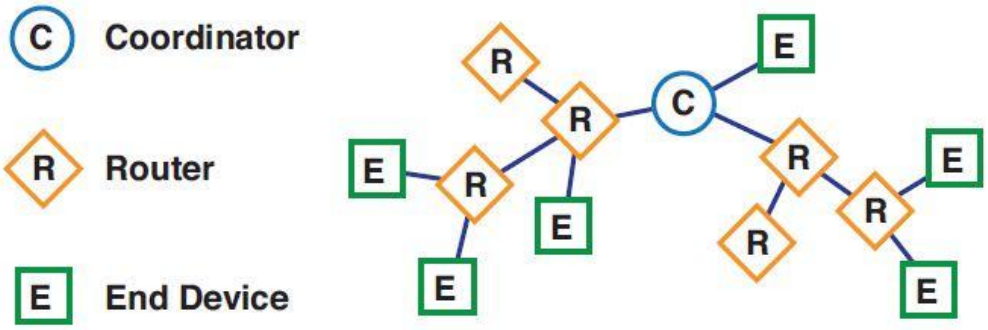

Figure 17 - ZigBee Mesh Network.
Image permission obtained from DIGI.

The alternative mesh network protocol to ZigBee is called DigiMesh. Figure 18 shows an example of a DigiMesh network. In this type of mesh, there is only one type of node: DigiMesh Node (DN). The fact that there is only one node type has many advantages. The mesh network setup is much easier, modules are easily replaced when one fails, and in the event of a module failure, other DNs compensate and route information around the damaged module (self-healing).

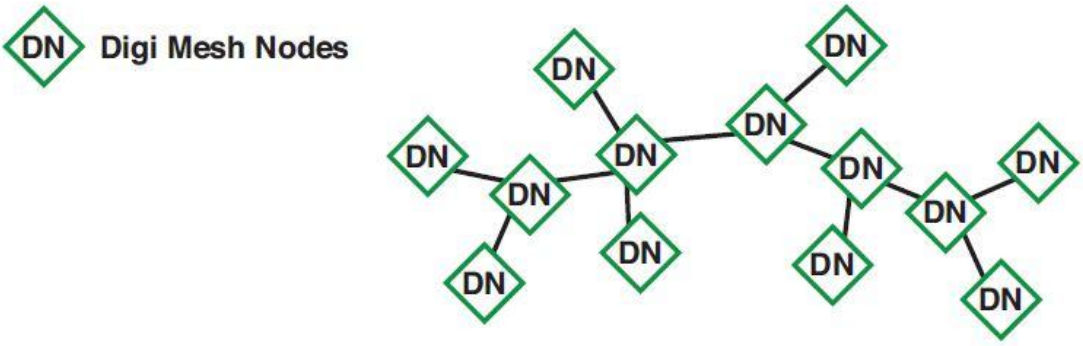

Figure 18 - DigiMesh Network.
Image permission obtained from DIGI.

As far as mesh networking is concerned, ZigBee is the better choice when there is need of interoperability with other ZigBee compliant components not made by Digi. For all other projects the DigiMesh protocol is superior in data rate, ease of setup, self-healing capability, potential for greater range, and ability for all nodes to sleep. Table 4 shows a comparison between the ZigBee Mesh and DigiMesh. [36]

	ZigBee Mesh	DigiMesh
Node Types	Coordinators, Routers, End Devices	DigiMesh Nodes
Sleeping	Only End Devices can sleep	All nodes can sleep
Range	Most Zigbee devices have range of less than 3.2 km per hop	With Digi XTend, up to 64 km for each hop
Throughput	Up to 80 bytes	Up to 256 bytes
Supported Frequencies and RF Data Rates	2.4 GHz (250 kbps), 900 MHz (40 kbps)	2.4 GHz (250 kbps), 900 MHz (10, 125, or 150 kbps)
Interoperability	Compatible with other ZigBee compliant devices	Proprietary
Addressing	MAC address (64 bit) and Network address (16 bit)	MAC address (64 bit) only

Table 4 - Comparison of ZigBee Mesh and DigiMesh. [36]

In addition to mesh networking, XBee modules also allow for point-to-point and point-to-multipoint network topologies. Point-to-multipoint communication is when a central hub can connect to numerous other devices like that of a wireless router. Point-to-point communication is another available option. This topology is exactly how it sounds: one wireless module communicating with exactly one other module. Point-to-point communication is also the easiest to set up because you are dealing with other two devices rather than many.

3.8.2 Wi-Fi Module

Another option for creating a wireless data link is using a Wi-Fi module. The RN-XV Wifly module by Roving Networks is one example of such a wireless transceiver. This module communicates using the 802.11b/g protocol and thus this device can communicate with any computer or other device equipped with a wireless card using this same protocol. In the case of XBee, it requires two microcontrollers and two XBee modules to interface with a computer, since most computers don't have an 802.15.4 wireless transceiver built in.

The data rate can be as high as 54 Mbps, which is an incredibly high speed, but this high data rate requires a high transmitting power and has a relatively short range. In PMCC, one of the crucial design goals was to have a low power (high efficiency) system, so a high transmitting power was avoided. Instead, the data rate was lowered, reducing the transmitting power. The Wifly module's transmitting power can be adjusted between 0 and 12 dBm. For PMCC, the desirable level of power would be 0 dBm, or perhaps a little higher if larger range is required. This module can be interfaced with a microcontroller using TTL UART, such as is available on the ATmega328P. The RN-XV has a built-in wire antenna and small form factor, the same footprint as an XBee module. The device also operates on secure Wi-Fi connections using WEP, WPA-PSK, and WPA2-PSK. Though wireless security is not much of an issue in solar applications, most Wi-Fi networks are encrypted and/or have password protection, which makes this feature extremely relevant. [37]

3.9 Sensors

Sensors are devices that allow a physical quantity to interact with instruments so that it can later be interpreted by a user or machine. The implementation of sensors in this project was essential to achieve the desired functionality of the system. An MPPT controller was designed to track the maximum power point produced by a solar PV panel at all times in order to use its energy generation efficiently. Unfortunately, there were several aspects that affected this energy production. The variance in temperature, weather conditions, cloudy or clear skies, light intensity and other environmental factors had a direct influence on the operating performance of the solar panel. This variance in performance was measured by the constantly changing watts of power that the solar panel delivered at a given time. An MPPT charge controller was then used to determine a real time value of the output voltage (V) and current (A) of the panel, which ultimately determined the overall output power of the system. The implementation of a voltage and a current sensor were therefore key factors of the MPPT controller that allowed it to accomplish the tracking. Another area where these sensors played a role was the detection of current and voltage of the battery.

In addition to these sensors, a temperature sensor and irradiance sensor were incorporated into the system as well. This allowed the user to have a log of the different temperatures and light intensity affecting the solar panel in relation to the output power that was delivered. Both of these sensors did not play a direct role in determining the MPP of the solar panel, but instead, they were used as an enhancement of the PMCC and also provided valuable data to the user where it could later be referenced in other applications such as research on solar power generation.

3.9.1 Temperature Sensors

In order to provide the user with information about the temperature of the solar panel, as well as the temperature of the batteries, a temperature sensor will need to be in direct physical contact with both the solar panel and battery. A reliable, inexpensive and easy to replace sensor needs to be implemented in the design so that an accurate reading of the temperature can be gathered and in case of an unexpected failure in the sensor, it should be easy to replace.

3.9.1.1 Thermocouple

As its name suggests, this temperature sensor is actually a junction of two dissimilar metals that will cause a voltage difference when the temperature is different between them. One of the two wires is at reference temperature (ambient temperature), while the other junction is at the location where the temperature is to be measured. As Figure 19 shows, the green line represents one type of metal in junction with the red line, which represents the other dissimilar metal. The small square with the arrow pointing to T°, is the junction that is in contact with the object to be measured, while the bigger square represents the temperature reference point.

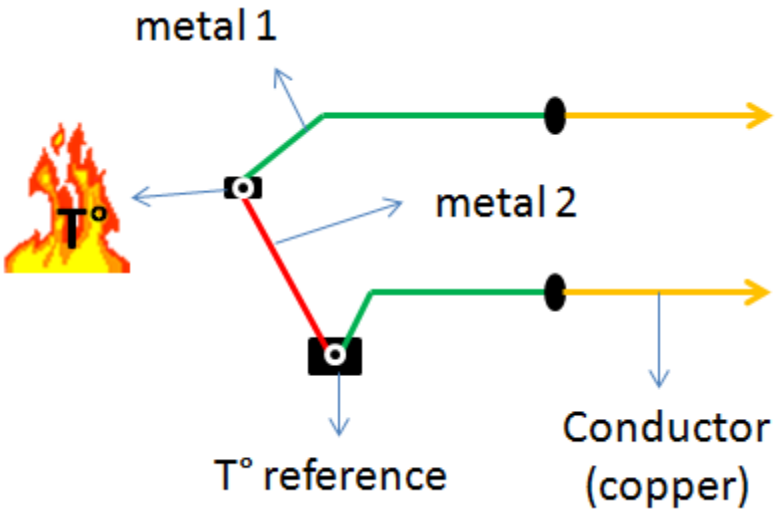

Figure 19 - Thermocouple schematic. [38]

These types of sensors are inexpensive, rugged and reliable over wide temperature range, and the output voltage is in the millivolts range. One key factor to think about when using thermocouples is that two dissimilar wires will be connected to two copper wires to integrate them in a circuit or into instrumentation. This connection will create two extra junctions (depicted by the black circles in Figure 19) that will generate a voltage difference that is temperature dependent, thus is important to make sure these connections are at some standard temperature otherwise errors in the readings may emerge. This

particular factor could potentially create a problem in the PMCC design due to the variance in temperature that a solar PV panel is subjected to by being exposed to direct sunlight. A temperature sensor that does not require a temperature reference was more suitable for this type of application. [38]

3.9.1.2 Thermistors

These are temperature sensitive resistors constructed of semiconductor material with a resistivity that is specially designed to sense temperature. Figure 20 shows a diagram of typical thermistor. Due to the properties of the material used to build these resistors, the way in which the sensor can behave can be as follows:

- Negative temperature coefficient: meaning its resistance decreases as the temperature increases
- Positive temperature coefficient: meaning its resistance increases as the temperature increases

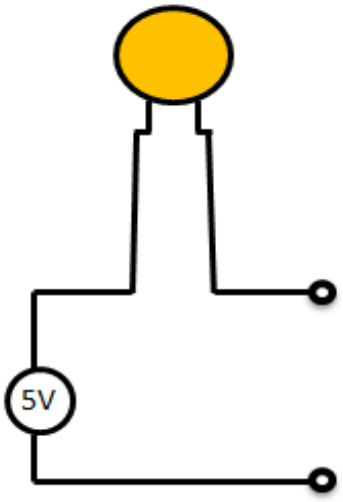

Figure 20 - Diagram of a Thermistor. [39]

These sensors are convenient because they are inexpensive, easy to implement and adaptable. They also have a reasonable output voltage compared to the millivolt outputs that thermocouples have. Because of these qualities, thermistors are widely used for simple temperature measurements but do not perform well at high temperatures. A disadvantage of this particular type of temperature sensor is that the equation used to translate the voltage output in relation to temperature adds unnecessary programming difficulties in the microcontroller and could cause potential errors in determining the actual temperature readings. [39]

3.9.1.3 LM35

The LM35 is an integrated circuit sensor produced by National Semiconductor that can measure temperature more accurately than using a thermistor. The sensor circuitry is sealed and is not subject to oxidation making it a durable sensor. The diagram of the pins is shown in Figure 21.

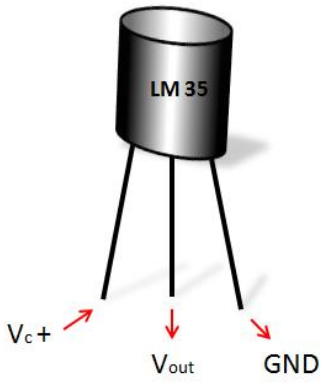

Figure 21 - LM35 Integrated Current Sensor. [40]

The LM35 measures temperature by outputting a voltage value that is proportional to the temperature in degree Celsius. This linear output voltage that it generates is higher than thermocouples and therefore no voltage amplification is generally necessary. The scale factor of the sensor is of .01V/°C. An easier way to calculate a certain temperature is by using the equation:

$$\mathrm{T(°C)} = \mathrm{Vout} * (100\ °\mathrm{C/V})$$

Where Vout represents the output voltage of the LM35 sensor which then is multiplied by 100 to represent the resulting temperature in degree Celsius. This linear scale would be perfect for the design since no conversion needs to be done which prevents errors in the calculations. The sensor itself does not require any external calibration or trimming and maintains an accuracy of +/-0.4 °C at room temperature and +/- 0.8 °C over a range of 0 °C to +100°C. Power consumption by the sensor from its source is extremely low, as little as 60 micro amps, and possesses a low self-heating capability. The sensor self-heating causes less than 0.1 °C temperature rise in still air. Unfortunately, there were limited number of analog pins in the micro controller, therefore a different sensor was implemented [40]

3.9.1.4 DS1624 Digital Thermometer

The Maxim DS1624 is a digital thermometer sensor that is extremely easy to implement in a system that requires temperature readings. The senor does not

require any external components and can be integrated directly with a micro controller via the pins described in Figure 22. The sensor is composed of a V_{DD} and GND pin, which is standard in most chips as the powering pin and ground pin respectively. The DS1624 digital thermometer communicated with the microcontroller using an I^2C-Bus. This method was designed by Philips to allow easy communication between components that reside on the same circuit board. In this case the pins that served this purpose are Pins 1 and 2, SDA and SCL respectively, which sent data back and forth. SDA, which stands for Serial-Data, is the actual pin where data regarding the temperature was sent to the microcontroller once this information has been requested. The microcontroller makes the request for this information through this same pin. The Serial-Clock (SCL) is the pin that is responsible for clocking in and out the data that is sent through the SDA pin. In this manner, no outgoing data interfere with incoming data and vice versa. The I^2C bus allows multiple devices to be connected to a single bus, without having to use multiple pins in a microcontroller, a feature that the other temperature sensors discussed did not have.

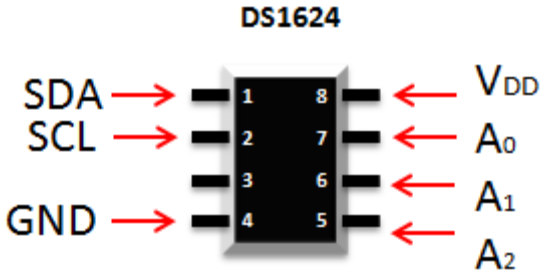

Figure 22 - DS1624 Digital Thermometer Pinout. [41]

The method used to access a specific device from the different devices connected to the same bus is to send the address and later send the request. The DS1624 Thermometer came built in with a unique 4 bit device code; this code distinguishes the device from others connected to the same bus. In addition to the 4 bit device code the chip possesses three pins, A0, A1, and A2, as shown in Figure 22, which correspond to pin 7, 6 and 5 respectively. Each of these pins corresponds to a 1 bit chip address input. Meaning, any desired 3 bit address can be assigned to the chip by combining these three pins. In this manner, multiple chips (up to eight) with the same device code were used in the same bus without any interference. One example would be setting all three pins to ground, implying the 000 address.

Aside from the benefit of bus transmission, the sensor is able to operate under a wide temperature range of +125°C to –55°C. This guaranteed that the sensors would keep providing information about the temperature even in extreme weather conditions. [41]

3.9.2 Voltage Sensor

As it name suggests, this sensor was responsible for calculating the voltage of the operating solar PV panel in real-time. In order to monitor and calculate the voltage output, the properties of a voltage divider circuit configuration were used. Two resistors (R1 and R2) were placed in series with each other and in parallel with the PV panel. The values given to the resistors were determined by the power specifications of the solar panel (75W) and the input specifications of the microcontroller ports. Basically, R1 had high resistance value. This high resistance value kept the sensor circuit from receiving high flows of current, which would result in energy loss and could potentially damage the circuit. The voltage across R2, denoted as V2, is the output voltage that was monitored to detect any variance in the voltage generated by the panel.

Before feeding this analog voltage into the microcontroller, it needed to go through some filtering to maintain an accurate reading. V2 was first fed into a filtering capacitor in order to smooth the output reading and prevent noise spikes in the signal resulting in false readings. Once the signal has gone through the filtering capacitor, it was finally fed into the Analog pin in the microcontroller where it was later implemented in the algorithm used to find the MPP.

The same concept and design was applied when keeping track of the voltage of batteries. The resistor values were altered according to the specifications of the battery. [42]

3.9.3 Current Sensor

The use of a current sensor was essential in the design in order to get the maximum power output from the solar panel array. The electric sensor was in charge of keeping track of the current that the panel outputs at all times. These readings were fed into the microcontroller in order to provide the user with real-time values of the current by displaying them on the LCD screen. Most importantly, the current sensor played a significant role in the realization of the MPPT in order to achieve the maximum output power from the panel. Two possible sensors were identified for the design; one was an AD8215 current shunt monitor from Analog Devices and the other was an ACS712 current sensor produced by Allegro Microsystems.

3.9.3.1 ACS712 Current Sensor

The ACS712 is a very cheap, accurate and easy to implement electric sensor chip available from Allegro Microsystems. It is a fully integrated current sensor that gave precise current measurement for both AC and DC signals. The great precision and accuracy of the sensor was due to factory trimming. The IC was an surface mount device (SMD) as shown in Figure 23.

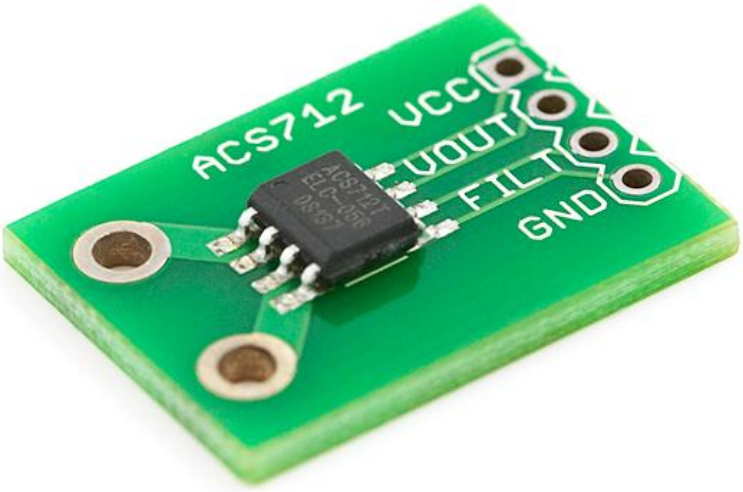

Figure 23 - ACS712 Current Sensor.
Reproduced with permission from Sparkfun Electronics.

The thick copper conductor and the traces allowed the device to support up to five times the amount of current without damaging the unit. The sensor required a DC voltage of 5 volts for the V_{CC} in order to operate. As well as with the other sensors, in order to keep it at an optimal accuracy, the integration of filters was recommended, so that the noise signals coming from the supplied 5 V do not impact the current readings from the sensor.

The device bandwidth can be easily set via the “FILTER” pin as shown in Figure 23. The output voltage that was delivered by the sensor is proportional to the AC or DC current depending on which is being measured. The sensor utilized a very precise, low-offset, linear Hall sensor circuit with a copper conduction path located near the surface of the die. When current was applied through this copper conduction path, the flow of current generates a magnetic field that is sensed by the integrated Hall IC and then converts that magnetic field into a proportional voltage. The accurated readings were achieved in the device by the close proximity of the magnetic signal to the Hall transducer. The output generated by the sensor has a positive slope when the current that is flowing through the current sensor pins is increasing. This conductive path has a 1.2 mΩ typical, which helps providing low power loss is the sensor. [43]

3.9.3.2 Current Shunt Monitor

AD8215 current shunt monitor from Analog Devices could’ve been implemented into the circuit using a design that is similar to the voltage sensor. In order to do so, a shunt resistor, or a resistor with a very low resistance value (around the milli-ohms), would’ve been placed in series with the PV panel as shown in Figure

24. The voltage across (a very small voltage) this resistor would be fed into a current sensor (AD8215) where it would monitor the voltage and then it would amplified about 20 times. Knowing the shunt resistor value and the voltage across it the value of the current could have been determined.

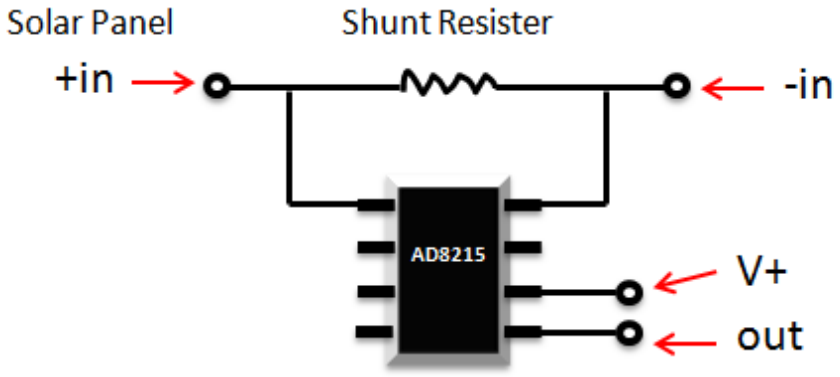

Figure 24 - AD8215 Current Shunt Monitor. [42]

Once the voltage has passed through the chip, its voltage output would have been fed into a unity amplifier or voltage follower to isolate the voltage and it is later fed into a low-pass filter to attenuate any noise spikes and it is ultimately connected into the A-to-D converter of the microcontroller for further use in the MPPT of the system. Once again, this same design and method could've also been applied to monitor the current coming from the battery. [44]

3.9.4 Irradiance Sensor

In order for light to reach the surface of the earth, it has to travel across a very thick atmosphere that is filled with different types of gases. During rainy or cloudy days, it becomes even harder for light to penetrate these barriers and make its way in. Considering that light is the fuel of this system, all of these physical and environmental factors that prevent light from reaching the solar panel would have an enormous impact in the overall performance of the PMCC. The intensity of light on a given day is extremely important for the project since this is the primary factor that will drive the energy production in the solar panel.

An irradiance sensor is the piece of technology that measures the intensity of light, and therefore helped the PMCC keep track of the amount of sunlight present when it is operating. By implementing this piece of technology in the PMCC, the user had the opportunity to use the system in more broad way. Not only did the system was able to power small appliances off the grid but it could also be used as a research tool. With the implementation of temperature sensors and irradiance sensor, the user now had more access to information that is relevant to the power output that is receiving from the system.

An irradiance sensor that is commonly used in industry with great results is the Texas Instruments TSL235 light-to-frequency converter. This sensor combines a

silicon photodiode and a current-to-frequency converter on a single monolithic CMOS integrated circuit. As light hits the silicone photodiode, it excites the electrons and generates a current flow that is later translated into a frequency that can be use in the microcontroller for further analysis and applications. The sensor encompasses three different pins. Pin 1, which is the ground pin (GND), pin 2, which is the input voltage pin V_{DD}, and finally, pin 3, which is the output in frequency.

The optimal operating input voltage is a value between 2.7 to 6 V max, though the recommended voltage is of 5 V. The output that is generated by this sensor is a square wave with a 50% duty cycle. As its name suggests, the light intensity, measured in μW/cm^2 is directly proportional to the output frequency. The reason the output of the TSL235 is frequency instead of voltage is due to the large amount of variance the intensity of light can have. Having a million steps of precision in a range of 0 to 5 volts is not going to prove efficient. Instead by using frequency more steps of precision were achieved since this will vary from a fraction of a hertz to the megahertz. [46]

Figure 25 shows the output frequency of the sensor vs. the irradiance. In that particular graph, the optimal input voltage of 5V has been fed into the input pin of the sensor; a λ = 6 nm wavelength has been used for the test and finally the ambient temperature (T_A) is 25° C. Due to the sensitivity of the sensor, it was necessary to include a decoupling capacitor in the design in order to have a more accurate measurement of light. The value of the decoupling capacitor was within the microfarad value; this helped attenuate the noise generated by the voltage being supplied to the sensor. In essence, the decoupling capacitor served as a low pass filter that enabled the generated signal to be more clear and accurate.

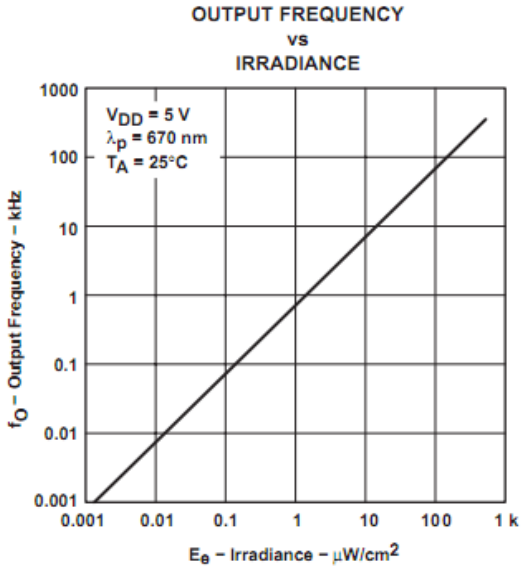

Figure 25 - Output Frequency vs. Irradiance Graph.
Permission obtained from Texas Instruments.

Another advantage of the TSL235 is that it is TTL compatible. This allowed the output of the sensor to have a direct interface with the microcontroller without the need of converting the output signal to other forms of message. The sensor has also been temperature compensated for the ultra-violet visible light in the range of 300 nm to 700 nm and also responds over the light range of 300 nm to 1100 nm.

Having the system integrated with sensors that can bring the user valuable information about the light intensity during the day, the temperature in the solar panel, all while sensing and monitoring the current and voltage that is being produced in the solar panel has an extremely valuable impact on the research side of the project. All of this information was later combined into a data log where it was later compared and correlated with the energy production in the system and helped find ways to improve the system by making it more energy efficient. [46]

3.10 Batteries

Batteries are divided into two main categories: primary (disposable) and secondary (rechargeable). Today, rechargeable batteries make up over 75% of the global battery market. Within each of these categories are a plethora of chemistries to choose from, each with certain advantages and disadvantages. The most prevalent materials used in batteries today are lithium, lead, and nickel. In addition to battery chemistry, a battery is rated with the following attributes: voltage, capacity in ampere-hours (Ah), cold cranking amps (CCA), specific energy, specific power, and C-rate.

Primary batteries have higher energy densities than secondary and are typically used when recharging is unfeasible. Lithium-metal and alkaline are among the most common primary battery types and are found in numerous applications from remote controls, watches, and toys, to name a few. However, off-the-grid photovoltaic systems require recharging so the focus was on secondary battery types.

Some of the chemistries used in secondary batteries are: lead-acid, nickel-cadmium (NiCd), nickel-metal-hydride (NiMH), and lithium-ion. NiCd batteries are an old and mature technology but are being replaced due to the environmental concerns associated with cadmium. Since cadmium is a toxic metal, it cannot be disposed of in a normal landfill and should instead be recycled. NiMH batteries offer some of the advantages of NiCd but without the adverse environmental effects. Even still, the NiMH battery today has only a small share of the global battery market because it is not as cheap as lead-acid nor as energy dense as lithium-ion chemistries. Thus for PMCC, the research focus was on the two most prevalent battery technologies: lead-acid and lithium-ion. [47]

3.10.1 Lead-Acid Batteries

Though numerous rechargeable batteries exist, the most commonly used battery in PV systems is the deep-cycle lead-acid battery. This is mainly because of the price to power ratio is superior to all other types and due to the fact that this is a proven technology.

There are three types of lead-acid batteries: starting, deep-cycle, and marine. The starting lead-acid is a typical automotive battery used to start a car. This type of battery has many thin plates of lead (high surface area) which allows for a high current output. These batteries are great for applications where a large current is needed for a very short time, but for deep-cycle applications this type of battery has a very short lifespan. The deep-cycle lead-acid battery has thicker lead plates which allow this type of battery to be discharged and recharged many times without degradation. One drawback is the fact that there is lower surface area between the lead plates and the acid electrolyte meaning smaller current. Though the deep-cycle lead-acid is designed to be discharged to 20% capacity, the battery will last longer if the charge never falls below 50%. A marine lead-acid battery falls somewhere in between the automotive and deep-cycle. The lead plates are thinner than deep-cycle yet thicker than a starting battery which gives it better current output and shorter lifetime when used in deep-cycle applications. [48]

In the domain of deep-cycle lead-acid batteries there are three types of battery construction: flooded, gel, and absorbed glass mat (AGM). Flooded lead acids are the cheapest and most common construction type. The electrolyte in this type of battery (30% sulfuric acid, 70% water) is in a liquid form. This allows for spilling and evaporation of the electrolyte, which shortens lifetime and is dangerous. The gel type batteries use a thickening agent to hold the electrolyte in place. This prevents leakage in the event that the case is damaged. This type of battery is sealed, which means that in the event that a significant amount of electrolyte is evaporated, it cannot be re-filled.

Absorbed glass mat lead-acid batteries are by far the most advantageous of the three types of construction. AGMs have Boron-Silicate fibers embedded in the electrolyte which prevents leakage even if the case is breached. In addition, the fact that this type of battery is sealed and pressurized forces Hydrogen and Oxygen to recombine into water while charging, thus greatly reducing water lost due to evaporation. They have a very slow self-discharge rate and are resistant to shock and vibration damage. The main disadvantage to AGMs is that they usually cost two to three times that of a flooded lead-acid of the same capacity. [47]

3.10.2 Lithium-ion Batteries

Li-ion batteries offer some of the highest energy densities as well as the lowest weight of all battery chemistries and constitute over one-third of the global market. They have a high cell voltage, low self-discharge rate, fast charging rate, and relatively good lifetime when deep-cycled. The two limiting factors afflicting Li-ion are cost and safety. Li-ion batteries tend to have one of the highest cost-per-watt ratios, much higher than lead-acid chemistries. In addition, it is imperative to build protection circuitry into the battery pack so that thermal runaway does not cause the battery to light on fire and/or explode. Lithium is also highly reactive with water so care must always be taken to not overexpose these batteries to water.

Rechargeable lithium batteries all use lithium ions to store the energy by the migration of these ions from the cathode to the anode. During discharge the anode undergoes an oxidation reaction which frees electrons to conduct current (do work) in an external circuit while the cathode undergoes a reduction reaction (gaining of electrons). The cathode is made up of a lithium-metal-oxide and the anode is made of graphite (porous carbon). Some common cathodes used in Li-ion batteries are: lithium-cobalt, lithium-manganese, lithium phosphate, and lithium-nickel-manganese-cobalt. The different cathodes offer differing levels of safety, specific energy, lifetime, and cost. Most of these Li-ion batteries use a liquid electrolyte to carry charge between the anode and cathode, but some use a polymer with a gelled electrolyte. These lithium-polymer batteries offer a slight advantage to liquid electrolyte types by the fact that there is no need for a rigid case, and thus can be made smaller, lighter, and more flexible. [47]

3.11 Battery Charging Algorithms

Though the specific charging algorithms for each battery chemistry are different, they all have the same general charge stages in common. In the first stage, called *bulk charging,* a constant current is applied to the battery. The charging voltage can range from about 11V to 15V (for a 12V battery), the only requirement being that the charging voltage must be set higher than the current battery voltage. Bulk charging is the stage used for a completely discharged battery to around 80 – 90% capacity. In PMCC, the battery bank used a 12V nominal battery voltage. A typical battery can be considered “fully discharged” when the voltage reaches 10.5V. At this time, little power can be extracted from the battery and discharging below this level can permanently ruin a battery. The MPPT charge controller contributed to improved efficiency of PMCC primarily in the bulk charging stage.

The second stage, called *absorption charging*, begins immediately after the bulk charging stage (when the battery voltage reaches a pre-determined limit). In this stage, the charging voltage is held at a constant value and current decreases as the internal resistance of the battery increases. As the battery reaches full

capacity, the current tapers off due to the increased internal resistance. When the current drops below a certain level, typically 0.5% of the battery's rated capacity (.05A for a 10Ah battery), it is considered fully charged.

The final stage in a typical three-stage charging process is called the *float charging* stage. In this stage the charging voltage is set to a constant value but at a lower level than the absorption stage. The float stage compensates for self-discharge, or gradual loss of voltage (power) over time, which plagues all battery chemistries. This stage maintains full charge by "topping off" the battery, keeping it at 100% capacity.

One crucial parameter to battery charging is temperature. The temperature should be monitored and charge voltage and current values should take the temperature into account. High current and environmental factors can cause battery temperature to rise and voltage decreases with increased battery temperature. The algorithms executed by the microcontroller factored in battery temperature when calculating current and voltage values to both maximize efficiency and provide emergency cutoff in the event that the temperature reaches an unsafe level. [48]

3.11.1 Lead-Acid Charging

Charging a lead-acid battery is best done using a three-stage process, shown graphically in Figure 26. The first stage is a constant current stage. For the 12V nominal battery bank, which was utilized in PMCC, a voltage between 11V and 15V were optimal. The exact voltage was found by using the MPPT algorithm to track the maximum power point. The corresponding current and voltage was then set at this MPP so that the most power was delivered to the battery during this bulk charging phase. When the battery reaches 80% capacity, each cell has a voltage of about 2.07 V while the entire battery has a voltage of approximately 12.42V. When this voltage level is reached, the next stage of the charging process takes over: the topping charge (absorption) stage. [47]

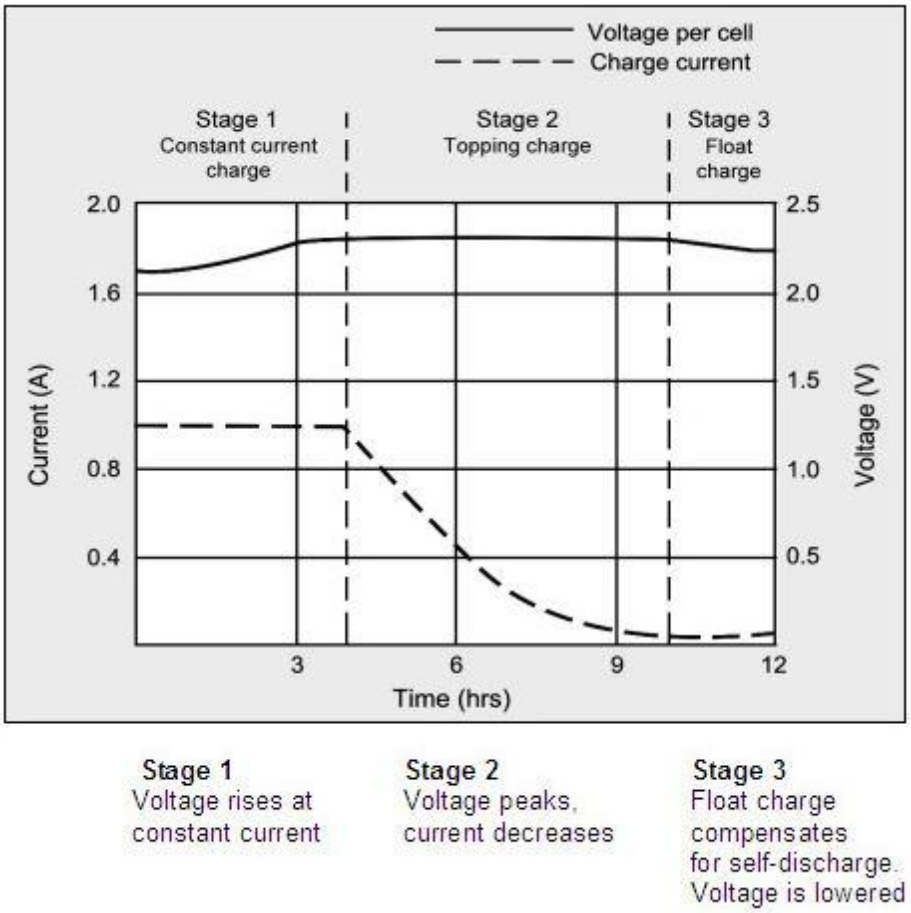

Figure 26 - Charging diagram for a typical lead-acid battery.
Image permission obtained from Battery University.

The topping charge phase sets a constant voltage instead of using a constant current. In this stage, the voltage per cell should be set to 2.385V which is around 14.3V for a 12V nominal battery at a temperature of 25°C. This voltage value is held until the current drops to a value of 0.5% of the battery capacity. At this point, the third and final stage of the charging algorithm commences: the floating charge stage. In this stage, the voltage is again set to a constant value, but is set to a value lower than used in the absorption phase. The voltage in this stage is set to around 13.3V at a battery temperature of 25°C for a 12V lead-acid battery. The float charge stage offsets the losses due to self-discharge, maintaining the battery at full charge.

Lead-acid batteries are sluggish to charge, usually taking between 12 and 16 hours to reach 100% capacity. This is, in reality, not such a bad thing for solar cell applications. The sun usually shines for many hours during a given day, delivering power at a rate that is slow enough to allow efficient charging of lead-acid batteries. Lead-acid batteries also have a high overcharge tolerance compared to lithium-ion. For instance, a lead-acid left at an “absorption level” voltage (~14.3V) for extended periods of time after reaching full charge will not destroy the battery like it would in Li-ion chemistry. [47]

3.11.2 Lithium-Ion Charging

Lithium-ion charging is similar to the lead-acid charging algorithm, but differs mainly in cell voltage and float charge. Figure 27 shows the stages in a lithium-ion charging process. The first stage in the process is a constant current stage. Here the voltage rises to a pre-determined level and then a constant charging voltage of about 4.4V is applied to the battery. A lithium-ion cell (nominal cell voltage 3.7V) has about 4.2V when fully charged. When this level is reached, charge should terminate, because Li-ion batteries do not tolerate a “float charge” well. If not used for a while, the Li-ion will self-discharge and will need to be topped off periodically to keep the battery at 100%.

Lithium-ion batteries can be charged much faster than can lead-acid batteries, typically being charged between 0.5 and 1 C. This means that a Li-ion can be charged in about one or two hours, much faster than the charge time of a lead-acid battery. Lithium-ion batteries are about 97 to 99% efficient in charging and stay relatively cool during the charge process. If a Li-ion battery is overcharged, then the production of CO_2 will begin and raise the pressure in the cell. If this pressure gets high enough, the cell will burst and vent out a flame and/or explode. Over discharging lithium-ion batteries is also not advised. If the cell voltage falls much below 3.0 V then the battery might become permanently dead so protection circuitry tries to shut off all current output when the cell voltage reaches around 3 V. [47]

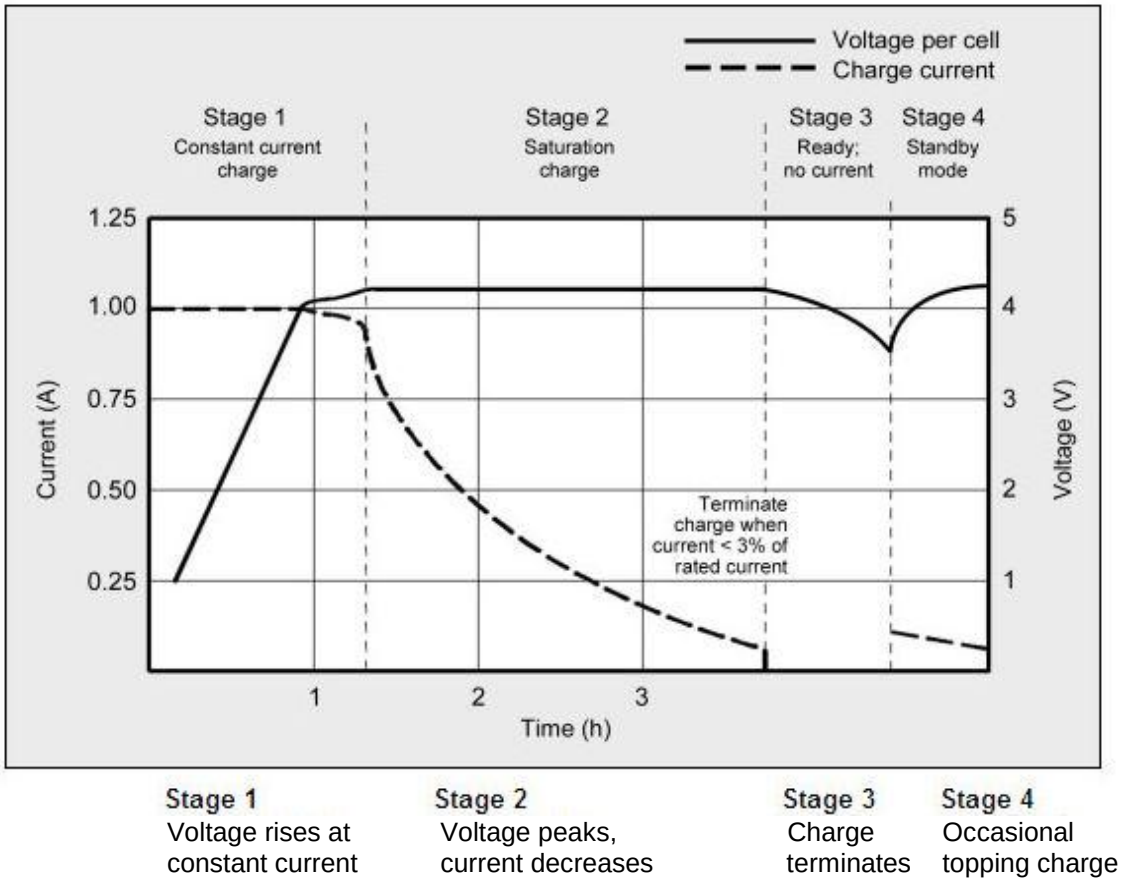

Figure 27 - Lithium-Ion Charging Diagram.
Permission obtained from Battery University.

3.12 Inverter and Power Distribution

Cell phones, PDAs, and MP3 players etc. are low-power devices that can run on DC power. Their power consumption is easily met by today's standard cigarette car plugs, which usually support up to 400 Watts of DC power. Now, for more demanding equipment such as household appliances, AC power is required and is more complicated when they are used off the grid.

With the fact that some of these devices use DC power while others are designed to take AC power from a regular wall outlet, this off the grid system is able to delivery both types of power to the end user to satisfy its needs.

3.12.1 Why an Inverter

An inverter enabled the system to deliver both the necessarily and correct energy to power the desired electronics. It was the final piece of equipment in the power distribution process, accomplishing the goal of powering small electronic devices off of the grid.

The main function of an Inverter is to convert direct current (DC) into alternating current (AC), the type that comes out of a wall outlet to power larger electronics in a house. In this particular system, the DC power was stored in one battery, and supplied the inverter with power using cables. Due to the high amperage that to runs through the connections, cables with a high enough rating were used.

3.12.2 Features of an Inverter

Even though, there are many kinds of inverters out there in the market, there are many things to be considered when buying one. There are four main features to look at when purchasing an inverter:

- Voltage of the Inverter: One of the first things to consider when buying an inverter is to look at the power sources to be use. It is extremely important to match the voltage rating of the inverter with that of the power source. If a 24 V battery were chosen, then a 24 V Inverter would be the appropriate one to buy. This guarantees that the inverter has been designed to support a power source of that specific voltage rating and will prevent a potential threat of catching on fire.

- Devices to be Powered: Another important thing to look at is what type of equipment the system is going to be powering. For this particular system, it was determined that the devices used should not exceed 600 W individually or combined. This means that the wattage in an inverter suitable for this specific job must exceed all the wattage required by the devices planned to be used.

- Peak or Surge: The peak rating or surge is the initial amount of power that is required to first power up a device. This phenomenon can be appreciated when a refrigerator turns back on and momentarily dims the lights in the house. This initial start up of the equipment draws high-energy consumption. Typically small appliances have small peak rating, and this information should be listed on the device's label. It is important to be aware of the peak rating in the inverter so that it can deliver the initial power necessary to power on a device.

- Wave output: The main function of the inverter is to take a continuous flow of current from a power source (DC), increases its voltage, and then change it to an alternating current source before sending it out to power a device. AC that comes out of a wall outlet if put through an oscilloscope displays a nice and smooth sine wave form, while on the other hand, the AC that comes out of an inverter will have a square wave form. This will not become a problem if trying to make coffee or powering a simple electric motor. The problem arises when the device to be powered is inherently sensitive to the signal produced by an AC wave. These devices typically receive or broadcast some kind of signal, such as audio or video

equipment. Navigation devices or sensitive scientific equipment are also likely to encounter problems, such as lines on a television screen or a steady buzz or hum. Cleaning up this square waveform to accomplish a smoother sine wave requires a series of filters, inductors and capacitors. Inexpensive inverters have little or no filtering, intermediate inverters output a “modified sine wave” and expensive inverters with a “perfect sine” range up to thousands of dollars and can virtually produce an even smoother sine wave than the one coming out from a utility company. For the scope of this project, a “modified sine wave” inverter was chosen, since the goal was be able to power up every day non-sophisticated or sensitive electronics.

3.12.2.1 Brand Comparison

Two brands of inverters were investigated for the process of incorporating it into the PMCC project. The Power Bright PW 1500 inverter and the Cobra CPI 800W power inverter. Both inverters have been widely implemented in off the grid solar power systems with the purpose of powering small appliances, and have proven to function in a successful manner. The main difference came when comparing the user interface and power. [49,50]

- One brand can deliver a continuous max power output of 1500 W for a period of one hour. This is sufficient to be able to power up small appliances such as: toaster ovens, coffee makers, and small microwave ovens. While the Cobra CPI 800 can deliver a max power of 800W for a period of one hour.
- They are both design to support a voltage source rating of 12 V.
- The Power Bright support a peak surge rating of 3000 W, which is important for appliances with a higher energy demand during their initial start up.
- The final AC voltage delivered by either of the two inverters is in the range of 110V to 120V, the necessary voltage to power up devices that require regular power from a wall outlet.
- Finally, both inverters produce a “moderate sine wave” output. Like mentioned before, this characteristic of the inverter is not essential in the scope of this project due to the type of electronics that are to be use by the end user.

3.12.2.2 Inverter Interface

When looking at the interface of both inverters, the Cobra definitely stood out over the Power Bright PW1500 inverter. Figure 28 shows the interface of the Power Bright PW1500 inverter. It possesses a dual 3-prong Ac outlet, next to an O/I switch to power on or off the electronics. It also contains a digital display with a display switch that enables the user to switch the display information from DC

voltage to AC watts. Finally, it includes an overload LED indicator that warns the user if a continuous power draw exceeds the 1500 watts. This LED will light up orange or red and will automatically shut down the inverter. [49]

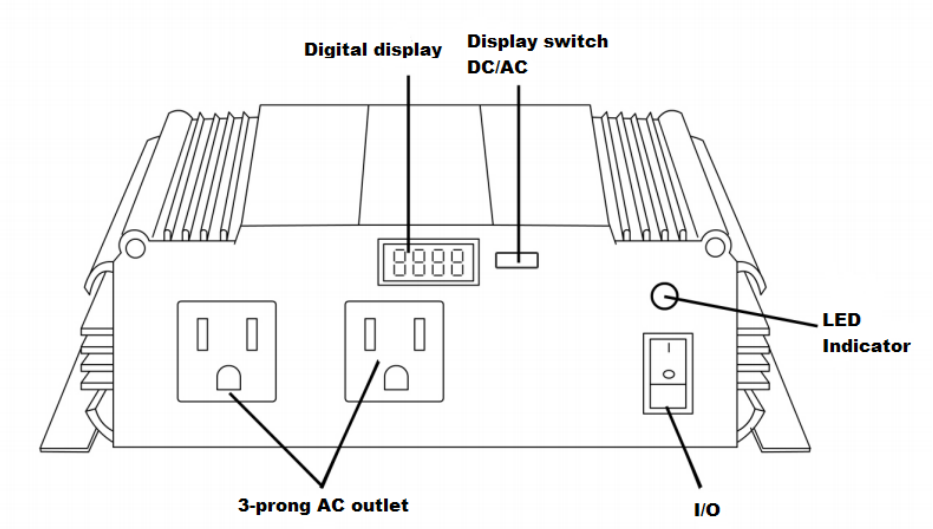

Figure 28 - Power Bright PW 1500 Inverter.
Permission obtained from Power Bright.

The Cobra model in Figure 29, possesses two 3-prong AC outlets, same as the Power bright inverter. Having multiple prongs enables the end user to get more things done by powering up multiple appliances at the same time. It also came with an incorporated USB port. As mentioned before, the goal of this system was for the end user to be able to not only power up AC devices, but also enable the system to connect to small gadgets. This 5 V USB port is ideal to power up small gadgets such as iPods, cell phones, mp3 players, etc.

The inverter also comes incorporated with power indicators that warn the user about the unit's power status and alarms for conditions that could cause it to shut down. [50]

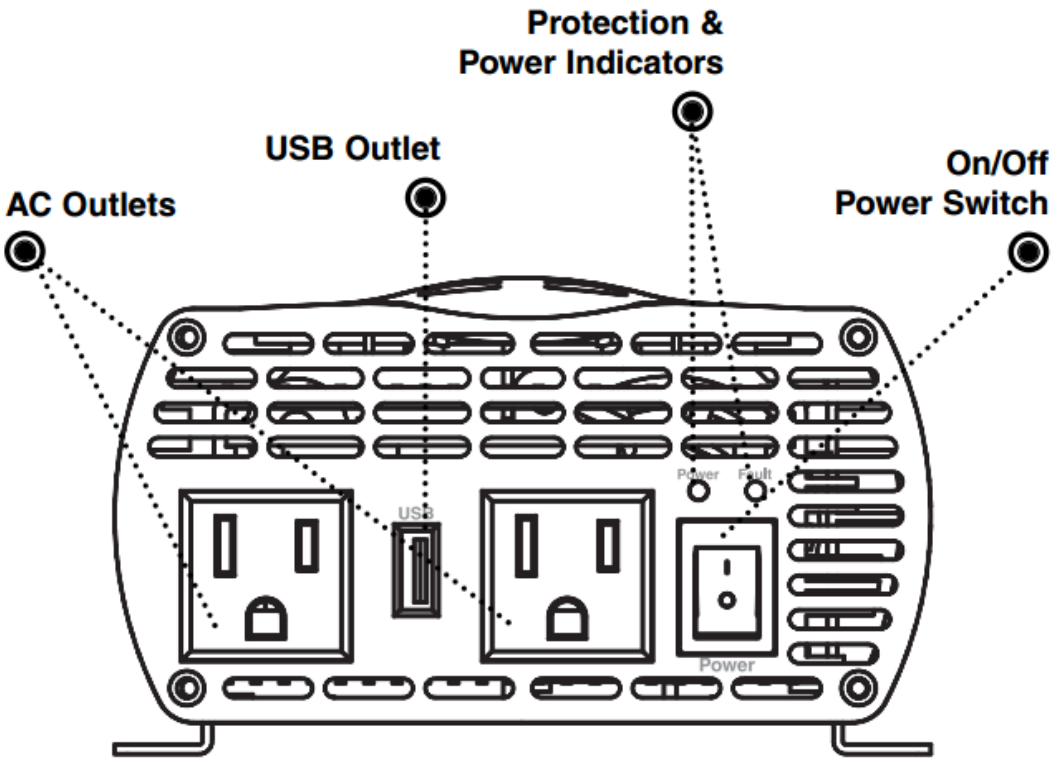

Figure 29 - Cobra CPI 800 Watt Power Inverter.
Permission obtained from Cobra.

Another great characteristic of the Cobra CPI Power Inverter is the built in Power indicators that will help keep the user informed of the status of the inverter while in operation. This inverter comes equipped with indicators that will help the user stay inform of potential malfunctioning and conditions that the equipment may be going through at some point during operations. The power and protection indicators include a green light, a red light and an alarm.

- Current Overload Protection - If at some point the loads that are connected to the inverter exceed the maximum load of 800 watts, this will automatically cause the power source to deliver a higher amount of current to the inverter in order to satisfy the power demand. If this scenario occurs, this will cause the inverter to overload and the inverter will automatically shut down to protect itself from any possible damage. There would be a momentary turn on of the red light. The inverter will continue to check for the current level in order to resume operation.

- DC input voltage shortage - The inverter as a warning will sound its internal alarm whenever the DC input delivered by the power supply drops below 10.5 volts. This is not the minimum required input voltage that the inverter requires to operate, but instead, it is an advance warning that the inverter gives to inform the user that it is close to reaching the minimum required input voltage

to operate. This scenario will typically take place when the battery that is supplying the energy to the inverter is close to being completely discharged. Another, possible scenario is if the cables used are not adequate for this type of use or they have not been connected correctly. These problems will cause the system to suffer an excessive voltage drop, therefore the inverter may shut down when drawing higher currents because the voltage at the inverter may have dropped below 10 volts. The inverter will detect the low input voltage and will respond with the sound of an alarm. At this point, the unit will keep operating until the input voltage drops to 10.0 V or less. If this voltage is ever reached, the inverter will shut down automatically to protect itself and the red light will turn on. The inverter will keep checking the input voltage until the voltage level reaches an appropriate level and then it will restart the load.

- DC input voltage overload – The inverter will detect a high voltage whenever the voltage supplied by the power source rises above 15 volts. This can occur if two batteries are connected in series instead of parallel. Another possible cause could be the use of a battery that has a voltage rating that is higher than 12 V while this inverter only supports 12 V batteries. If for any reason the DC input voltage rises above 15.0V, the inverter will automatically shut down to protect itself from any internal circuit damage and the red light will turn on to indicate voltage overload. At this point the inverter will continue to check the levels of the input voltage and once this have come back to normal the inverter will resume work.

- Temperature Overload – As its name suggest, temperature overload will trigger in the inverter whenever the internal temperature rises above the alarm threshold. This increase in temperature would typically occur if the equipment is operated in a high heat environment. Another possible cause would be if the fans or vents were being blocked during operation. This would prevent air from flowing into the unit, and therefore proper ventilation would not be achieved. If this were to occur, the red light in the inverter will start to blink and the inverter will shut down. This usually will occur when internal temperature in the inverter continues to increase up to 40ºC (104ºF). By shutting itself down automatically the inverter will protect itself and prevent any potential fires. In order to restore the inverter back to normal, it is necessary to turn the unit off and allow it to properly cool down until it has reach a normal operational temperature. Once it has reach an operational temperature the inverter will automatically return to normal operation after it has been turned back on. [50]

3.12.3 Batteries to Inverter

Power wires and wiring are very important factors to consider in the performance of the inverter. Connecting a cable from a battery source to the back inputs of an inverter may seem as an easy task, but there are many things to consider when doing this. Due to the characteristic of the inverter (low voltage and high current

input) low resistance wiring is essential between the battery and inverter. Figure 30 shows the two batteries connected in parallel to maintain the desire 12 V output. If the end user were to use the entire 800W that the inverter can deliver, it would mean that 120 V of power are going to be supplied at 6.7 amperes of current. On the other hand, the batteries will have to deliver 800 W of power to the inverter in order to supply the energy in demand. With the fact that the batteries can deliver a voltage of 12 V, in order to achieve the 800 W of power in demand, a current of 66.7A would have to run through a cable from the batteries into the inverter. [51]

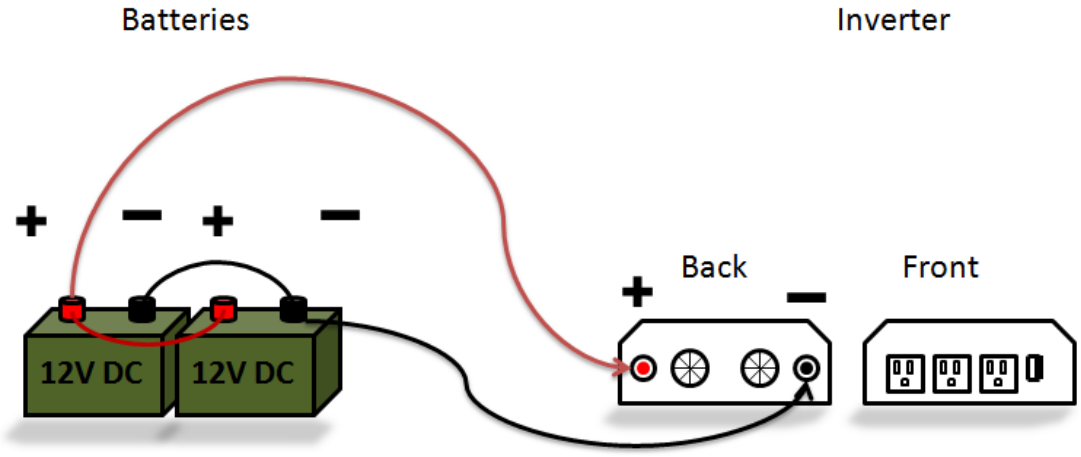

$$Pin = 800\ w \qquad Pout = 800\ w$$
$$Vin = 12\ v \qquad Vout = 120\ v$$
$$Iin = \frac{800}{12} = 66.7\ A \qquad Iout = \frac{800}{120} v$$

Figure 30 – Connecting batteries to inverter.

In order to keep the power loss to the minimum and the amount of energy deliver to the load at its maximum, the use of copper wire was used in the design opposed to aluminum wires. Aluminum wires have about one-third more resistance than copper wire of the same size. The cables were also relatively short and thick as possible, reducing the voltage drop between the power source and the inverter. These characteristics in the cable have a great impact in the overall performance of the system and prevent the inverter from shutting down due to low voltage input; improving the design efficiency.

3.12.4 Fuses and Fuse Holder

Fuses are a great piece of technology that helps protect electrical equipment from being blown up due to extremely high flows of current. The implementation

of fuses was decided as an extra precaution to protect the circuit from higher amperage that might be experience from over loads or currents being fed back into the circuit from the battery. The electric fuses of Figure 31 were placed in both the input and output of the panel. These fuses support the current flow of up to 10 amps. This value is the maximum allowed current in the circuit itself. Having a high current value does not interfere with the operational performance of the inverter and nor will allow it to go beyond its safe performance. [52]

Figure 31 - 10 A Fuse and Fuse Holder.
Permission from Digikey.

4. Design

4.1 Solar Panel

Although there are many options for solar panel technologies, it was quite clear that the main candidate for this project was the mono-crystalline panel. Polycrystalline silicon panels are not far behind in efficiency but they are not much cheaper than mono-crystalline panels. The small savings in initial cost does not cover the savings in energy cost through the lifetime of the panel use. CdTe and thin film or amorphous silicon modules were ruled out for their inferior efficiencies. CIGS and GaAs panels were ruled out due to their expensive price and availability, even though they would be a front-runner considering their good performance at higher temperatures. The main company considered in the solar panel market was SunWize. The panel that was chosen for use in this project is the SunWize SW120. It is the highest power output panel in the SW mono-crystalline series as seen from comparison Table 5. Another advantage in choosing this specific panel is the price point. Solar Sphere offers this panel close to $500 below its $870 manufacturer suggested retail price.

Model	Power (Watts)	Voltage (Vmp)	Current (Imp)	Voc	Isc	Dimension (Inches)	Weight (lbs)
SW85	85	17.4	4.88	21.4	5.7	57 x 22.8	23
SW90	90	17.4	5.17	21.4	5.9	57 x 22.8	23
SW100	100	16.7	6	21	6.7	57 x 25.4	26
SW115	115	16.7	6.89	21	7.7	57 x 25.4	26
SW120	120	16.7	7.18	21	8	57 x 25.4	26

Table 5 - SunWize SW-Series Panel Comparison. [53]

4.1.1 Mounting

SW-series modules should be firmly fixed in place, making them suitable to withstand wind and snow loads for locations where these weather conditions are most common. The tempered glass face of the laminated solar module is rated to withstand 100+ miles per hour wind speeds, which is very important for the Central Florida area. A module support structure should be equally rated for such loads considering the number of modules to be supported. In this project the system includes only one solar panel, therefore the mount was designed to support one panel. The glass surface is impact resistant and rated to withstand up to 1” diameter hailstones at 50 mph, but a hard impact by a rock or tool may cause breakage. Precautions should be taken when assembling solar modules on the mounting frame. The user should avoid leaning solar modules or panel

assemblies upright, as they can fall and break. Repairs to broken solar panel glass are not possible.

The solar module frame has intermediate mounting holes on the longer sides. These mounting holes are positioned to provide the best possible location for mechanical attachment of supporting structures. Four stainless steel bolts are recommended in the mounting procedure for best support of the panel. These bolts were included in the designed selected. Re-drilling the panel for different mounting holes is not recommended as this may result in loss of strength and void the warranty. If flush mounting is selected, the SW-series panels include four end frame holes for bolted structural attachment. The use of proper support structure anchoring fasteners should be important in order to provide maximum holding strength to the supporting material in which attachment is to be made.

Solar panels can be mounted in many different locations. A location with good solar exposure away from trees and structures should be selected. For commercial and residential use, the panels are primarily mounted on rooftops for better sunlight exposure. At least a six inch clearance between the solar module and roof is needed, in order to let air flow across the back of the module for cooling and to provide space for output cabling to exit. For portability, they can also be mounted on the ground by using mounting brackets and ground-fixed poles. Since the angle of the solar angle changes during the day and even during the time of the year, it is important to mount the panel on an adjustable fixture. Besides good water drainage, a tilted solar panel will allow for about 50% more daily power output than horizontally mounted modules. [53] It is calculated that the optimal panel mounting angle for Orlando will change according to Table 6. Panels located in the northern hemisphere should face due south and oppositely, panels located in the southern hemisphere should face due north. In Table 6 the vertical angle (V°) represents the angle between the panel and the vertical direction. These angles can be used to calculate the angle between the panel and the horizontal direction or leveled ground. H° = 90° - V°

Month	**Jan**	**Feb**	**March**	**April**	**May**	**June**
Angle	46°	54°	62°	70°	78°	86°
Month	**July**	**Aug**	**Sep**	**Oct**	**Nov**	**Dec**
Angle	78°	70°	62°	54°	46°	38°

Table 6 - Vertical Mounting Angle for Solar Panels in Orlando. [54]

The solar panel mount can be passive, such as a fixed angle, or adjustable pivot mount. The pivot mount is an angle adjustable passive mount, which can result in better efficiency throughout the year. This feature is needed since the angle of the mounted panel can vary with location (longitude) and time of year. The mount can even be an active type, which means that the panel is fixed on a “smart” mount. Solar tracking can be implemented with the use of an active mount. Solar

tracking is achieved by mounting the solar panel(s) on a swivel type mount. This mount can be constructed to adjust around one or two axis and is usually powered by some type of an electrical motor(s). Solar tracking uses light sensors and a control module that operates the electrical motor(s) in accordance to the light variation sensed by these light intensity sensors. Since the solar tracking technique is the most efficient of all, it is important that its benefits are worth the energy consumption that such system would require. This method would require a certain level of battery power, which defeats the purpose of its use, considering the scale of this project and its short testing period.

The panel will be mounted on a rack, constructed from a lightweight and weatherproof metal such as aluminum. The advantage of such a mount is that it increased the mobility of this project for testing purposes. A similar mount is pictured in Figure 32. This base can be fabricated by one of the group members or purchased for around $50. The two sides can be joined together by using two separate rails. The length of these rails would be determined by the mounting width of the solar panel, which according to Table 5 is close to 25.5 inches. By doing so, the solar panel mount forms a square shaped base with a 25 inch side. This newly formed base can be used as a frame for a nonconductive panel such as Plexiglas or plywood. The panel is able to hold the battery, the charge controller box and mount the power inverter.

Mobility is also a very important issue, since the combined weight of the selected panel and battery is close to 60 pounds. Another method that can increase mobility is to design a mount that incorporates caster wheels at its base. Obviously these wheels would have to be rated at 15 pounds or higher since a total of four wheels are needed. Similar wheels as the polyurethane ones in Figure 32 can be purchased from local hardware stores for around $5 each. [55]

Figure 32 - Pivot Mounts and Caster Wheels for Solar Panels.

4.2 Microcontroller

The Atmel ATmega328P microcontroller pre-loaded with the Arduino bootloader is used in PMCC. This microcontroller contains the adequate hardware and software for all design goals, providing enough digital and analog pins to handle all sensors, LCD, and transmitters, while at the same time being able to control the MPPT circuit using pulse-width modulation (PWM) outputs. A list of specifications for the ATmega328P is given below: [26]

- 8-bit microcontroller
- Up to 20 MHz clock
- 32 KB flash memory
- 1 KB EEPROM
- 2 KB SRAM
- 6 PWM channels
- 6 analog inputs (10-bit ADC)
- 14 digital input/output pins
- Hardware Serial USART

- SPI Interface
- Two-Wire (TWI) or Inter-Integrated Circuit (I^2C) communication
- 5V DC power
- Low-power modes
- DIP or SMT packages

The six analog pins are utilized in PMCC. In order to implement I^2C communication in this microcontroller, analog pins 4 and 5 were used. This reduced the effective number of analog inputs to four, since PMCC will utilized I^2C components (DS1624 temperature sensor). Two analog current sensors and two analog voltage sensors take up the remaining four analog input pins. I^2C employs a clock and data bus, and all I^2C devices connect to these two lines (in this case analog pins 4 and 5). All I^2C devices have a unique address, and up to 127 unique peripherals may be contained on a single I^2C bus. Thus, for any future additions to PMCC, I^2C chips will be preferred over analog devices. No additional analog devices may be used, unless an analog-to-digital (I^2C) converter was added to the system.

Many of the 14 digital I/O pins are required. The XBee wireless module uses the TX and RX (Serial transmit and receive pins), which are also digital pins 0 and 1. The LCD also uses serial communication so this too requires TX and RX pins. Since there is only one set of hardware USART available on the ATmega328P, two digital pins instead can be used and the serial port can be set up in software (using Arduino's SoftwareSerial library). The irradiance sensor requieres one digital input pin. Lastly, four digital pins are used as PWM outputs, controlling the buck-boost circuit. The total digital pin count was 9 out of 14 pins, which allowed little room for additional peripherals.

This microcontroller was found to contain all of the hardware required for the charge controller, but a choice between software now had to be chosen. The first choice was to utilize AVR's IDE (AVR Studio) and programming language. The code could be written in either a C-like or in assembly language. The main drawback was the fact that an external programmer is needed to load new code to the flash memory. In an embedded application, or one that does not allow easy access to the microcontroller, programming of the device would be impractical. Using an external programmer is both time consuming and the user risks damaging the IC (bending pins, electrostatic discharge) every time the chip is removed from a socket. This would be extremely inconvenient in PMCC, for the charge controller was contained in a small housing, and thus removing the microcontroller every time programming is needed would not be ideal.

The Arduino was chosen as the microcontroller to be used in PMCC. The Arduino bootloader allows direct programming through USB, eliminating the need of a separate hardware programmer to implement new code. In order for a program be loaded via a USB, a USB connector and a USB-to-TTL IC are required on the PCB. An ATmega8U2, reprogrammed as a USB-to-Serial

converter, was used to communicate between the microcontroller and the computer which is programming the chip.

The other major factor that influenced the decision to choose Arduino was the programming language. After doing research about AVR's programming languages, it was found that all the necessary functions needed in PMCC are available. However, the Arduino programming language was chosen due to relatively shorter learning curve and a large and active community which facilitates faster learning. The language and IDE are completely free and open source, and many resources concerning sensors, motors, LEDs, communication tutorials, etc. are readily available on the Arduino website. The language is both easy to use and robust, providing all the functionality needed for interfacing with analog sensors, I^2C components, and TTL serial peripherals among others. In addition, numerous libraries have been written for common sensors and other peripherals which helped in the learning and implementation of components in PMCC. [26]

In PMCC, two microcontroller integrated circuit (IC) chips were required. One was designed into the printed circuit board (PCB), and another was on an Arduino Uno development board connected to a data acquisition computer receiving data transmitted from the PCB microcontroller. The Arduino Uno board receiving data will be an off-the-shelf component, but the ATmega328P that was part of the charge controller was implemented in a PCB. A second Arduino Uno development board was used for prototyping and testing before designing the PCB incorporating the microcontroller and additional components in the final prototype.

In order to make the ATmega328P into an "Arduino" microcontroller, a few components were needed to be added to the PCB: a 16 MHz crystal oscillator, USB connector and USB-to-TTL circuitry, 5V and 3.3V regulators, and a reset button. On the PCB the pins were traced from the microcontroller to these components as well as the various sensors, LCD, MPPT circuit, and wireless peripherals. Arduino is open source hardware which means that schematics can be easily obtained for integration into the PCB design. [26]

4.3 Electrical Configuration

The ATmega328P microcontroller is responsible for monitoring and controlling numerous sensors and other peripherals. Figure 33 shows the different components of PMCC's electrical system connected to the correct pins of the microcontroller. All of the analog pins and a large number of digital pins are used in PMCC, making expansion very difficult.

The XBee wireless transceiver module requires a UART serial port to communicate. The serial transmit pin (TX) and receive pin (RX) are mapped as shown in Figure 33. This is the only set of hardware UART on the ATmega328P and thus for all other peripherals which communicate via serial, it is necessary to

set up a software serial port using two general purpose digital pins, as are addressed during the LCD discussion.

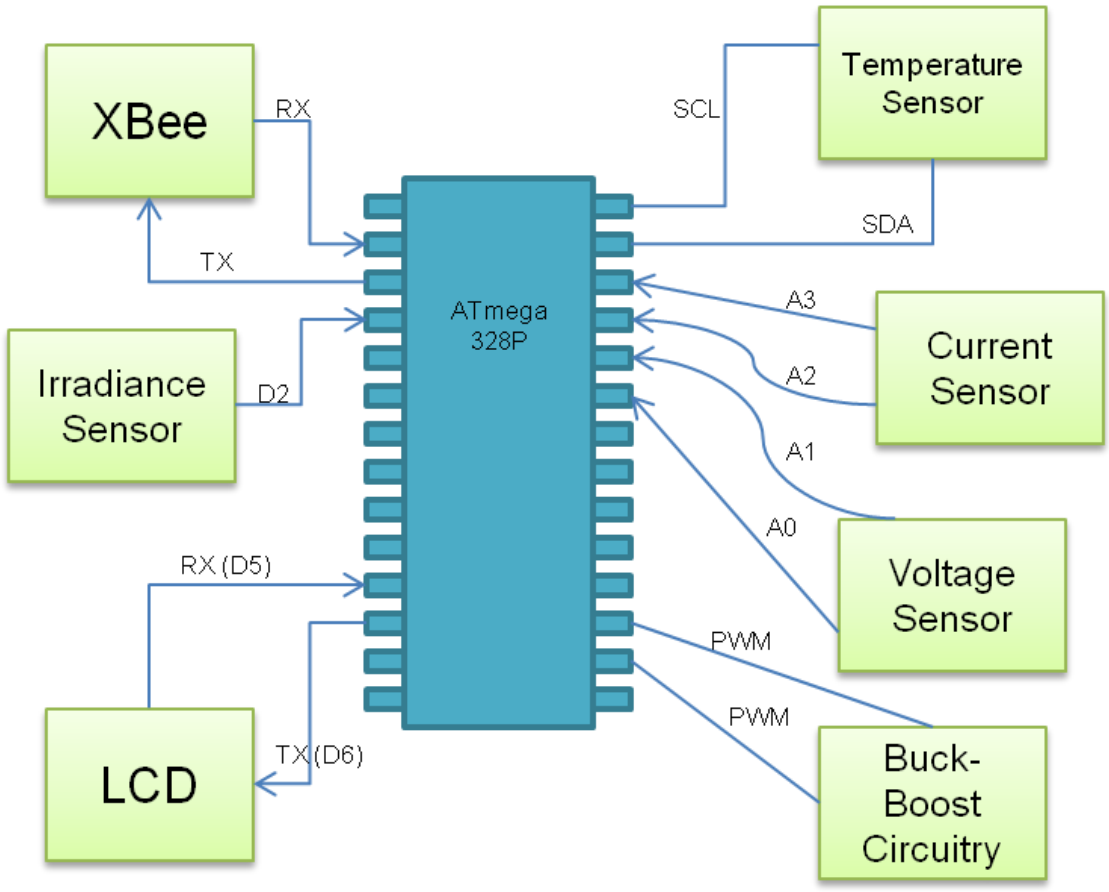

Figure 33 - PMCC Microcontroller Interfacing with Peripherals.

The irradiance sensor is connected to digital pin 2 of the microcontroller. This sensor outputs different frequencies depending on light intensity, and this pin is capable of reading this change in frequency. This device is used for measuring the light intensity in order that the efficiency of the system can be obtained.

The LCD is interfaced using TTL serial communication. Since the ATmega328P only has one set of hardware UART serial ports, the LCD is wired to digital pins 5 and 6. Any of the general-purpose digital pins can be configured to act as serial ports, 5 and 6 were chosen because of spacing issues. The serial port can be implanted in code, thus allowing communication between the microcontroller and LCD.

Out of the 14 digital I/O pins of the ATmega328P, 6 can be configured as PWM outputs. These PWM pins are crucial to PMCC because they allow the voltage to be changed dynamically in order to find and track the maximum power point. Either two or four PWM outputs are required, depending on the design of the buck-boost circuitry. In PMCC, the buck-boost circuit uses two PWM lines. In

Figure 37, two PWM lines are shown at pins 9 and 10, two of the possible six PWM output pins. Lowering the duty cycle of these PWM reduces battery charging voltage, while increasing the duty cycle raises it. In addition to these PWM lines, two addition digital lines are needed to switch between the buck and the boost stages (not shown in figure).

The voltage and current sensors output an analog voltage, which are read in using analog pins A0, A1, A2, and A3. The voltage inputs to the microcontroller must be between 0 and 5 volts, else the values cannot be read and there is risk of damaging the device. There is two voltage sensors and two current sensors in PMCC: one set measuring solar panel voltage and current, and the other measuring battery bank voltage and current.

The temperature sensors are required for both tracking MPP and equipment protection. One temperature sensor was placed on the solar array, and another at the battery bank. The temperature sensors chosen use Inter-Integrated Circuit (I^2C) communication. The decision for this was because of the fact that all of the analog pins are used up, and thus any expansion of the electronics would require analog-to-digital converters. Instead, it was deemed better to use the I^2C bus to avoid having to use addition integrated circuits in the system. On the ATmega328P, analog pins 4 and 5 double as the clock and data lines for I^2C communication. Pin 4 is the I^2C data line (SDA) and pin 5 is the I^2C clock line (SCL). Since the I^2C bus can handle up to 127 unique device using only two wires of the microcontroller, additional circuits can be added as necessary without severe disruption of other functionality.

4.4 LCD

One of the most significant design constraints of the charge controller overall is that the components included should use as little power as possible, as not to detract from the power available for charging the battery. For this reason, the graphical display was ruled out because it did not provide significant advantages in usability for the extra power it consumed. For example, a graphical display might consume hundreds of mA while a character LCD would consume less than 100 mA when fully backlit. In addition, the incorporation of a graphical LCD screen would introduce added programming complexity, which could not be justified for use in this system based on the minimum specifications needed. Furthermore, the decision against the inclusion of a graphical LCD screen simultaneously rules out the possibility of a touchscreen interface. While it could be argued that a color touchscreen LCD would provide increased user operability, it was deemed unnecessary because the specifications could be fulfilled using only characters; there was no need for graphics.

The power consumption was the primary reason not to select the graphical LCD however even though the segmented/alphanumeric LCD consumes the least amount of power, it does not have enough flexibility for this application and was

therefore dismissed as well. The 14-segment characters are generally very large per character and do not allow the system to display detailed messages. The segmented LCD option was deemed inefficient because it could not display several status values such as current and voltage simultaneously.

Ultimately it was determined that a character LCD screen provides the right balance of power consumption and image size/quality making it the most viable option. In addition, backlighting was also believed to be a necessary feature of the LCD so that the status could be read in any lighting situation. Backlighting makes the screen more versatile and allows the user to quickly and easily view the text in varying conditions.

Based on these considerations a 20x4 character LCD was chosen for implementation into the charge controller design. This should provide ample space to display several quantitative values as well as any status indicators that need to be included. The specific display chosen is the serial enabled LCD-09568 from SparkFun Electronics, shown in Figure 34. The actual LCD is 87.3 x 41.8 mm while the PCB footprint measures 105 x 59.9 mm. This display is monochrome (black on green) and has adjustable backlighting.

Figure 34 - Serial Enabled Black on Green LCD.
Reproduced with permission from SparkFun Electronics.

Other than the size of the display, consideration was given to the serial communication aspect and was chosen over the alternative, parallel LCD screens. While serial LCD screens are generally more expensive, they make up for the increase in cost with their simplification of use and reduction in the number of pins that they use.

The 20x4 serial LCD screen chosen has an easy interface with the Arduino microcontroller using the one of the many standard software libraries available to the public for open source use. Since this LCD utilizes serial communication, the LCD will communicate using the “SoftwareSerial” Library, which facilitates serial communication on digital pins. Table 7 shows an example code in which the user defines the baud rate as well as reads and writes a sensor value.

Library: `SoftwareSerial.h`		
Function	**Code**	**Description**
Initalize	`SoftwareSerial()`	Set up a new serial port
	`serial.begin()`	Establishes the baud rate
Read a value	`serial.read()`	Reads in a value
Print to screen	`serial.Print()`	Prints characters to the screen
Check serial port	`isListening()`	Test to see if serial port is listening

Table 7 - Required functions for LCD programming. [56]

4.5 Sensor Implementation

4.5.1 Voltage Sensor

Figure 35 is a flow chart describing the different parts that the voltage sensor circuit is composed of. This sensor is responsible for calculating the voltage in real-time of the operating solar PV panel which is depicted to the left of the flow chart. The output terminal of the panel will run into the voltage divider circuit where the voltage is distributed across resistors R1 and R2 accordingly based on the resistor values that are going to be determined next.

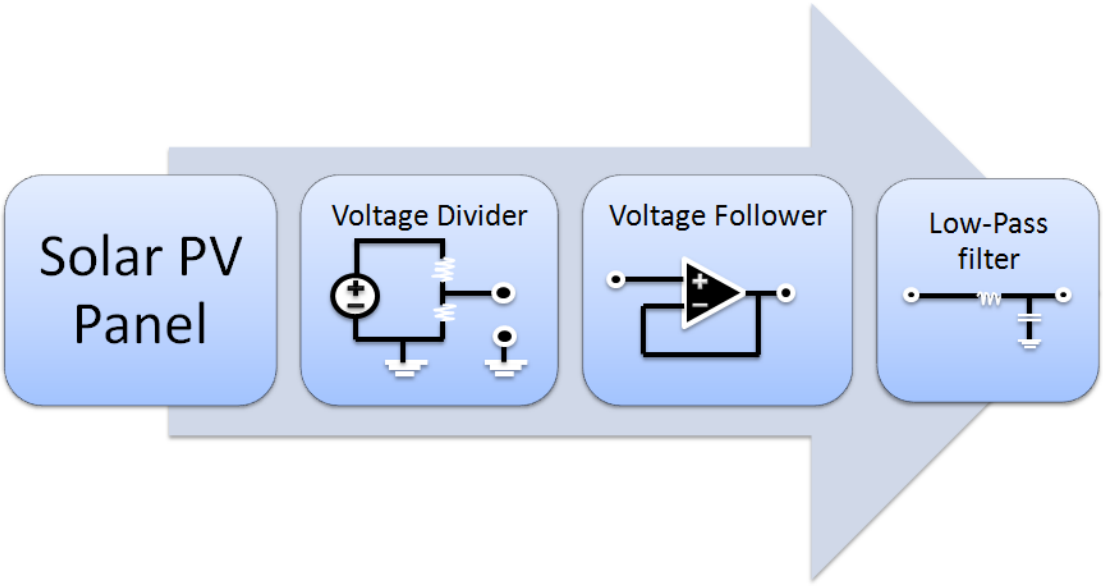

Figure 35 - Voltage Sensor Flow Chart.

The voltage across R_2 is the voltage that is monitored and measured for the MPPT, therefore it must follow the electrical specifications of the Solar PV Panel and the micro-controller to prevent any damage or malfunctioning of the system. The appropriate resistor values were determined as following given the specs:

$$R1 = \ 1M\ ohms$$

$$V2 = \frac{R1}{R1 + R2}\ Vp$$

where, V_2 represents the voltage across R_2 as a function of V_p which is the voltage the solar panel is delivering at a certain point in time. Given the electrical specs of the solar panel, the Voc of the panel is of 21 V. Since V_2 is the voltage that is going to be fed into the micro controller, this voltage cannot exceed the 5 volts DC mark due to the specs in the micro-controller.

$$Voc = Vp = 21\ v$$

$$V2 = 5\ v\ max$$

$$5v = \frac{1M}{1M + R2}$$

$$R2 = 312.5\ K\ ohms\ \cong 309K\ ohms\ (available\ resister\ value)$$

In this way, in a worst case scenario where the panel would deliver 21 volts, the voltage across resistor R2 will never exceed the 5v input in one of its pins. Then, V2 is fed into voltage follower which will be responsible for isolating the voltage divider circuit from the rest of the components in order to prevent the other components in the circuit from altering the actual voltage reading coming from the panel.

Finally, the voltage output coming from the voltage follower is fed into a filtering capacitor where noise spikes and fluctuation of the voltage was prevented from making it into the micro controller given the user a false reading of the actual voltage measurement. A simulation of the voltage sensor to be implemented in the design is shown in Figure 36. A power supply of 21 volts has been used to simulate a worst case scenario in the design. As the first voltmeter shows, the voltage across R2 is of 4.956 votls, which confirms that the voltage has not exceed the maximum voltage of 5V given by the micro control given a worst case scenario. Moving toward the voltmeter number two and three, the voltages remained pretty constants with just 5 milli volts difference after the voltage follower. At the output terminal of the low-pass filter, the voltage is guaranteed that it will never exceed the 5 volts threshold given by the micro controller.

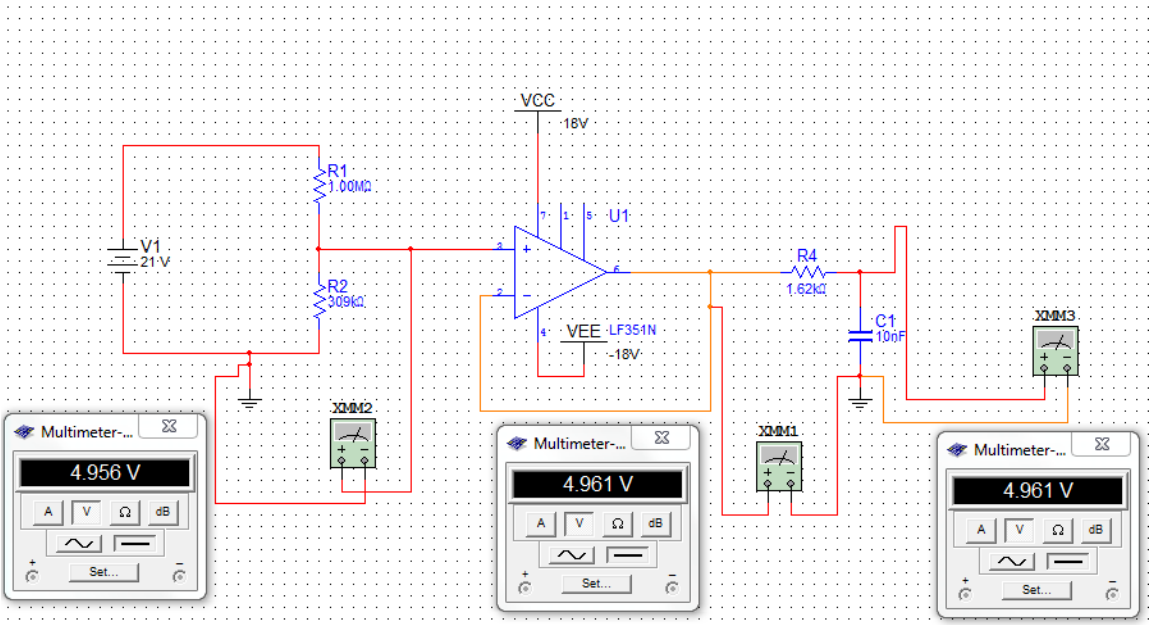

Figure 36 - Voltage Sensor Circuit.

This same approach was used when measuring the voltage in the batteries; the resistor values are calculated the same way following the electrical specifications of the battery for that case. [42]

4.5.2 Current Sensor

The flow chart for the current sensor shown in Figure 37 follows a similar path as the voltage sensor but this time the current that is output by the solar panel is what needs to be measured, and therefore it is done a little differently. The output of the panel is connected in series with a shunt resistor. These resistors typical have a low resistance that is around the milli-ohms. The purpose here is not to block the flow of current coming out the solar panel by placing a higher resistor value; instead, it is important that the current flows as freely as possible so that an accurate reading can be recorded. The focus is to let as much as current through as possible with a very little resistance so that just a small voltage drop is generated across the shunt resistor and then monitored by the AD8215. Since the voltage across the shunt resistor is too small to be used for actual measurements in a device, this voltage is amplified by the AD8215 by about twenty times. Once the voltage has being amplified, the output generated by the AD8215 chip is now useful for actually readings purposes.

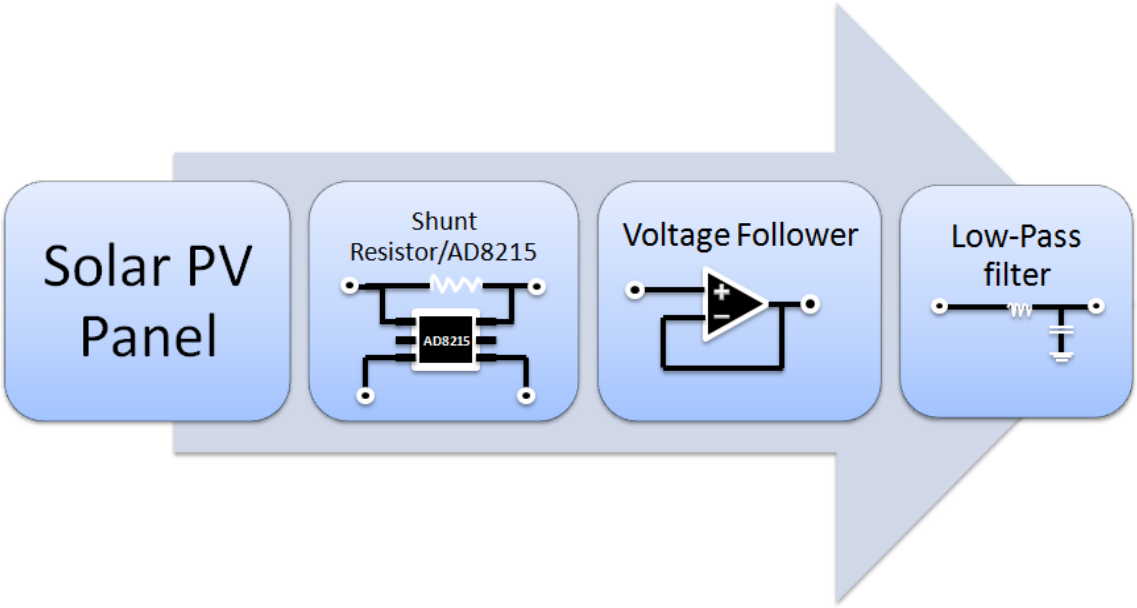

Figure 37 - Current Sensor Flow Chart.

From this point on, the way the signal is treated is similar to that of the voltage sensor. First, the output is isolated from the rest of the circuit by a voltage follower, and then it is finally fed into a filtering capacitor where any noise spikes are rejected. Once the signal has been filter out from potential noise, it can finally be fed into the AD converter pin of the microcontroller to be implemented in the MPPT. [43] Some of the features of the ACS712 Current Sensor from Allegro Microsystems are:

- Low-noise analog signal path
- 5 μs output rise time in response to step input current
- Handles a 80 kHz bandwidth
- Total output error of 1.5% at Temperature ambient of 25°C
- 1.2 mΩ internal conductor resistance
- 5.0 V, single supply operation
- 66 to 185 mV/A output sensitivity

4.5.3 Temperature Sensor

The DS1624 Thermometer from Maxim is a digital temperature sensor that fits all of the desire characteristics that are needed in this system. This makes the sensor extremely easy to use in the design with no extra circuitry needed in the implementation process. Each DS1624 needs to be in direct contact with the solar PV Panel and the batteries in order to provide accurate information of the temperature in the panel itself and the batteries and not the environment. The main specifications of the sensor are as follows:

- Communication type: I^2C Bus

- V_{DD} of 2.7 to 5.5 V input power
- Range of temperature is of -55°C to +125°C
- The temperature is read as 13-bit value
- 8- pin DIP

The big range of temperature from of the sensor enables the sensor to operate normally with accurate readings even if it is exposed to high temperatures as well as low temperatures. The implementation of the sensors both from the batteries and the solar panels are connected in the same bus due to the facilitating method that I^2C allows in the communication process with the microcontroller.

As seen in Table 8, pin 1 and 2 are in charge of the communication so they are connected directly with the microcontroller. Pin 3 is a pin that is not used therefore is left unconnected. Pin 4 and 8 are responsible for powering the chip and grounding the chip respectively. The voltage applied at the V_{DD} should be between 2.7 to 5.5 volts. And finally pins 5, 6 and 7 used to assign different address to the sensors so that no interference between the sensor occurs when providing data to the microcontroller. [41]

Pin	Symbol	Description
1	SDA	Data input/output
2	SCL	Clock input/output
3	NC	No connect
4	GND	Ground
5	A_2	Address input pin
6	A_1	Address input pin
7	A_0	Address input pin
8	V_{DD}	Supply voltage

Table 8 - Temperature Chip Detailed Pin Description.

4.5.4 Irradiance Sensor

The implementation of the irradiance Sensor in the ESCC is crucial in the design in order to provide the user with information regarding the light intensity during the day. Due to the characteristic of the TSL235, its incorporation in the design does not require extensive circuitry for a proper performance. As shown in Figure 38, the sensor is composed of four main parts.

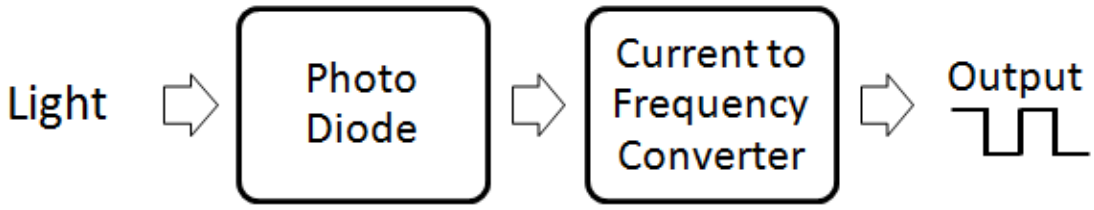

Figure 38 - Light to frequency converter. [45]

Light is the sensor's input quantity which is received by a silicon photodiode. This information is converted into frequency and later output as a square waveform. This output signal is later fed into the micro controller where it is translated to lumens in order to have a value that the user is able to work with on the data logs.

The sensor is powered with a DC voltage of 5 V. Due to the nature of the sensor, the implementation of a decoupling capacitor was necessary in order to keep the accuracy of the sensor at a maximum. The decoupling capacitor that was used fell in the microfarads range; This capacitor is integrated in the same pin as the V_{DD} as shown in Figure 38. [45]

4.6 Wireless Transceiver

In choosing a wireless transceiver, many factors were taken into consideration. The range, power, throughput, communication protocol, form factor and other variables had to be consistent with the design goals of PMCC. Table 9 shows a comparison between the XBee modules and the RN-XV Wi-Fi modules.

	XBee DigiMesh Module	RN-XV Wifly Module
Protocol	802.15.4	802.11b/g
Operating Voltage	3.3V	3.3V
Transmitting Power	1 mW	1 – 4 mW configurable
Hardware Interface	TTL Serial UART	TTL Serial UART
Max Data Rate	250 kbps	52 Mbps
Frequency Band	2.4 GHz	2.4 GHz
Antenna	Wire (built-in)	Wire (built-in)
Outdoor Range	90 m	150 m (at 4mW)

Table 9 - Comparison of Xbee and Wifly Modules. [35]

The wireless transceiver chosen for PMCC is the XBee module with wire whip antenna. From Table 9, it is evident that these two chips have very similar specifications. The main distinction comes down to wireless protocol: 802.15.4 or 802.11b/g. Wi-Fi is an inherently high bandwidth (Mbps) communication protocol while the 802.15.4 is more for applications which require much less throughput. In addition, 802.15.4 point-to-point communication is an efficient and effective

way to communicate data between two modules. For this reason, the wireless transceiver chosen for PMCC was an XBee module.

Now that the 802.15.4 protocol was determined to be superior to 802.11 for PMCC, A choice of different XBee modules had to be undertaken. The numerous XBee modules offer differing functionality such as transmitting power, range, antenna type, and Mesh protocol. First the antenna type was chosen from among the four choices: chip, wire whip, U.FL, and RPSMA. The latter two, U.FL and RPSMA, both require external antennas and though they will allow for increased range, the smaller footprint of the chip or wire whip antennas was deemed more desirable. The chip antenna provides the smallest footprint of all the antenna types, but at the expense of decreased range. The antenna choice for PMCC is the wire whip antenna, due to decent range, and small form factor.

The next decision was the choice of transmitting power. All other factors being equal, the more power a wireless module outputs, the farther the range. For a given Mesh protocol, two variant of module exist: XBee and XBee-Pro. The Pro versions offer the same functionality as the ordinary XBee modules, but have increased transmitting power (and therefore greater range). The transmitting power of the XBee-Pro maxes at 63 mW while the XBee transmit at 1 mW. This increase in power provides an outdoor (line-of-site range) of 1.6 km and an indoor (obstructed path) of 90 m. The ordinary XBee modules have outdoor and indoor ranges of 90 m and 30 m, respectively. The other factor between these two chips is cost: the Pro version costs about twice as much as the ordinary version. For PMCC, it is deemed unnecessary to have such an increased range provided in the Pro version, and thus in order to keep the system cost low, an ordinary XBee module was used. However, the system is designed to handle an XBee-Pro module if longer range was required.

The last parameter that needed to be taken into account was the Mesh protocol. As discussed in the research section, there are two main Mesh protocols used in XBee modules: DigiMesh and ZigBee Mesh. The ZigBee mesh is a solid and prevalent industry standard which makes interoperability with other manufacturers' devices easy and efficient. In contrast, DigiMesh provides a much easier communication protocol as long as all the devices in the network are from Digi. In PMCC, two Digi XBee modules will communicate with each other and therefore DigiMesh is the protocol of choice.

The XBee DigiMesh 2.4 GHz RF modules with wire whip antenna are the wireless modules chosen for PMCC. These transceivers have an RF data rate of 250 kbps, more than is needed to transfer the sensor data that will be collected. The chip communicates at 3.3V TTL UART serial which can plug in directly to TX and RX pins on the ATmega328P microcontroller. The small form factor of the XBee modules is another advantageous trait. The goal was to make the charge controller as compact as possible and some wireless transceivers (especially their associated antennas) are large in size. The small size of 1.087"X0.96"

allows this module to be designed onto the PCB without taking up too much space. [35]

4.7 Wireless Methodology

The wireless capability on PMCC allows both monitoring and logging of sensor values and system performance. The methodology is to use two wireless transceivers to send or receive data. One device, the transmitter, is a part of the charge controller. The other, the receiver, is stationed at a computer within range of the wireless distance. This computer takes all the data received and delivers it to a user in a user-friendly manner using tables, graphs, etc. Figure 39 below shows how the wireless system was implemented. The figure only contains the parts of PMCC that are directly involved in the wireless data link, thus the solar panels and battery bank are not included in the figure.

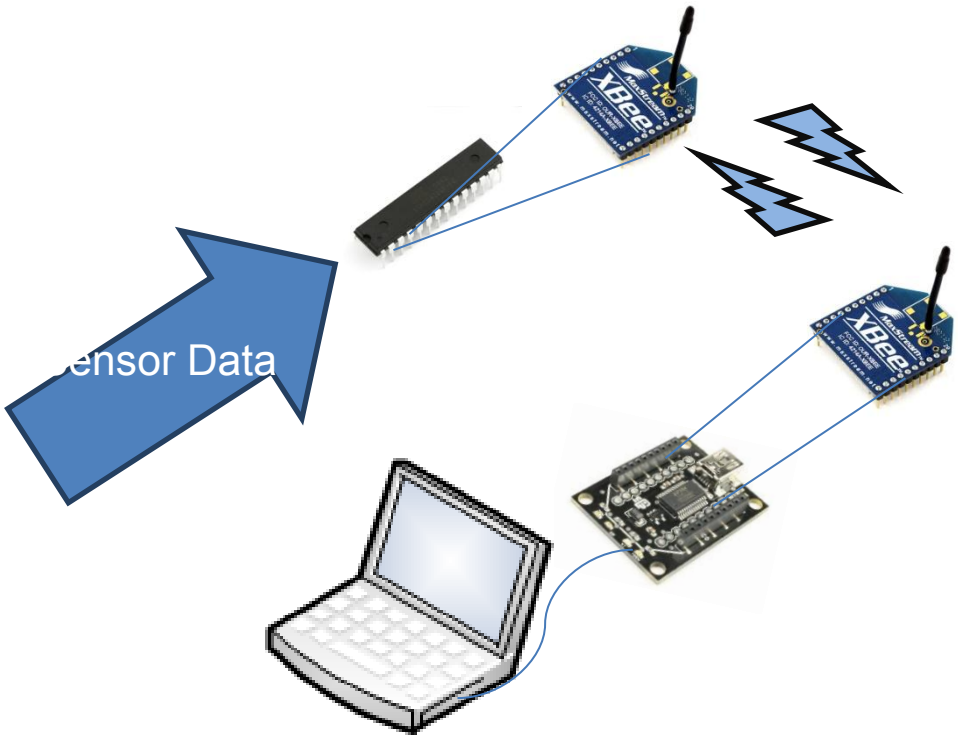

Figure 39 - Wireless Subsystem Setup.
Component pictures used with permission from Sparkfun Electronics.

The charge controller contains an ATmega328P microcontroller and XBee module as part of the printed circuit board. All sensor and performance data that is read in and processed in the microcontroller is transmitted via the XBee module utilizing the serial communication protocol. The baud rate was first tested at 9600 bits per second (bps) but was increased to up to 57,600 bps to provide the necessary bandwidth for all data. On the receiving end the XBee module was be placed on an Explorer Board that allowed the user to connect to any computer

via Universal Serial Bus (USB). The Explorer Board was less expensive than purchasing a second microcontroller and made the receiving end more compact.

Since the wireless link is composed of only two wireless modules, point-to-point communication was used. This scheme is much easier to work with than a mesh protocol such as DigiMesh or ZigBee Mesh. Both the DigiMesh and ZigBee Mesh XBee modules are capable of point-to-point communication. However, the DigiMesh modules have a much easier software setup when used in point-to-point mode, and so the DigiMesh XBee module was chosen. Figure 40 shows how the XBee modules interface with the ATmega328P and Explorer Board.

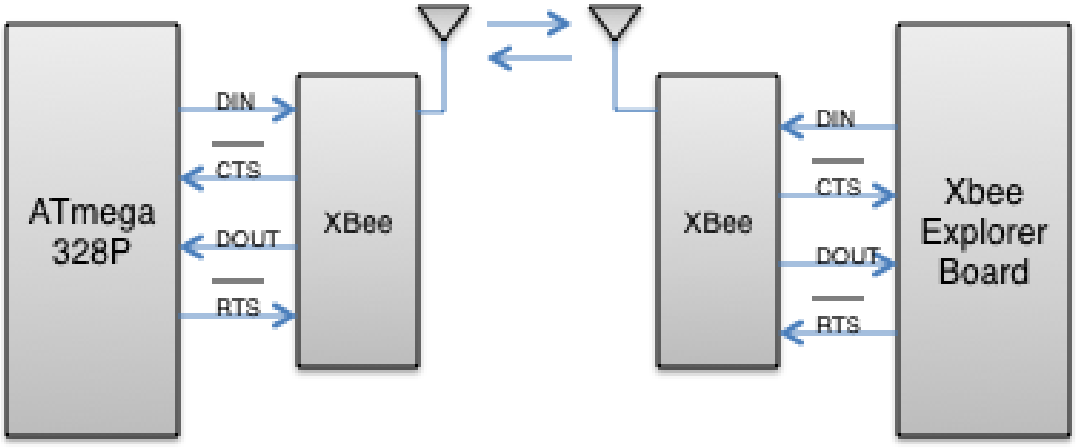

Figure 40 - Xbee to microcontroller configuration. [35]

Four connections are required between the microcontroller and XBee module. The data in pin (DIN) is the TTL serial data to be transmitted (TX) and the DOUT pin is the TTL receive pin (RX). The RTS pin is the “Request-to-Send” pin and tells the XBee module that the microcontroller has now processed and packaged the information and is ready for this data to be transmitted. The CTS pin stands for “Clear-to-Send” and is used to let the microcontroller know that the XBee is ready to transmit data. These two wires are optional and are used to reduce potential conflicts of data transmission. [35]

4.7.1 User Interface

At the receiving end of the wireless configuration the Xbee module communicates with the Arduino Uno board which was connected to a computer via USB. At this interface, the serial data that has been transmitted wirelessly is loaded on to the PC. Initially the baud rate will be set at 9600 bits per second but

was increased to 57,600 bps. This rate determines the speed at which the data is received.

Once it has been obtained, there is a need to present the data in a way that is informative and useful for the user. Since the system obtains data from several sensors, it is ideal to present a series of columns that detail the different aspects of the system and make it simple for the user to create graphs from it. The current and voltage data may be combined into a graph of the power, and can also be compared against the temperature and irradiance data, which are commonly correlated.

Since Excel is a widely used software package in both industry and academia, it will be the program of choice for developing a user interface. A spreadsheet was created that allows the user to quickly view the sensor and system data. Figure 41 shows a basic interface that saves the historical data of the system. As shown, each column contains information on each sensor, and makes it easy to plot graphs of the data.

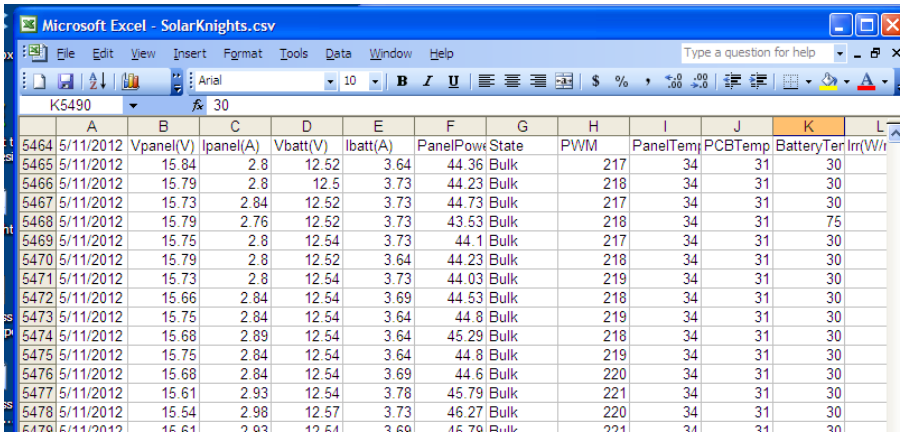

	A	B	C	D	E	F	G	H	I	J	K	L
5464	5/11/2012	Vpanel(V)	Ipanel(A)	Vbatt(V)	Ibatt(A)	PanelPow	State	PWM	PanelTem	PCBTemp	BatteryTer	Irr(W/
5465	5/11/2012	15.84	2.8	12.52	3.64	44.36	Bulk	217	34	31	30	
5466	5/11/2012	15.79	2.8	12.5	3.73	44.23	Bulk	218	34	31	30	
5467	5/11/2012	15.73	2.84	12.52	3.73	44.73	Bulk	217	34	31	30	
5468	5/11/2012	15.79	2.76	12.52	3.73	43.53	Bulk	218	34	31	75	
5469	5/11/2012	15.75	2.8	12.54	3.73	44.1	Bulk	217	34	31	30	
5470	5/11/2012	15.79	2.8	12.52	3.64	44.23	Bulk	218	34	31	30	
5471	5/11/2012	15.73	2.8	12.54	3.73	44.03	Bulk	219	34	31	30	
5472	5/11/2012	15.66	2.84	12.54	3.69	44.53	Bulk	218	34	31	30	
5473	5/11/2012	15.75	2.84	12.54	3.64	44.8	Bulk	219	34	31	30	
5474	5/11/2012	15.68	2.89	12.54	3.64	45.29	Bulk	218	34	31	30	
5475	5/11/2012	15.75	2.84	12.54	3.64	44.8	Bulk	219	34	31	30	
5476	5/11/2012	15.68	2.84	12.54	3.69	44.6	Bulk	220	34	31	30	
5477	5/11/2012	15.61	2.93	12.54	3.78	45.79	Bulk	221	34	31	30	
5478	5/11/2012	15.54	2.98	12.57	3.73	46.27	Bulk	220	34	31	30	
5479	5/11/2012	15.61	2.93	12.54	3.69	45.79	Bulk	221	34	31	30	

Figure 41 – Excel spreadsheet for data recording and plotting.

The free software Gobetwino is used to capture the serial data that is transmitted by the Xbee. After designating the file name and location, the software will continue to append the incoming data to the same spreadsheet. A statistical analysis of the data could be implemented to determine the correlation of certain characteristics, such as temperature and output voltage, or irradiance and temperature. It would be useful to identify physical trends that lead to positive or negative situations so that they could be accounted for in the future.

4.8 Algorithm Implementation

The major objective of power point tracking is to extract the maximum amount of power from the photovoltaic array as possible. Choosing an MPPT algorithm that will realize this goal was essential to efficient operation and system health. Conceptually, the incremental conductance method would be more efficient

because it is able to identify the precise maximum power point and does not oscillate around it as the perturb and observe algorithm does. However, some studies show that in implementation, these two methods operate at almost the same efficiency. [30] The increased complexity of the incremental conductance method, and its increased computation time, are not justified through sizable gains in power.

An extremely simple alternative was the constant voltage method. Although it takes very little computational power, it also contributes significant losses during the time it takes to determine the open circuit voltage. The current is set to zero for a short period in order to measure this voltage and is extremely inefficient. Furthermore, this process is repeated based on the designated cycle time. In addition, by designating a static value for the operating voltage the system cannot possibly function at the maximum power point because this value is based on an approximation.

Ultimately the perturb and observe method was implemented due to its balance between the relative simplicity of design and overall efficiency. As shown in Figure 42 below, the microcontroller computes the power and continually adjusts the operating voltage based on the result. This process runs continually as long as the system is powered on and the battery is in the bulk charging state.

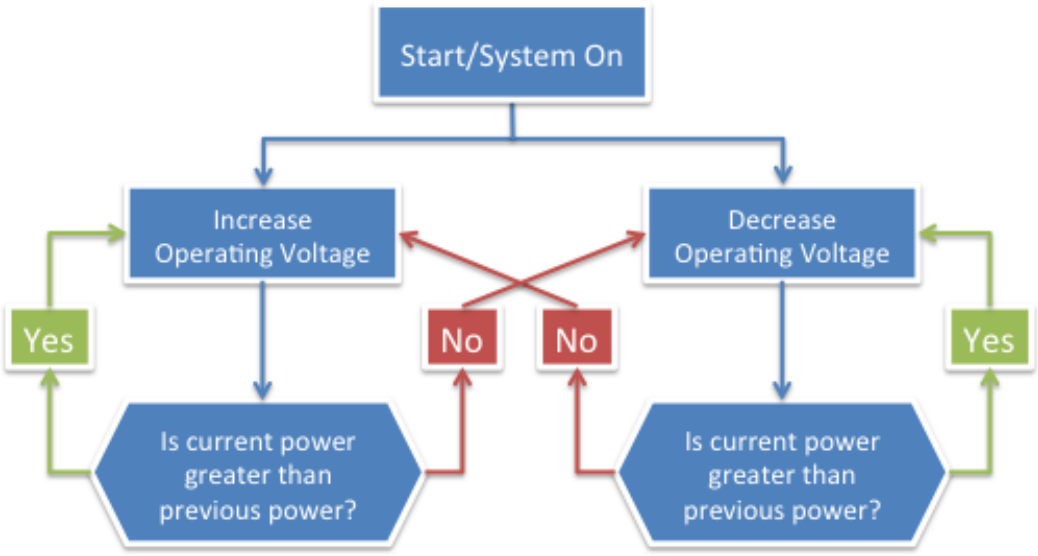

Figure 42 - Block Diagram of Perturb and Observe Method.

Once the microcontroller reads in the sensor values, it can also take into account other relevant information before adjusting the current and voltage sent to the battery. As shown in Figure 43, the ATmega328P microcontroller not only reads in the current and voltage from the PV system but also considers the current, voltage, and temperature from the battery bank. The MPPT algorithms are in place to make sure the maximum power is delivered to the battery, but the value to be supplied can change based on what state the battery is in. The

microcontroller also has various thresholds in place to designate when to switch between these stages.

In order to physically adjust the voltage, the microcontroller controls toggle switches using two of its digital output pins. This in turn controls the buck and boost converters, which receive the solar input in parallel. The boost converter is used to raise the voltage when the battery charging voltage is higher than the panel voltage. The opposite is true for the buck converter which is used to decrease the voltage that is sent to the battery. The microcontroller is able to designate what voltage this should be using the PWM output.

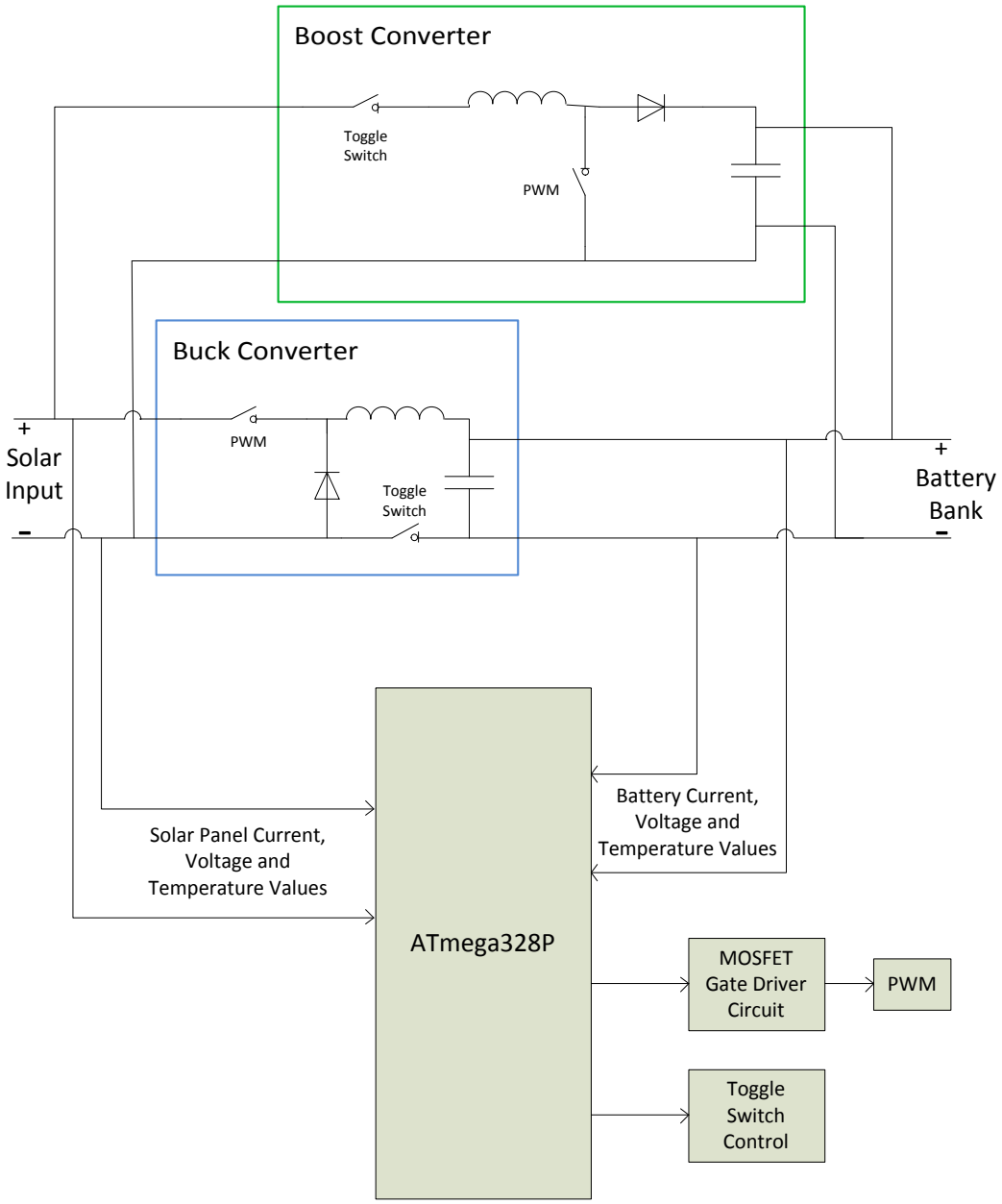

Figure 43 - Buck-Boost Circuit Diagram for MPPT.

4.9 PCB Design

A custom printed circuit board (PCB) was designed for this project. The board was designed using the circuit board design software, CadSoft's Eagle PCB Design. The components were mounted in house, since the majority of the parts were through hole. The main reasons for using a custom PCB versus a prototype board were design optimization, durability and appearance. Durability is important to this project because the board needed to be designed to handle the 4.8 A maximum current rating of the solar panel. The board needs to dissipate heat so thermal pads were also required in the design of the PCB.

When considering durability, the physical structure of the custom-printed PCB seems to be better quality than a prototype board. One reason is because on a custom-printed PCB, the copper conductors are bonded to the board, while prototype uses point-to-point wiring. With vibrations, or excessive heat, which can happen within a charge controller, the point-to-point wiring can become loose. Also, the through hole circuit board components will be soldered in, which will make the PCB very sturdy. Mounting holes were added to the design of the board in order to mount it inside the electrical box.

As mentioned earlier, cost depends on the complexity of the design and the quantity of the components used. To prevent downtime in case of a defective PCB or component, two boards were ordered. The final consideration was appearance considering the board was mounted inside the device casing with a clear Plexiglas cover to display the interior design. However, design optimization is just as important as appearance is optimization. An Eagle-designed PCB allows for the best performance and optimization, along with a nice clean look.

PCBs also allow for features like surface mount and multi-level circuit designs. The circuit components can be evenly split between two layers in a dual-layer design. If a PCB is used, the parts will be equally spaced and the traces symmetric, which was very important for our voltage and current sense circuits. In spite of all these advantages, PCB's cannot be changed altered or repaired. Once a PCB is printed, there is no room for changes and repair. In order to avoid mistakes in PCB design a lot of time was dedicated to selecting the right components and circuit simulation. The circuit was built on a bread board first, to ensure proper operation and design. Using a prototype board has its own advantages, such as design flexibility and ease of use and repair. No software knowledge is required to build a designed circuit onto these boards, even though it can be used to design and simulate the board. These boards allow for design change and repair with very little to almost no downtime. In case of a bad component these boards are easier to work with in order to replace a burnt component. The main disadvantage with the prototype boards is the use of surface mount components. Surface mount components cannot be used safely with these boards.

In order to fully understand and appreciate the dual layer capability design needed for this project, it is important to discuss the differences between surface-mount and through-hole. So it is necessary to consider the advantages and disadvantages of each. Most people who work with electronic boards know that surface mount technology (SMT) has provided many benefits both in the design and manufacturing process for printed circuit boards (PCB). The key element that stands out with SMT is the fact that less space is taken up on the PCB, since the components mounted are both small and can be mounted on either side of the board. Some other benefits of SMT are the weight and electrical noise reduction. Surface-mount components can significantly reduce the total weight of the surface mount assembly, which can weigh as little as one-tenth of through-hole parts. A few more advantages of SMT are reduced propagation delays and package noise from shorter lengths of leads, and increased resistance from shock and vibration due to lower component mass. However, there are some known disadvantages for SMT. Due to the small sizes and lead spacing, manual assembly and repair of surface-mounted boards can be very challenging—especially without proper tools. Also, surface-mounted parts can't be used with breadboards, meaning each prototype requires a custom PCB.

The other choice for the printed circuit board was through-hole technology (THT). Some advantages of THT are ease of assembly and soldering. Hole-boards are best for beginners because design failures are easier to repair as compared to SMT boards. Through-hole leads have proven to be much more durable than the joints for surface-mount boards. Prototype boards can be used with THT, which is what the group members are used to working with, and any design changes could be easily made to the breadboard. Also, the availability and pricing of components for through-hole seemed to be better than surface-mount. Some disadvantages of THT are of course space on the board because the parts are not as small, and the board would also weigh more.

4.9.1 PCB Software

Cadsoft's Eagle PCB Design software was used to design and implement the charge controller circuit. This software allowed the design of a circuit board from a sketch to a production board. It features a wide range of component libraries from a large number of manufacturers. It has a multilayer option which means that the user can design multilayer PCB.

The first step in designing a PCB using Eagle is the laying out the components in circuit schematic and selecting the right manufacturer and model for each. All the RCL components should be assigned their values as in the circuit design or simulation. All nodes should be marked manually for future reference since Eagle does not automatically mark nodal connections. Eagle has a full range of common Spice software features such as; cut, copy, paste, move, grab, mirror, rotate, add and delete. The program has many more advanced features that will not be used in designing the circuit. The circuit was then transferred to a board

design by using the most important feature of Eagle, which is the ability to transfer components from a schematic to a board with the click of a button. The board design allows the user to select the board size and shape down to the millimeter. All the components are grouped on the bottom corner of the board design screen. The user can define a specific place in accordance to their manufacturer requirements. The components are still connected in accordance with the schematic design of the circuit, so it is wise to follow a certain schematic-order when placing the components on the PCB. Eagle features such as the "Ratsnest" button will adjust the wiring to the shortest and most optimal route.

Once all the parts are placed on their strategic places then the user will have to trace the actual copper wiring connections between parts. Copper tracing can be routed manually or automatically through the auto router. Manual wire tracing is a bit more tedious if the board will carry a lot of components. But it can be very useful, because it allows the user to manually select different trace bends to control trace direction. Most importantly manual routing enable the user to chose the width of the wire trace according to the current load that the trace will support. Automatic wire tracing is enabled by another unique feature the Eagle has; AutoRouter Setup. This button, located towards the end of the left-side toolbar, makes a circuit designer's job a lot easier by allowing Eagle to optimize the traces. It will automatically and intelligently select the best possible route for all the copper traces on the board. These traces will be divided between both top and bottom layers of the board in such order that the wire paths would not cross. It is important that before running the AutoRouter Setup, the grid setting selected on the board matches that of the AutoRouter Setup. This auto feature works like a program within a program to shorten the design time allocated to copper wire tracing.

The next step is running the ground plane or copper pour as it is sometimes called. This feature allows the user to cover the rest of the designed PCB with the ground copper pad. It allows for the ground plane to be spaced from any positive or power trace by a user defined distance. Once the ground plane is finished for both sides, the next step is to use the Ratsnest button to run the copper pour. After the copper pour the board is ready for silk screen. Silk screening is used to print indicators on the PCB that show the locations and mounting position of all the components used. This step is very important in the component mounting procedure. Silk Screening can be used to add additional user selected text on any part of the board.

The last step in designing a PCB with Eagle is the creation of the CAM files by running Gerber generation script. These files generated at this point were submitted to a board house to manufacture the PCB. Board houses or PCB manufacturers are available on the Web, and www.4pcb.com by Advanced Circuits was selected because of price and quick turnaround times. [58]

4.10 Battery Bank

When choosing a battery for PV applications, many factors were taken into account, namely capacity, voltage, lifetime (number of deep cycles), cost, safety, cold cranking amps (CCA), C-rate, and weight. In researching the numerous battery chemistries, nickel-based rechargeable batteries such as nickel-cadmium and nickel-metal-hydride were deemed less favorable to PMCC and therefore lead-acid and lithium-ion chemistries were compared. The advantages and disadvantages are presented for lithium-ion versus lead-acid batteries. A breakdown of some typical characteristics of these two types of batteries is shown in Table 10.

	Deep-Cycle Lead-Acid	Lithium-Ion
Specific Energy Density (Wh/kg)	30 - 50	100 – 200
Cycle Life	500 - 1000	500 - 1000
Charge Time	8 – 16h	1 – 4h
Overcharge Tolerance	High	Low
Self-Discharge rate/month	5%	10%
Cell Voltage (nominal)	2V	3.7V
Safety Concerns	Thermally Stable	Protection circuitry required
Toxicity	Very High	Low
Cost	Very Low	High

Table 10 - Lead-acid vs. Li-ion Batteries. [47]

Lithium-ion batteries currently lead the global battery market, controlling over one-third of the total market share. The reason for this is mainly due to the specific energy of Li-ion batteries; the energy capacity per unit mass is the highest of all battery chemistries. This is why they are used in our laptops, cell phones, music players, and other portable devices. Lithium-ion batteries allow a lot of energy for a small amount of weight. Some other advantageous characteristics of Li-ion batteries are: high cell voltage, fast charge rate, long lifespan, and low toxicity. The biggest disadvantage of this type of battery is cost. When doing research of large, stationary Li-ion batteries for solar applications, very few had the capacity found in lead-acid batteries and were many times more expensive. Therefore, for PMCC, deep-cycle lead-acid batteries was chosen.

Once deep-cycle lead-acid batteries were chosen, a choice between flooded, gel-electrolyte, and absorbed glass mat (AGM) had to be made. Flooded is the cheapest type of battery, but require maintenance and cannot be transported using normal shipping methods due to potential acid leakage. Gel-electrolyte removes the risk of leakage, but has a short lifespan (especially in hot climates) because the water in the electrolyte evaporates and cannot be replaced because this type of battery is “sealed.”

PMCC used AGM batteries for energy storage. AGMs cannot leak acid, even if the case is breached, and thus can be transported as “non-hazardous,” lowering shipping costs. In addition, AGMs are sealed and kept under pressure, forcing hydrogen and oxygen to recombine when charging at an extremely efficient rate, making water loss negligible. AGM batteries have a low internal resistance, low self-discharge, can handle shock and vibration very well, and can survive freezing temperatures. The only disadvantage this battery has is the fact that an AGM costs two to three times more than a flooded battery.

The battery chosen for PMCC was the Sun Xtender PVX-420T AGM Battery. This battery is manufactured by Concorde and was purchased from www.wholesalesolar.com for $145. The battery is rated for nominal 12V and 42Ah capacity at a 24h (0.042C) charge rate. The battery can deliver about 40 CCA and can be deep-cycled 1000 times if never discharged lower than 50% capacity. In PMCC, when the battery bank reaches 50% depth of discharge (DOD), no power will be delivered to the load. This battery has the dimensions 7.71 x 5.18 x 8.05 cubic inches and weighs 30 lbs. This battery is extremely resilient to shock and vibration forces, and will not leak even if the case is broken. In addition, the PVX-420T can withstand below-freezing temperatures, which would ruin a flooded lead-acid battery. The battery also features small self-discharge of 1 to 3% per month and never needs additional water to be added since electrolyte evaporation is negligible. This battery is a great battery for photovoltaic purposes. It provides a high capacity, long deep-cycle lifetime, and efficient energy storage, all in a reliable and spill proof casing. [59]

The charging algorithm used for these batteries, as specified in the Sun Xtender datasheet, is very close to the typical lead-acid charging algorithm discussed in the research section. A bulk charging stage will be used from 50% (or lower) to 80% battery capacity. In this constant current stage, our MPPT algorithm functions by finding the maximum power point and setting the voltage accordingly. Next comes the absorption stage of charging, in which the voltage is set between 14.2 to 14.4V, depending on battery temperature. When the current into the battery has dropped to 0.5% of capacity (0.42A in this case), the battery is considered fully charged. When this current is reached, the battery then goes into the floating charge stage in which the voltage is dropped to between 13.2 and 13.4 volts. This floating stage is used to offset the loss due to self-discharge, even though the self-discharge value is small in the Sun Xtender PVX-420T. The exact charging voltages for the absorption and floating stage can be computed as follows: [S8]

$V(Absorption) = 0.00004T^2 - 0.006T + 2.510$

$V(Float) = 0.00004T^2 - 0.006T + 2.340$ (Where T is in °C)

Table 11 gives the specifications of the battery storage. It consists of a Sun Xtender PVX-420T AGM Battery connected in parallel.

This configuration keeps the voltage at 12V and double available output current to 80A. The weight battery bank will weigh 60 lbs and the form factor of 8x10 square inches will be able to easily fit on the mount consisting of solar panel and charge controller. The maximum C-rate is derived from the maximum current that can be generated from the solar panel. In PMCC, a 120W solar panel is used. If 100% efficiency was possible, then the voltage would be 12V, and the current would be 10A. Thus the maximum current possible is 10A into the battery bank. The C-rate is found by dividing the current by capacity of the battery bank, in this case 10/84 = 0.12C. Since lead-acid batteries take a long time to charge, typically between 0.05 and 0.2C, this maximum value of 0.12C is perfect for efficient battery charging in PMCC.

Battery Specifications	Value
Nominal Voltage	12V
Max CCA	40 A
Capacity	42Ah
Lifetime (50% DOD)	1000 cycles
Max C-rate (from 75W panel)	0.12C
Weight	30 lbs
Cost	$145

Table 11 - Sun Xtender PVX-420T AGM Battery Specifications. [59]

4.11 Inverter

When deciding which inverter to use in the project two different brands stood out; the Power Bright and Cobra Power inverters. Both of them contain the specifications necessary to be implemented in the system, but the Cobra 880 model was ultimately chosen because of cost. They are both designed to support a voltage source rating of 12 V, which is ideal for this system where a 12 V Deep Cycle Lead Acid battery is connected to maintain the desired 12 V output voltage. [10] The Cobra inverter, which has been chosen for implementation in the design, outputs a maximum power of 800 W with a power surge rating of 1600 W. The inverter outputs a moderate sine-wave and 109V – 120V in the two 3-prong AC outlets, it also has a 5 V USB port.

4.11.1 Power Cables

To maintain the good performance of the inverter and efficient power distribution the use of a four foot long 4-AWG copper cable (90°C insulation rating) has been determined to be the minimum size for connections between the battery and inverter. This low resistance wire enables the system to deliver the maximum amount of energy to the load in a safe manner. These cables are designed to run up to 135 amps of current.

Two 4-AWG power cables, red for the positive terminal and black for the negative terminal, run from the power source into the terminals of the inverter. The end of the cable that connects to the inverter has been stripped off its protecting insulation for about an inch in order to insert the bare copper into the terminal. Once the input terminals in the inverter have been appropriately identified by its polarity (+) or (-) the bare ends of the cables are inserted and the internal screws are tightened to clamp the wires securely within the unit. Adjusting the screw holds the cable tightly in place. Once the power cables have been securely connected to the inverter, the other end is connected to the power source in its appropriate terminal (positive with positive (red +) and negative with negative (black -)). [51]

4.11.2 Mounting

Finding a location where the inverter can be securely placed and be easily accessible for the user was important in the mounting process. The inverter was placed on a flat surface with the mounting bracket against the mounting surface. Corrosion resistant mounting hardware was considered in the mounting process in order to have a more durable base but ultimately the inverter was left unattached to allow for ease of movement of the system.

4.12 Packaging

The packaging or casing design was very important for this project. The 75 W solar panel rating means that the current flowing through part of the charge controller is high enough that heat dissipation needs to be considered. The high voltage switching MOSFETs in the voltage regulating part of the system need to be connected to a heat sink. The MOSFETs were strategically placed on the PCB so that they all fit, even with their individual head sinks.

Ventilation was also a design consideration for the charge controller casing. In this project the use of case fans were considered however that would defeat the purpose of a low powered system since the fan(s) would draw a relatively high amount of power. The heat created from the system inside the case will was thought to be a design restraint, but through testing, it was determined that the PCB does not reach high temperatures and could be housed in a plastic box.

LCD and PCB placement was also important to packaging design. The LCD was mounted on the front/top side of the casing while the PCB was mounted on the bottom of it. The board was mounted using spacers in order to achieve better air circulation and component protection from a short circuit. Since the bottom of the casing is made out of a nonconductive material, short circuit protection wasn't as important. However, as mentioned earlier for performance reasons the circuit components had to be properly ventilated. Since the PCB is a dual layer design, adequate spacing is needed between the bottom side of the board and its mounting surface.

The top cover of the casing was designed in Plexiglas for esthetical and PCB exposure purposes. Plexiglas is also easier to work with for LCD mounting. Plexiglas is clear so that the PCB design can be seen through the front of the charge controller casing. This allows the user to quickly and easily view the LEDs that indicate the system power.

System placement is another issue that was addressed when selecting the proper material for the casing construction. If the charge controller was designed to be mounted close to the solar panel, it will mean that the packaging could be exposed to common Central Florida weather condition such as a rain storm. In this case the packaging would have had to be weatherproof and not have any vents. It was decided that the charge controller be placed inside a separate weatherproof enclosure if outdoors mounting were necessary. In this project the packaging was designed for indoor use and proof of concept, therefore waterproofing was not necessary.

4.13 Equipment Protection

Equipment protection was considered since some components, such as the panels and the batteries, were expensive and need specific care. These parts are very valuable and it is important to protect them for a longer and efficient performance. Longer performance means more return for the higher initial investment that is usually associated with a full Solar Panel System. First are the solar panels. The panels are the only component that is constantly exposed to the outdoor weather conditions. Even though these components are waterproof, they are not hail proof. Fortunately hail storms are very rare, but hurricanes are a common weather factor that should be considered when deciding on the location of the solar panel mount. If installing a permanent mount, the mount would have to be strong enough to withstand hurricane force winds. Grounding is also important in protecting the solar panel array from lightning damage during a thunderstorm. Proper size exposed copper (grounding) wire would be needed to connect the panel casing with an earth grounding electrode. In this case, the panel was not permanently mounted for demonstration purposes.

Other than physical protection, the solar panel's charge controller and battery required protection of their own. The Siemens SP75 panel selected for this

project has its own equipment protection. The panel has a protection box on the back that incorporates the use of bypass diodes. The diodes eliminate the risk of current reversal from the battery during night time, in case the battery is directly connected to the panel. Bypass diodes prevent reverse voltage across the PV module during shading of individual cells. This results in currents being forced through the shaded areas creating undesirable heating called hot spots. The bypass diodes, included in all of the junction boxes of the SW series modules, allow a shaded or damaged module to bypass other solar modules in the circuit. This will minimize hot spots and significant loss in array power.

Wire selection was also important. The gauge of the wire that connects the solar panel to the charge controller was selected in accordance with the amperage of the system. The correct wire gauge was also selected for the connections between the charge controller and the batteries. The solar panel selected is rated at 75W at 4.8A short circuit current. That means that the wires between the solar panels should be rated up to about 8 A.

Another system protection that was incorporated in the system is polarity reversal protection. High voltage diodes are used at the PV and Battery inputs on the solar charge controller that will protect the circuit from user mistakes. The polarity on the charge controller is clearly marked for a safer user experience. Dual ultra-fast rectifier diodes such as BYV42E, by Philips Semiconductors, were used between the positive and negative terminals of the input PV voltage and output battery voltage. This rectifier diode pair resembles a MOSFET in outside appearance. It has three separate pins, A1 (pin1), KK (pin2) and A2 (pin3). A1 and A2 are the separate Anodes for each diode. Pin 2 or KK is the common Cathode for the rectifiers. Connecting the A1 and A2 pins (anodes) to the negative terminals of the charge controller connectors to the panel and battery, while connecting the KK (common cathodes) pin to the positive terminals of the charge controller connector, ensures a normal operation of the system if the terminals are connected correctly. In addition, it will ensure a short circuit if the polarities are reversed for either the panel or battery. Figure 44 is a quick reference for the circuit connection, pin configuration and symbol of these rugged, fast-switching, rectifying diodes.

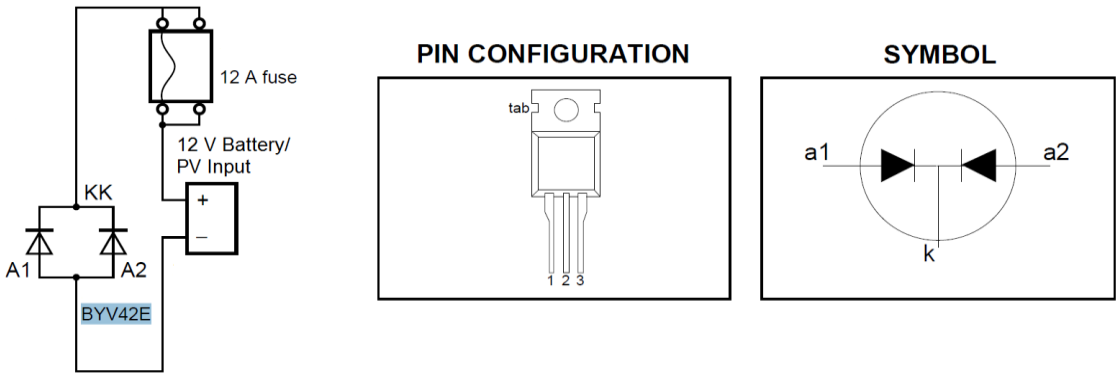

Figure 44 - BYV42E Rectifier Diode Connection, Configuration and Symbol. [60]

Additional circuit protection is provided with the use of 12 A fuses. The fuses were connected as in the figure above between the batteries positive terminal and the common cathodes of the rectifier diodes. Fuses are designed to protect the circuit in case of high current flow. In other words, the fuse is designed to burn out and create an open circuit scenario and disconnect, if the current through the battery's positive terminal will somehow exceed the current rating of the fuse. The fuse was only used on the battery side of the connection terminals since the panel side will not see any current reversal due to the circuit design.

5. Design Summary

The overall system design for this photovoltaic charging system consists of a solar panel, MPPT charge controller, battery, and power distribution. These main subsystems were either design or integration stages. The design portion was the charge controller, which encompasses the microcontroller, sensors, transceivers, and display peripherals. This is the part of the project that the team researched and designed so that the various subsystems came together to provide an efficient and cost-effective MPPT charge controller. The integration stages were the solar panel, battery, and inverter. These are the components that were purchased and integrated with the charge controller. The value of this is demonstrated by the fact that an entire prototype was created and tested, instead of only using simulation and modeling to “test” PMCC.

The entire system diagram is given in Figure 45. Sunlight incident on the solar panel generates electricity via the photoelectric effect. This unregulated power feeds into the charge controller. The charge controller measures the voltage, current, and temperatures of both the solar panel and battery. Using this sensor information, a regulated output is delivered to the battery bank. The goal was to have efficient charging of the battery using the MPPT algorithms implemented in software by the microcontroller. From the battery bank, power is delivered to various loads as 120 V AC using an off-the-shelf inverter, as well as 5 V DC and 12 V DC using DC voltage regulators.

The charge controller is comprised of a microcontroller, numerous sensors (namely voltage, current, temperature, and irradiance), LCD screen, wireless transceiver, and MPPT buck-boost circuitry. All of these components were designed onto a printed circuit board. This PCB was designed to be as compact and low-cost as possible. The wireless subsystem consists of the microcontroller on the PCB with an accompanying wireless RF transceiver which will transmit data to a remote data logging and monitoring computer. This data acquisition computer incorporates an additional wireless transceiver module, connected to the explorer board via USB, which acts primarily as the receiver. In addition to this hardware, the MPPT algorithm was implemented in software on the microcontroller.

Eric was tasked with integration of solar panels and designing the MPPT circuitry. Amber was the lead on the MPPT algorithm software and the LCD component. Steve was working with the microcontroller, wireless system, and batteries of the system. Sebastian was responsible for researching and integrating various sensors that were crucial in PMCC. In addition, Sebastian was working with the power distribution from the battery bank to a load.

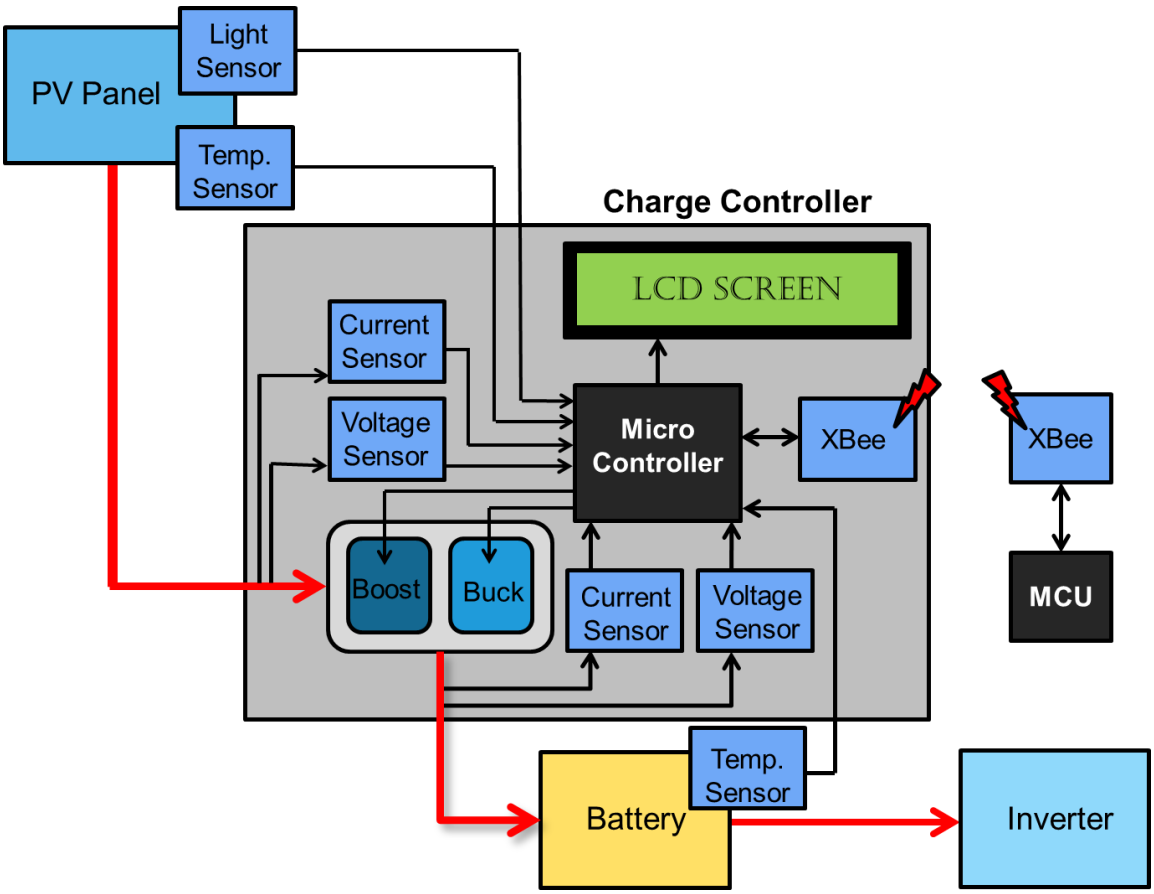

Figure 45 - Overall System Block Diagram.

The first component decision in the design was the solar panel. The solar panel chosen was the Siemens SP75. This panel is rated at 75W, at the maximum power voltage of 17.0 V and maximum power current of 4.4 A. The panel also has an open circuit voltage of 21.7 V and a short circuit current of 4.8 A. These maximum values were used in the design of the wiring and power electronics so that all components of the charge controller can handle this amount of wattage (amperage). The panel footprint is 47 x 21 square inches and weighs 16.7 lbs. These parameters were taken into consideration when designing the mount and assembly of the system.

The microcontroller chosen was the ATmega328P with Arduino bootloader. This microcontroller provides all hardware functionality required in the charge controller; all the analog and digital pins required by the sensors and other peripherals are satisfied by this microcontroller. In addition, the 16 MHz clock speed, TTL serial, I^2C communications, and robust programming language were also deciding factors in this decision.

Figure 46 below shows the electronics design inside the charge controller. The Atmega328P is connected to the peripheral devices as shown in Figure 51. The XBee is attached to the hardware UART ports of the microcontroller. The LCD

screen uses two general-purpose digital I/O pins to connect to the microcontroller. In software, a serial port can be established on pins D5 and D6. The irradiance sensor uses one digital input pin to deliver the light intensity. The current and voltage sensors utilize four of the analog input pins, where an analog voltage between 0 and 5 V is read in. The temperature sensors use I^2C to communicate with the microcontroller using analog pins 4 and 5, which were configured as an I^2C data link. Finally, the microcontroller controls the buck-boost regulator to deliver the appropriate charging voltage to the battery bank. Two PWM lines are required and two additional digital outputs are required to control switches that turn on or off the buck or boost part of the MPPT circuit.

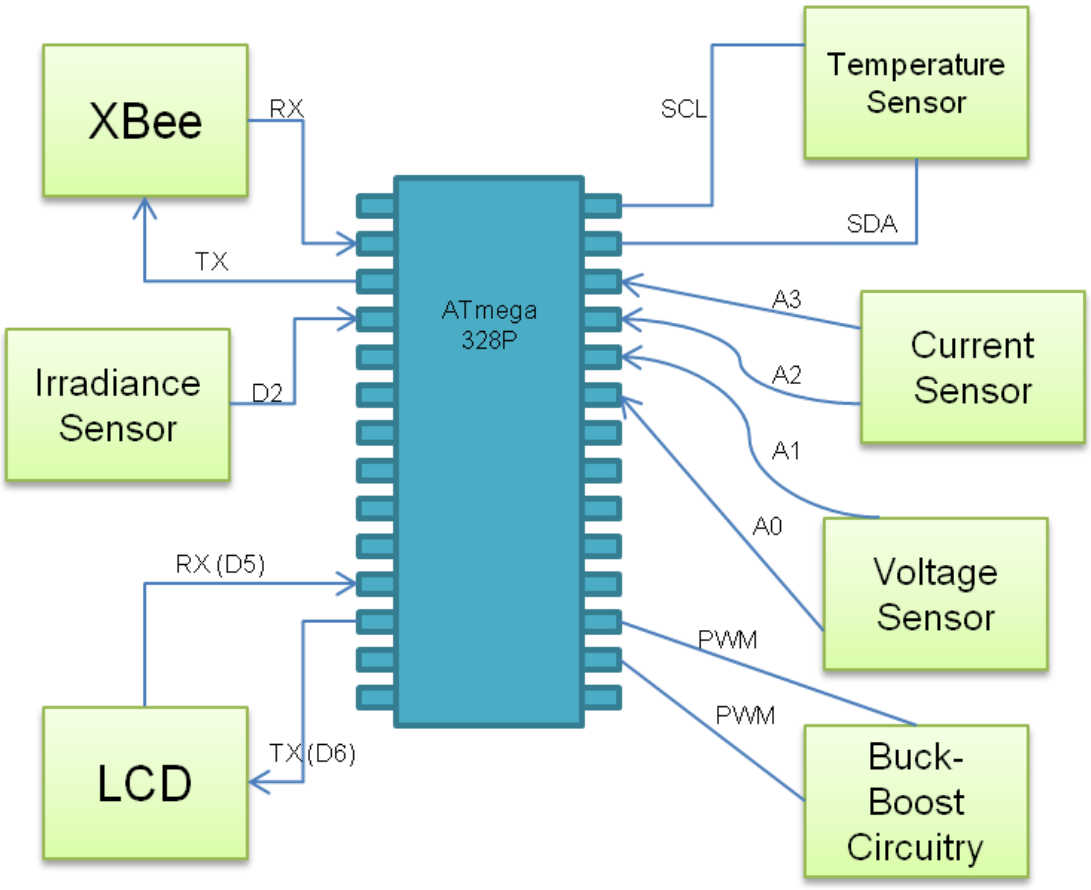

Figure 46 - PMCC Microcontroller Interfacing with Peripherals. [25]

The LCD is used to display sensor data to a user who is physically at the charge controller. The specific display chosen was the serial enabled LCD-09568 from SparkFun Electronics. The fact that this device uses TTL serial allowed for easy integration with the ATmega328P. This LCD is a 20x4 character display in order that many values can be displayed simultaneously. The LCD also features an adjustable backlight, and is monochrome (black on green).

Using a voltage divider configuration circuit as a voltage sensor in the design was extremely convenient. The resistor values used in the circuit were relatively easy

to calculate, which makes the overall implementation of the circuit easy to modify and/or adjust as required if needed in the future.

The same approach was used to find the appropriate current sensor. The AD8215 Current Sensor is a current sensor chip that does not require complicated circuitry to operate; therefore it was easily implemented in the design. The AD8215 Current Sensor is a very precise low power circuit, which provides accurate current readings while using very little resources.

On the temperature sensor side, the DS1624 temperature sensor had all the pros in its favor. This low power, precise digital temperature sensor supports a large range of temperatures from -55°C to +125°C without limiting its performance. This sensor has the capacity to be assigned a digital address which allows up to eight temperature sensors to be use in the design and they can all be accessed from the microcontroller through the same I^2C bus line.

Finally, the irradiance sensor's part in the project is determining the light intensity that the panels are subjected to during the course of the day. The TSL235 Irradiance Sensor is in the form of a photodiode that traps the light and then it is converted to frequency for output. Since frequency is the output, minimal changes in the light intensity can be detected in the frequency change of the output, therefore providing the user with up-to-date accurate readings. On the implementation side, the sensor only required a decoupling capacitor in order to keep the accuracy of the sensor to its maximum by attenuating the noise generated by the power supply.

The wireless transceiver selected was the XBee DigiMesh RF module from Digi. A breakdown of the specifications is given in Table 12. This module was chosen because it is low-power, has a decent range, and can be easily interfaced with the ATmega328P using a TTL serial port. The small form factor and built-in antenna were also preferable traits.

Specification	XBee DigiMesh Module
Protocol	802.15.4
Operating Voltage	3.3V
Transmitting Power	1 mW
Hardware Interface	TTL Serial UART
Max Data Rate	250 kbps
Frequency Band	2.4 GHz
Antenna	Wire (built-in)
Outdoor Range	90 m

Table 12 - List of Specifications of Chosen XBee Module. [35]

The wireless subsystem is an additional feature not found in most photovoltaic charge controllers. This added functionality aids the user in remotely monitoring and logging the sensor and performance values of the system. Figure 47 gives the setup of the wireless subsystem used in PMCC.

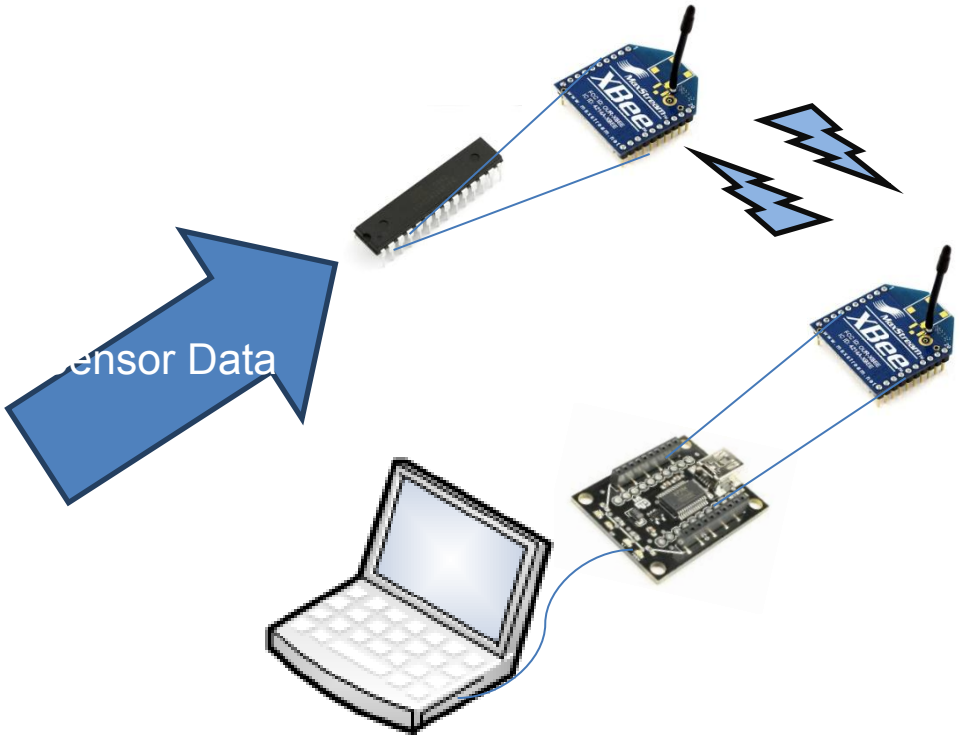

Figure 47 - Wireless Subsystem Setup.
Component pictures reproduced with permission from Sparkfun Electronics.

The wireless subsystem has two distinct parts: the transmitting module located at the charge controller itself, and the receiving module located at a remote computer. At the charge controller, sensor data is continuously fed to the microcontroller, where it is processed and packaged for transmission through the XBee transceiver. On the receiving end, another XBee module will be connected via USB to the computer using the XBee Explorer Board. From here the data is processed and given to the user in an easy-to-read format. The computer stores the serial data that is received into an Excel spreadsheet.

The Perturb and Observe Method was chosen as the MPPT algorithm that was implemented in PMCC. Figure 48 gives the general idea of this algorithm. First, the voltage is set to default value. The battery voltage and current are read through their respective sensors into the microcontroller. Then the current and voltage are multiplied to get power. Next the voltage is changed slightly higher or lower and the power is again checked. For example, if the voltage was increased, and the power is now higher than the previous value, then the voltage is again increased and power checked again. If the power value is less than the previous value, the voltage is then lowered. This way, the circuit can track the maximum power by way of current and voltage values.

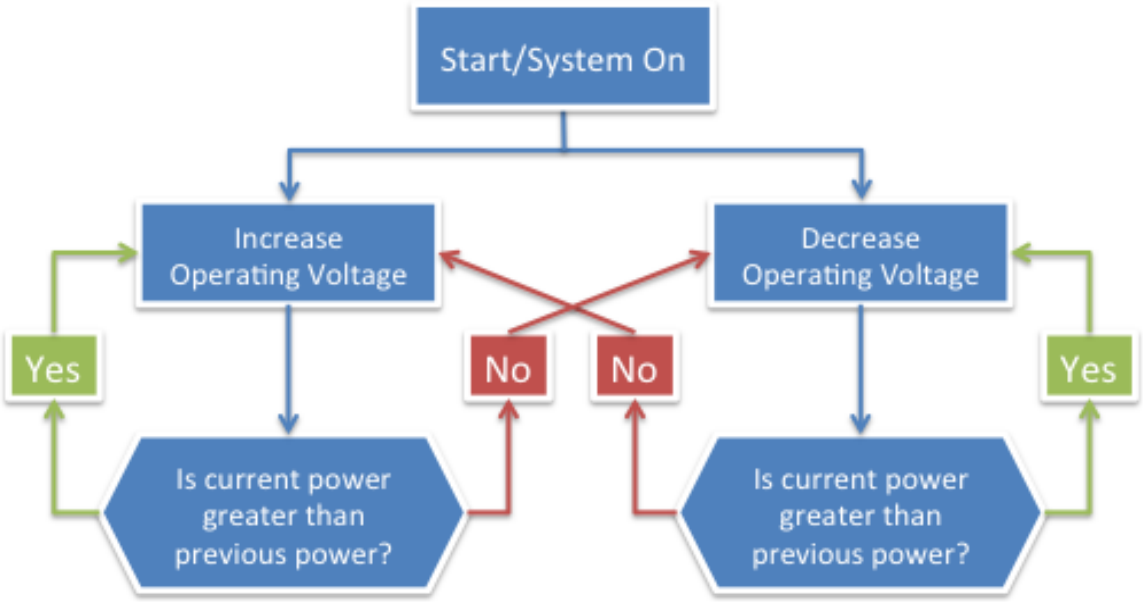

Figure 48 - Block Diagram of Perturb and Observe Method.

The circuit design for the maximum power point tracker is shown in Figure 49. The solar input is fed into a buck and boost circuit in parallel. The ATmega328P microcontroller has the task of monitoring the values (current, voltage, and temperature) of both the solar panels and batteries. The microcontroller also controls the buck and boost converters by way of toggle switches and PWM output generators. The two toggle switches are controlled by two digital output pins of the microcontroller, and the two PWM outputs are also digital output pins configured as PWM. Depending on the sensor readings gathered from both the solar array and battery bank, the appropriate voltage will be selected. If the battery charging voltage is less than the solar panel voltage, then the buck converter toggle switch is closed, the boost converter toggle switch is opened, and the voltage is lowered to a specific voltage determined by the duty cycle of the PWM. If on the other hand, the charging voltage is higher than the panel voltage, the boost toggle switch is closed, the buck toggle switch opened, and the voltage is determined again by the duty cycle of the PWM output.

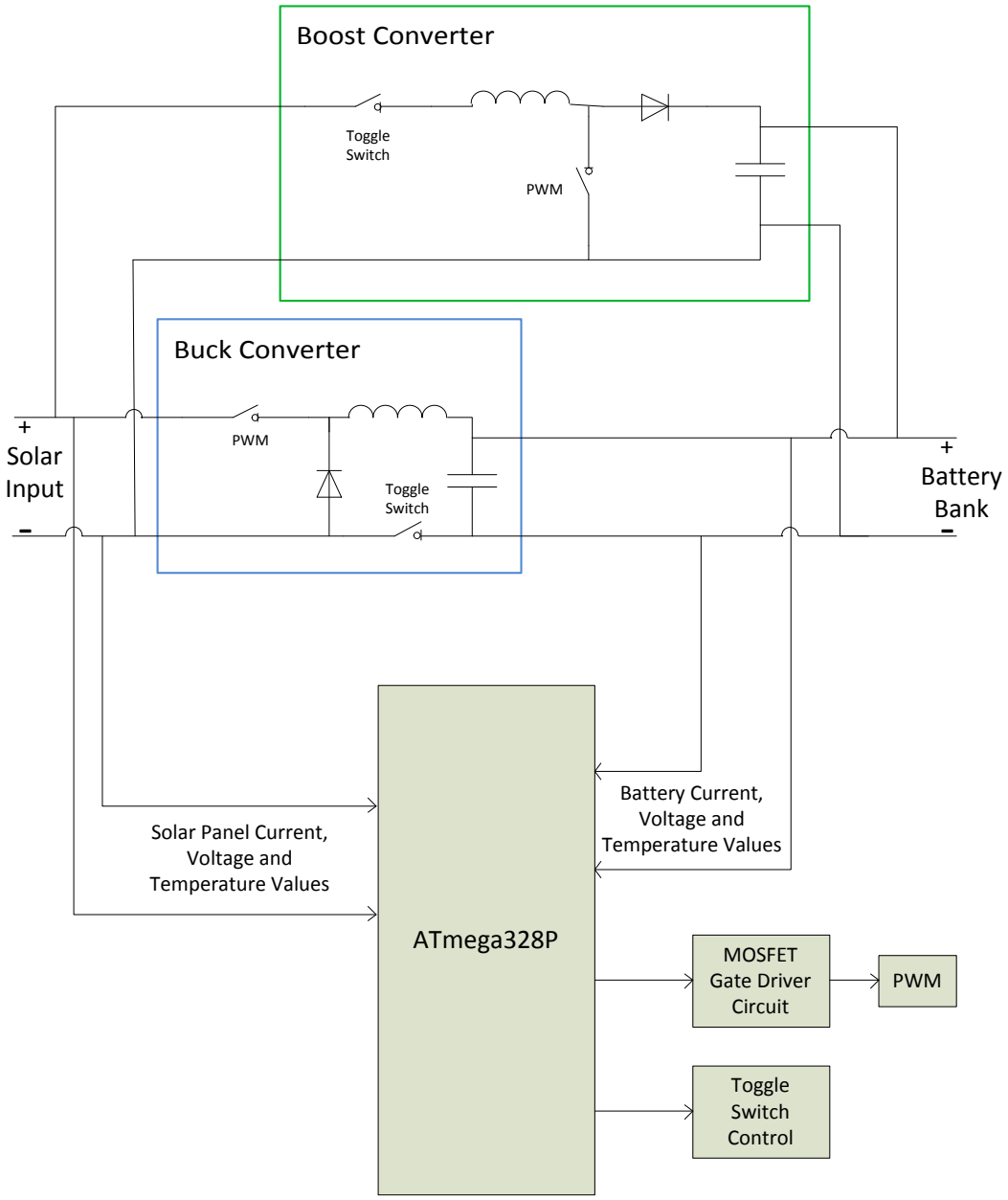

Figure 49 - Buck-Boost Circuit Design for MPPT.

Many different types of batteries were researched for the battery bank including lead-acid, nickel-cadmium, lithium-ion, and nickel-metal-hydride. Of all these types of batteries, the deep-cycle lead acid was deemed most cost effective and favorable for photovoltaic applications. Next a choice between flooded, gel-electrolyte, and absorbed glass mat had to be decided. Out of the three types of lead-acid chemistries, the AGM battery was found most favorable due to long lifetime, resistance to damage, and requiring no maintenance. The specific battery chosen for the system was the Sun Xtender PVX-420T AGM lead-acid battery. The battery specifications are presented in Table 13. The battery features 40 cold cranking amps, long lifetimes, and cost under $150.

Battery Bank Specification	Value
Nominal Voltage	12V
Max CCA	40A
Capacity	42Ah
Lifetime (50% DOD)	1000 cycles
Max C-rate (from 75W panel)	0.12C
Weight	30 lbs
Cost	$145

Table 13 - Sun Xtender PVX-420T AGM Battery Specifications. [59]

The Cobra 880 power inverter contained all the characteristics needed in the design to provide the end user with a smooth powering experience. The Cobra Power inverter was designed to receive 12 volts from its power source and would can deliver an output voltage of 109-120 VAC at 60Hz. It can also provide a continuous max power of 800 Watts with a surge of 1600 W. Both of these specs went beyond the desired output power of 200 W. This oversize in specs was mostly implemented as a safety precaution. In the scope of this project, no sensitive devices are intended to be powered by the system therefore a moderate sine-wave output complies with the requirements.

As shown in Figure 50, the inverter comes incorporated with two 3-prong outlets that allow the user to power multiple AC devices. In addition to these outlets, it also comes integrated with a USB port that enable low power devices such as cell phones, iPods, etc, to be charge off the grid.

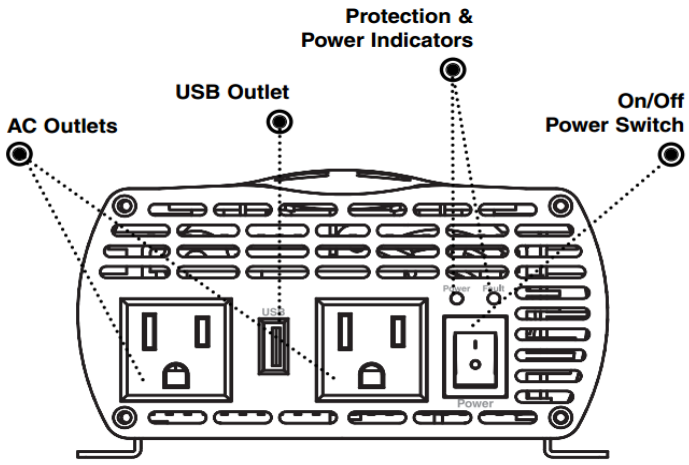

Figure 50 - Cobra CPI 880 Power Inverter.
Image permission obtained from Cobra.

This custom printed circuit board shown in Figure 51 has been designed using CadSoft's Eagle PCB Design software. The final design will be 7.5 x 5.5 in and was manufactured by Advanced Circuits. The largest trace widths are 0.07 in. allowing them to handle a maximum of 5 A at a rise temperature of 15°C. The bottom layer of the two-layer board will be a ground plain which will help reduce external noise to the electronics and help keep all grounds well connected. In the power electronics circuitry, top copper plains where added in place of traces to assure high current capacities could be handled without overheating. A similar technique was used for the 5 V and 3.3 V switching regulator, where plains of copper served as traces to keep the circuit as tight as possible for best efficiency.

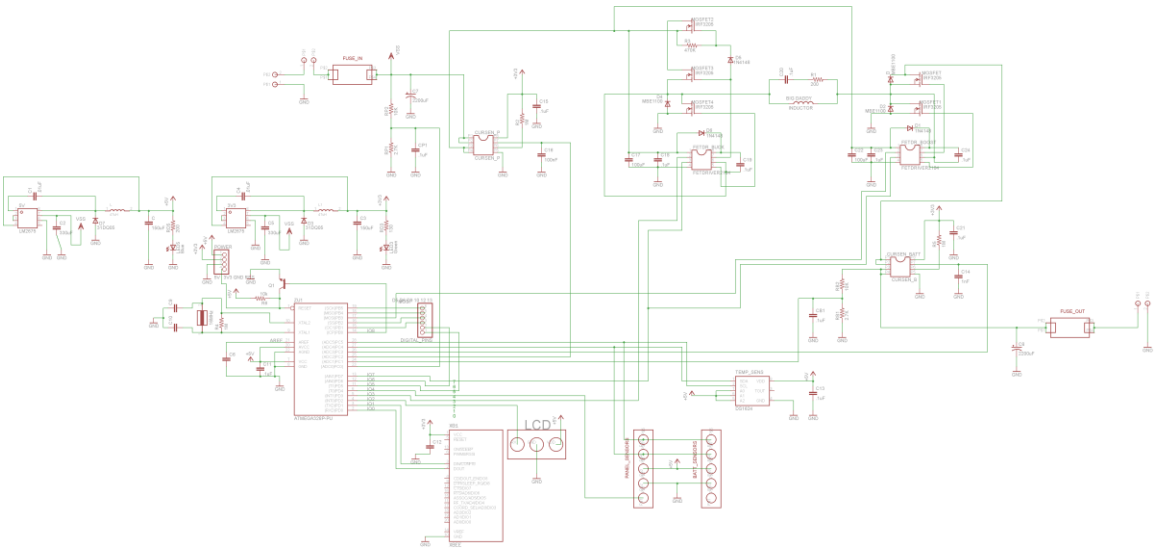

Figure 51 – Overall PCB Schematic.

The final enclosure consisted of an electrical box, with a custom Plexiglas top where the LCD was mounted. As shown in Figure 52, the power and sensors from the panel plug into the left side of the box and the power and sensors that connect to the battery are attached on the right side. The LCD is mounted in the Plexiglas towards the bottom of the box so that it does not obstruct the user's view of the circuit board and the power/status LEDs that are on the lower right side.

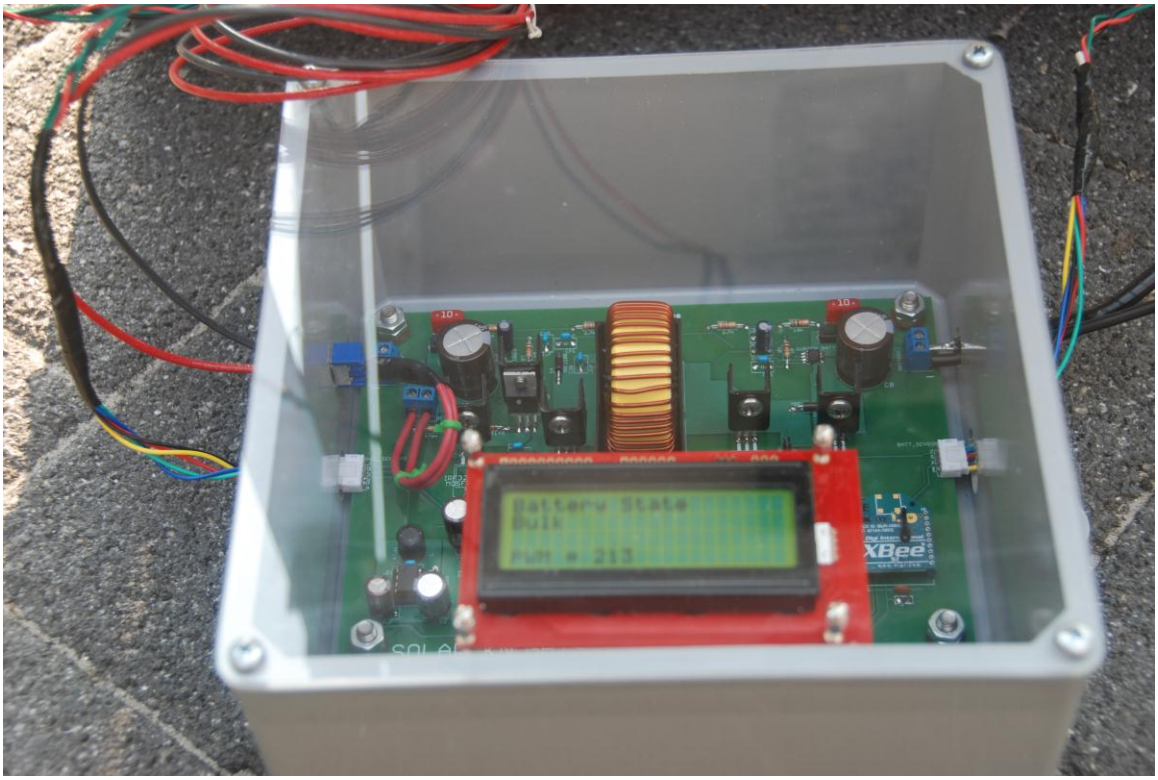

Figure 52 – Final packaging of the PMCC system.

6. Testing

6.1 Solar Testing

Solar testing was useful in verifying the IV characteristics of the solar panel. The group visited FSEC (Florida Solar Energy Center) located in Cocoa, Florida to see firsthand how solar panel modules are put through physical and performance tests. These tests are performed to provide certain specifications to either the public or the manufacturer. The group met and toured the facilities with Kris Davis who is a Solar Research Engineer at FSEC. His duties include researching novel materials in the Solar PV Panel industry that will increase module efficiency and cost while reducing module size and weight. An in depth discussion was conducted in order for the group members to understand the battery of tests needed to define the module's performance capabilities. The group was invited to FSEC for further testing on the solar panel that the system will use, in order to identify its true IV characteristics in a real life situation.

Additional solar panel testing was conducted at the UCF main campus close to the Engineering 1 building where the Senior Design Lab is located. Amongst other tests the panel was tested daily for output current and output voltage fluctuation in a full range of weather conditions. The objective of solar testing is to fully understand and derive the panel output in order to calculate the time it would take to fully charge the system's battery. Charge time is also dependent on charge controller efficiency. Figure 53 is the IV curve taken from the solar panel manual. It is important to understand that the IV curve in this picture portrays the highest possible output from the panel at an optimal temperature. This curve is an ideal curve and is different from the tests that were conducted in outdoor conditions.

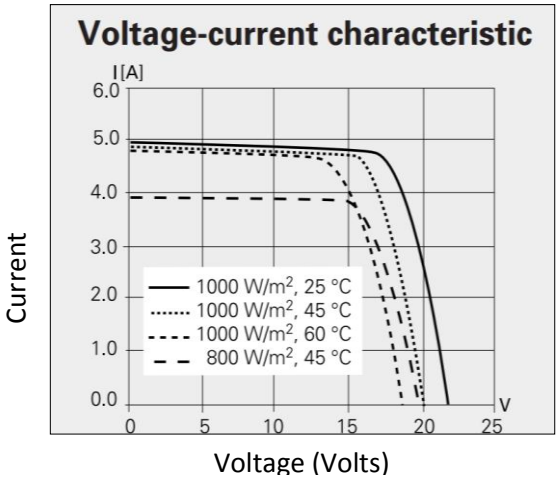

Figure 53 - Siemens SP75 IV Characteristics. [61]

6.2 Battery Testing

Battery testing, as described in Table 14, was needed to gauge the time of charge needed from the panel for the battery to fully charge. Time of battery charge mainly depends on solar panel output power, which in turn depends on the irradiance level. Battery discharge time is also important to determine the maximum charge supplied to the inverter.

Step #	Procedure	Expected Results	Actual Results Stat.
Battery Charge Time			
1	Connect the battery to the system with no load	Battery should start to charge	Complete
2	Connect Multi-meter to battery to check for voltage	The Multi-meter should read a voltage that coincides with the charging stage	Complete
3	Connect Multi-meter to battery to check for current	The Multi-meter should read a current that coincides with the charging stage	Complete
4	Monitor the time it takes for the battery to reach the Float charging state	According to the battery and charge controller ratings, it should take 8 hrs.	Complete

Step #	Procedure	Expected Results	Actual Results Stat.
Battery Discharge Time			
1	Connect the battery to the inverter with a predetermined load	Battery should start to discharge	Complete
2	Connect Multi-meter to battery to check for voltage	The Multi-meter should read battery-full voltage that will gradually decrease	Complete
3	Connect Multi-meter to battery to check for current	The Multi-meter should read a current that is being drawn	Complete
4	Monitor the time it takes for the battery to reach the Float charging state	According to the battery and load ratings, it should take 8 hrs. at a 5Ah load rate.	Complete

Table 14 - Battery Testing Plan.

6.3 Sensor Testing

A testing plan, shown in Table 15-18, has been utilized to make sure that all of the sensors that were incorporated work the way they were supposed to work and eliminated the possibility of any factory defects before they were implemented in the final design. The following table contains each sensor that was tested followed by the test plan that was put in place for each sensor, then the expected results, and finally the status of the test.

Step #	Procedure	Expected Results	Actual Results Stat.
Voltage Sensor			
1	Come up with a voltage divider configuration	Should be easy to implement	Complete
2	Calculate appropriate resistor values based on the Solar panel and microcontroller specs	R1= Mega ohms value R2= Kilo ohms value Vout < 5 volts in worst case scenario	Complete
3	Build a voltage divider circuit in MultiSim	Circuit simulation should reflect previous expected results	Complete
4	Build a voltage follower connected to a low pass filter	Vout should be equal at the designated points	Complete
5	Built circuit at the lab and test it	Results should reflect the simulation results	Complete

Table 15 – Voltage Sensor Testing Plan.

Step #	Procedure	Expected Results	Actual Results Stat.
Current Sensor (AD8215)			
1	Implement the shunt resistor monitor in the a circuit design	Shunt resistor should be in series with voltage source	Complete
2	The current value is going be verify in both the Arduino and voltmeter	Results should match with each other	Complete

Table 16 – Current Sensor Testing Plan.

Step #	Procedure	Expected Results	Actual Results Stat.
Temperature Sensor (DS1624)			
1	Temperature sensor is connected to the Arduino	Some sort of value should be output by the sensor	Complete
2	Sensor is tested room temperature and compare with thermometer	Both temperature results should be close to equal.	Complete
3	Extra heat is applied to both thermometer and DS1624 temperature sensor	Increase in Temp. reading in the thermometer should match the DS1624 readings	Complete

Table 17 – Temperature Sensor Testing Plan.

Step #	Procedure	Expected Results	Actual Results Stat.
Irradiance Sensor (TSL235)			
1	The TSL235 is connected to the Arduino board	Raw data should be received from the output of the TSL235	Complete
2	Increasing and decreasing ambient light	Noticeable changes in the raw data should be observed, especially at both extremes of light intensity.	Complete
3	Testing with direct Sun light and Shade	Similar results as the previous testing should be obtain	Complete
4	Implement the algorithm to translate the reading to lumens	Direct sunlight 100,000 lux. Filtering of clouds etc. b/w 5,000 and 10,000 lux, Moonlight as little as 0.25 lux.	Complete

Table 18 – Irradiance Sensor Testing Plan.

6.4 Software Testing

The MPPT software and the algorithms that it encompasses were tested using the test plan explained in Table 19. In addition the LCD coding was tested as well.

Step #	Procedure	Expected Results	Actual Results Status
Software Testing			
1	Hard-code values for current and voltage	Should calculate the correct value for power	Complete
2	Write a string of text to print to the screen	Text displayed on LCD	Complete
3	Hard-code values for different charging states	Algorithm will change into different states based on the current and voltage	Complete

Table 19 - Software Testing Plan.

6.5 Wireless Testing

The transceivers were tested by developing two identical prototypes, each consisting of an XBee module, Arduino Uno development board, and a computer. The three components were wired together using the correct pin assignments. After the hardware had been set up, the system was programmed and tested, using the plan in Table 20, to evaluate whether the data be sent was being received and could be viewed on the receiving computer. When the wireless link had successfully been created, the transceivers were tested for range and speed (data rate).

Step #	Procedure	Expected Results	Actual Results Stat.
Battery Discharge Time			
1	Test XBee with ATmega328P	Should act as an ordinary TTL UART serial port	Complete
2	Transmit increasing amount of sensor data	Will saturate at certain point, this is max data rate	Complete
3	Increase transmitter distance	Find the maximum range of the wireless link	Complete

Table 20 - Wireless Testing Plan.

6.6 Safety Procedures

6.6.1 Batteries

There are a few things to know and consider in order to handle batteries in a safe manner. The first thing to look at is the physical appearance of the battery, identify if the container has any cracks, or signs of fluids on or around the battery. If this were found around the battery, then it could be that the electrolyte is

spilling, leaching or leaking out. If any of these signs are present, gloves or some kind of protection should be used since the electrolyte is a solution of acid and water, therefore skin contact should be avoided. As a result, the battery would need to be replaced immediately.

It is also important to keep the connection terminals free of dirt in order to avoid a flawed connection. The cables used to connect to the battery should not be extremely tight because it could lead to post breakage or meltdown. It is important to be aware of the weather condition the battery is going to be exposed to. It is important to keep the battery above freezing temperature and limit exposure to heat. Temperatures above 80°F degree will accelerate the discharging process of the battery.

Finally, it is important that during any process of using the batteries, the terminals should not be shorted, since this will cause a very high current flow from one terminal to the other, therefore draining the battery and could potentially cause an overheat in the shortage object and cause a fire.

6.6.2 Power Cables Precaution

When making the appropriate connections between the inverter and the power cables, it is important to have the unit completely off by making sure that the power button on the inverter is in the off position and the inverter is not connected to the power source.

Once the unit is securely off, the polarity in the inverter terminal should be appropriately identified. Finding out the correct polarities in the inverter terminal is extremely important; otherwise this will cause internal fuses in the inverter to blow and may permanently damage the unit. Once the input terminals in the inverter have been appropriately identified by its polarity (+) or (-), the bare ends of the cables are can be inserted and the internal screws can be tightened to clamp the wires securely with the unit. Once the power cables have being securely connected to the inverter, the other end can be connected to the power source in its appropriate terminal (positive with positive (red +) and negative with negative (black -)).

An initial spark may be observed when connecting the cables to the power source due to current flowing to charge capacitors in the unit, thus this final connection should not be done when in the presence of flammable fumes or liquids. It is important to make sure that the connections among the power source, power cables and inverter are not loose since this will result in excessive voltage drop and may cause over heated wires and melted down the insulation.

Once the unit has been successfully installed, regular checks of the screws in the terminals of the inverter should be performed since they can become loose by vibrations or thermal cycling. Finally, 115 volt AC power is potentially lethal, therefore under no circumstance should any AC wiring connections should be

performed while it is connected to the inverter regardless of its power status (ON/OFF). This type of work should only be performed while the inverter is completely disconnected from the power source. [52]

6.6.3 Power Inverter

When buying new equipment that has been fabricated to deal with high amounts of current and voltage, it is always required to perform a few specific tests on the device in order to make sure that is operating in a proper and safe condition and that it is doing what it is supposed to do without endangering its surrounding as well as the user.

In the case of an inverter, this device has been design to convert DC power into AC power, a process that often involves the use of high current flows as well as high voltages. This conversion from DC to AC typically causes huge amounts of heat to be produce within the device which could potentially turn into a fire if is not cool down properly. The first step towards a safety operation of the device is to make sure that all of the safety instructions including the CAUTION and WARNING statements given in the user's manual are read in its entirely. [50]

6.6.3.1 General Installation Precautions

It is important to install the device in a dry area, where it is not exposed to rain, snow, bilge water, spray or in an environment where there is a potential threat of flooding. The optimal ambient temperature should be between 30°F and 105°F, keeping in mind that the cooler the better. The inverter should have at least one inch of clearance around for proper airflow and the ventilation openings should never be obstructed which could potentially cause overheating to the device and result in a potential fire. If the inverter has been dropped or damage in any way, check with manufacturer before installation. In order to prevent potential fires or explosions, do not install the inverter in areas or compartments containing battery fumes, flammable materials or in locations that require ignition-protected equipment since inverters contain components that tend to produce arcs or sparks.

These are some of the guidelines that should be followed in order to have a successful and safe installation to get the most out of the inverter and have a peace of mind that it will operate properly. Once a safe area has been determined where the installation process can be completed successfully, it is extremely important to check the inverters performance while being aware of the different built-in safeties that the device comes equip with. [50]

6.6.3.2 Mounting Precautions

It is important to place the inverter on a flat surface where it is of easy access to the user. The use of mounting brackets should be used to keep the unit secure in the surface and lifted off the surface for appropriate ventilation. Depending on the designated place to mount the inverter, the device can either be placed horizontally or vertically. If a vertical mounting is decided in the final mounting process, neither end of the unit should be at the top in order to avoid foreign material from falling or settling inside the unit. It is important to connect the Ground-screw that comes built in the inverter's chassis to ground in order to prevent any internal short circuit from striking the user. It is recommended by the manufacture that a #8 AWG copper wire be use to ground the unit connecting the cable to a ground road, or if available, another proper ground entrance. [50]

6.6.3.3 Operating Limits

Just as with any equipment in the market, each has its own operating limits that the user should be aware of in order to receive a flawless experience. In the case of the Cobra power inverter, there are a few aspects of the input voltage and the power output that the user should know about before operating the inverter to its full capacity. By keeping the inverter within this these few operating limitations, the inverter will provide the user with a great experience.

The Cobra CPI 880 power inverter has been design to operate with an input voltage in the range of 10 to 15 volts. The optimum performance of the inverter will occur when the voltage being supply is around the 12 to 14 volts. If for any reason the input voltage is alter so that is either receiving a voltage higher than 15v or lower than 10 volts, as a protection mechanism the inverter will automatically shut down in order to protect itself. If this ever happens during normal operation, an audible alarm will warm the user of the situation.

The Cobra CPI 880 power inverter is capable of delivering a max output power of 800 watts for a period of time of 60 minutes. After operating at this max power for about an hour, the inverter must cool down for about 15 minutes in order to resume any further work at its max power. The 15 minutes idle time should be done with the inverter completely off with no loads being powered. It is important to take into account that the wattage rating given by the inverter refer to a resistive loads. In general the inverter will operate most AC loads within its power rating, but there are a few devices that may encounter problems when being power by the inverter. The inverter may fail to start some induction motors used in freezers, pumps and other motor-operated equipment that requires very high surge currents to start though its rated current draw is within the inverter's limits. The typical motors that the inverter will normally start are single phase induction motors that are rated at one-half HP or less. [50]

7. Operators Manual

CAUTION: Read Section 6.6 - Safety Procedures before proceeding with the integration of PMCC in a fully powered photovoltaic system.

All connections should be made prior to exposing the PV panel to the sun.

Step 1: Remove the front cover of the PMCC unit. Disconnect the LCD connector to the PCB prior to fully removing the cover. Make sure the power switch is in the OFF position, before connecting the panel or the battery to the PMCC unit.

Step 2: Connect the input and output sensor cords to their appropriate position on the PMCC unit. The input side is the one with the toggle switch next to it as shown in Figure 54.

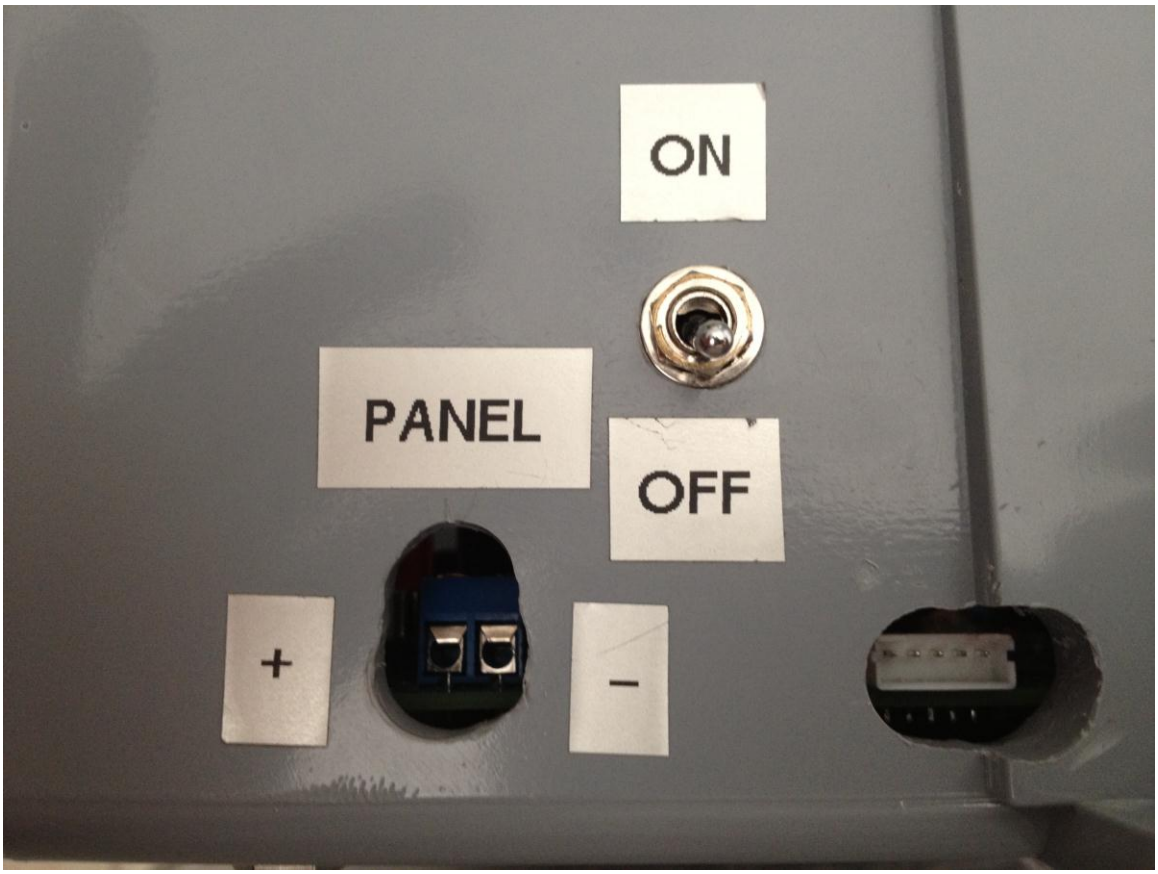

Figure 54 – Input (Panel) Side and Toggle Switch.

Step 3: Connect the battery to the output terminals of the PMCC unit. Pay attention to the polarity before tightening the wires into the PCB terminals.

Step 4: Connect the inverter clamps to the correct terminals on the battery. Avoid polarity reversal.

Step 5: Connect the PV panel to the input terminals of the charge controller. Pay attention to the polarity before tightening the wires into the PCB terminals.

Step 6: Connect the LCD cord to the PCB before placing the cover on the PMCC unit.

Step 7: Toggle the PMCC unit power switch to the ON position. Verify that the green (3.3 V) and blue (5 V) LEDs are lit. These are indicators that the circuit is being supplied sufficient power.

Step 8: Toggle the power switch on the inverter to the ON position. Observe the status of the system on the LCD screen.

CAUTION: Do not connect a load higher than the rated output power on the inverter (800W)

8. Administrative Content

8.1 Budget

While the predominant purpose of the project was to design the efficient charge controller, the proof of concept was demonstrated through a fully functional stand-alone photovoltaic system. The following budget presented in Table 21 includes the required parts that were obtained to create an off-the-grid solar charger.

Parts List	Cost per part	Number of parts	Total Cost
Solar Panels			
SunWize SW120, 120 Watts 12V Solar Panel	$382.89	Donated	$0
Charge Controller			
Printed Circuit Board (Student Special)	$33.00	2	$66.00
Serial Enabled 20x4 LCD - Black on Green 5V	$29.95	1	$29.95
DS1624 Temperature Sensor	$3.75	5	$18.75
Solderless Plug-in BreadBoard	$5.50	2	$11.00
Various Circuit Components (op-amps/caps/Inductors)	$50.00	1	$50.00
Wire/Solder	$25.00	1	$25.00
Battery			
Sun Xtender PVX-420T AGM Battery	$145.00	2	$290.00
Inverter/Outputs			
Scobra CPI 1575	$189.95	1	$189.95
Heavy-Duty AC Power Inverter Cable Kit	$25.49	1	$25.49
Fuse Holder	$6.95	3	$20.85
150 Amp ANL Fuses	$7.06	3	$21.18
Microcontroller			
ATmega328 with Arduino Bootloader	$5.50	5	$27.50
Arduino Uno SMD (ATmega328)	$30.00	2	$60.00
Wireless Components			
Xbee Module	$26.00	4	$104.00
		Total:	**$939.67**

Table 21 - Budget.

The project can be broken down conceptually into four major sections. The first phase consisted of the photovoltaic array. A 75 Watt, 12 V solar panel was obtained from the Florida Solar Energy Center for use in the project. The second partition includes the actual charge controller. This is where the microcontroller, LCD and other electronics reside. In order to fabricate the printed circuit board,

there was first a period of testing and building the circuit on a solderless plug-in breadboard. Once it was determined that the design performed the required tasks, the custom circuit board was ordered. Since there is a wireless component that will receive the information and is attached to the computer, a separate explorer board was used. The third and fourth components of the system are the battery bank and inverter respectively. These items were purchased and required little or no design, but were incorporated into the system in order to create a working prototype that demonstrated the ability to store and distribute power.

The funding for this project was provided through a grant from Workforce Central Florida. The grant was a new program entitled the New and Emerging Industries (WCF-NEI) and was intended to support senior design projects working on projects in these industries. There were several industries that were designated new and emerging and the solar charge controller falls into the Renewable and Sustainable Energy category. Groups were required to provide a proposal and an initial budget for their project in order to apply for the funding. The group was funded based on the proposed budget provided to Workforce Central Florida.

8.2 Industry Mentor

One of the stipulations of the Workforce Central Florida funding was that the senior design group identifies and communicates with an industry mentor in a relevant field. This took place during the first weeks of the senior design class and was required for the initial funding application. The mentor was required to meet with the group periodically and give advice about design as well as provide an industrial perspective about their project and its relevance. The goal of the Workforce Central Florida program is to stimulate relationships with local companies and employees.

Because this project is relevant to the solar industry, a mentor was identified from a nearby power utility company that has demonstrated significant investments in the solar market. Alan Shaffer, the assistant general manager of delivery, has worked at Lakeland Electric for over 30 years. He oversees the planning, maintenance, operations, and construction of Lakeland Electric's transmission and distribution systems. [62]

Lakeland Electric's mission is to provide safe, reliable, competitive and environmentally responsible energy solutions to enrich their customers' quality of life. This describes some of the motivation behind their recent involvement in several solar projects in the area. They provide a solar hot water program as well as a net-metering program for residences and businesses that have incorporated their own solar generation. Furthermore, they are consulting and advising on several research and commercial projects, such as a solar farm that is currently being installed. [63]

Alan consulted with the group during several status presentations in the Fall semester and again during the Spring. In March, the senior design group visited

Lakeland Electric and also took a tour of the solar farm at the Lakeland Regional Airport.

8.3 Milestones

The Senior Design 1 semester took place between August and December 2011. During this time the primary focus was to conduct thorough and well-documented research. The majority of the research took place between mid-October and the end of November and was relatively complete by the end of the Senior Design 1 class as depicted in the Gantt Chart of Table 22. Significant emphasis was placed on the electrical components of the charge controller as this constitutes the majority of the design work. This schedule allowed the group to choose parts that could be ordered early in the spring semester.

	Research						
	Solar Power	Charge Controllers	Sensors	Microcontrollers	Wireless	Batteries	Inverters
18-Oct							
25-Oct							
31-Oct							
7-Nov							
14-Nov							
21-Nov							
28-Nov							

Table 22 - Gantt Chart depicting research timeline.

The design phase slightly overlapped both the research and parts acquisition portions of the project which come before and after. The design began once each section had been researched and the parts that needed to be purchased were identified. As indicated in Table 23, this took place in the final weeks of senior design 1 and continued through the first month of senior design 2. The University was closed from the week of December 12th until January 9th for winter break. During this time, parts were still investigated as the design progressed.

	Design						
	Charge Controller	Current Sensors	Voltage Sensors	Other Sensors	MPPT Algorithm	Microcontroller	Wireless
…							
28-Nov							
5-Dec							
12-Dec							
19-Dec							
26-Dec							
2-Jan							
9-Jan							
16-Jan							
23-Jan							
30-Jan							
6-Feb							
13-Feb							
20-Feb							
27-Feb							
5-Mar							

Table 23 - Gantt Chart depicting design timeline.

Over winter break as certain aspects of the design were finalized, some parts were ordered for early prototyping in the spring semester. Parts acquisition increased significantly following the break and continued for the first month. The goal was to have ordered all of the necessary parts for the project by mid-February. The parts necessary for the packaging of the final circuit board and electronics were acquired later, as shown in Table 24, once the design had been tested and the final board has been fabricated.

	Acquire Parts							
	Microcontroller	Sensors	Display	Wireless	Batteries	Inverter	Solar Panels	Packaging
…								
19-Dec								
26-Dec								
2-Jan								
9-Jan								
16-Jan								
23-Jan								
30-Jan								
6-Feb								
13-Feb								
20-Feb								
27-Feb								
5-Mar								
12-Mar								
19-Mar								
26-Mar								
2-Apr								

Table 24 - Gantt Chart depicting parts acquisition timeline.

Table 25 shows the schedule for prototyping. This phase began immediately following parts acquisition and also included component level testing. Once a part was acquired, the component testing consisted of individual parts testing to confirm that it worked and provided reasonable information. This was especially important with sensor implementation, to make sure they are scaled correctly and provided meaningful data. The circuit design was first prototyped on a solderless breadboard and also incorporated the Arduino break out board for simplified programming and design. As previously stated, the development of the packaging did not commence until the main modules had been finalized.

	Prototype							
	Microcontroller	Sensors	Display	Wireless	Batteries	Inverter	Solar Panels	Packaging
…								
16-Jan								
23-Jan								
30-Jan								
6-Feb								
13-Feb								
20-Feb								
27-Feb								
5-Mar								
12-Mar								
19-Mar								
26-Mar								
2-Apr								

Table 25 - Gantt Chart depicting prototyping timeline.

The final stage of the project consisted of testing. The testing plan and methods as described in section 6 covered component level, module level, and system level testing. Table 26 shows testing commenced in March, overlapping with the final stages of prototyping. The testing and documentation encompassed all of April up until the last week in which the final presentation took place.

	Testing							
	Solar Panel	Battery Charging	Hardware	MPPT Algorithms	Wireless	Data Storage	Safety Proceedures	Packaging/Transport
…								
19-Mar								
26-Mar								
2-Apr								
9-Apr								
16-Apr								
23-Apr								
23-Apr								

Table 26 - Gantt Chart depicting testing timeline.

9. Conclusion

9.1 Changes to Design

The initial concept for this design has been modified to make it more relevant to industrial practices and needs. The most significant change was the addition of the wireless capability. This adjustment was believed to be a major value added to the project. This feature allows the user to not only remotely monitor the status of the system, but to record and store historical data. Again, this provides live monitoring in addition to creating a database of environmental situations and the system's condition in response to them.

Live and historical data is of great value to both industrial and research entities. Over time both could benefit from learning about how atmospheric conditions affect the efficiency of the photovoltaic system. Meanwhile, live monitoring is inherently useful for maintenance and alerting the user of any status issues, significantly reducing down time and unnecessary field surveys.

Another added feature, which was incorporated immediately following feedback from the group's consulting solar research engineer, was the incorporation of an irradiance sensor. While this sensor data does not incorporate into the maximum power point tracking or the charging of the battery, this allows for more meaningful documentation of the atmospheric conditions. Furthermore, it gives insight into determining the efficiency of the system. When the irradiance is known, the efficiency can be tested because the power output can be compared to the known amount of incoming sunlight.

In the original design, it was proposed that the system would integrate several photovoltaic panels in order to generate a significant amount of power. This was later revised upon discussion with Kris Davis, of the Florida Solar Energy Center. It was explained that an inexpensive charge controller that could be implemented at each panel in a system would be of interest in the research of new PV solutions. Current designs involve sending all of the power to one charge controller but if charge controllers, equipped with maximum power point tracking, could operate at each panel it may increase efficiency. This panel-integratable concept inspired the down scaling of the photovoltaic configuration to work on what could be a proof of concept for an inexpensive solution.

For example, in a large solar farm or grid not all of the panels will undergo the same irradiance levels at once, due to shadows or other external factors. For this reason, a singular charge controller attempting to perform maximum power point tracking could not possibly allow the system to reach the maximum power point for each panel, therefore reducing the efficiency overall because it is addressing the system as a whole. [64]

9.2 Future Work

With the panel-integratable model in mind, following the proof of concept and demonstration of efficiency, future work could include simplifying the design to create the most cost effective charge controller possible. This would be necessary to reach a competitive price point that would allow the expense to be justified through energy savings.

A significant savings could be achieved through the elimination of the LCD screen. The cost of the LCD in this system is approximately $30 and would not be necessary to implement at each charge controller in a solar panel field. For an industrial or consumer application the LCD screen is redundant with the wireless data that is being transferred to the computer so it would be easily removed without losses in functionality.

Depending on the need, wireless capability could be removed as well. Wireless capability would provide unique insight into the system status, MPPT efficiency, as well as allow for remote distress alerts. However, if these benefits are not necessary for the given application, the removal of the wireless Xbee modules and the supporting circuitry would equate to a substantial savings. Each Xbee module used in this design costs about $25.

Oppositely, in order to investigate a more robust system, additional features could be added that would increase the system performance and allow for advanced operations. One concept that could be applied might be a charge controller with memory so that it could save relevant data and establish good starting points for calculating the maximum power point. This would enable faster acquisition of the MPP therefore making the system more efficient. This would in turn require a faster and more capable microcontroller as well as the addition of memory to the system as previously stated.

A different direction to pursue would be to adapt the maximum power point tracker for use with other renewable energy sources. This tracking technique can be applied to sources such as small water turbines and fixed-pitch-rotor wind-power turbines. Similarly to the photovoltaic system, these sources vary regularly based on the atmospheric conditions and would find great benefit in the ability to maximize the power extracted during non-ideal circumstances. While this may seem like a drastically different application, the MPPT controller is conceptually blind to the function that is generating the power and instead only sees the input current and voltage. For this reason, adapting the charge controller for use with these other sources would be relatively simple but would involve modifying some of the electrical components such as the size of the capacitors or diodes to account for different levels of power. [65]

9.3 Industrial Scaling

This maximum power point tracking device serves as a proof of concept but has the potential to be scaled to industrial implementation. Research is being conducted into the concept of implementing a micro-inverter solution that would be installed at each PV panel before connecting them in series or parallel. As previously discussed, this project could act as a precursor to a type of charge controller that could be realized at individual PV panels. In order to do so, the competitive price point would need to be determined through a thorough study of the cost of implementation and market research. Once this number was identified, the features could be scaled down appropriately to reach this goal.

Consequently, if a charge controller of this type was to be produced at an industrial scale, it would drive down the cost of the parts and manufacturing significantly and should be considered in the initial research into the feasibility of producing such a system.

Another possible design change for an industry ready design might involve replacing the current Xbee wireless device with another, more expensive, module that enables the data to be transferred over much larger distances. Another alternative would be to incorporate a Wi-Fi transceiver which also has a larger range than the current design. This device was not used in the current project because although it transfers data at a high rate, it consumes more power.

Finally, the photovoltaic charge controller design presented is meant to be an off-the-grid system and uses a battery to store its power. In some industrial scenarios it would be beneficial to develop an MPPT charge controller to interface with a grid tied system.

Appendix A: Works Cited

[1] http://www.solarserver.com/knowledge/basic-knowledge/photovoltaics.html
[2] http://www.timnolan.com/uploads/Arduino%20Solar/ppt.pde
[3] http://www.edn.com/article/471969-Solar_array_controller_needs_no_multiplier_to_maximize_power.php
[4] Isidor Buchmann: http://batteryuniversity .com/learn/article/charging_the_lead_acid_battery
[5] http://eecs.ucf.edu/seniordesign/su2010fa2010/ga/
[6] http://bama.ua.edu/~bwbuckley/projects/mppt.html
[7] http://www.livestrong.com/article/241911-10-facts-about-solar-energy/
[8] http://www.eia.gov/cneaf/solar.renewables/page/trends/rentrends.html
[9] http://www.cleanedge.com/reports/clean-energy-trends-2011
[10] http://www.nrel.gov/learning/re_photovoltaics.html
[11] http://en.wikipedia.org/wiki/File:PV_Technology.png
[12] http://en.wikipedia.org/wiki/Monocrystalline_silicon
[13] http://www.solarec.co.za/~solarecc/index.php/solar-electricity/photovoltaic-modules.html
[14] http://en.wikipedia.org/wiki/Copper_indium_gallium_selenide_solar_cells
[15] http://en.wikipedia.org/wiki/Cadmium_telluride_photovoltaics
[16] http://www.azom.com/article.aspx?ArticleID=1166
[17] http://photochemistry.epfl.ch/EDEY/NREL.pdf
[18] http://infogreenglobal.com/the-practical-full-spectrum-solar-cell-comes-closer/#more-2162
[19] http://www.solarpower2day.net/solar-cells/efficiency/
[20] http://www.nrel.gov/gis/solar.html
[21] http://services.eng.uts.edu.au/~venkat/pe_html/ch07s1/ch07s1p1.htm
[22] http://www.national.com/an/AN/AN-2124.pdf
[23] http://ptm2.cc.utu.fi/~ptmusta/kuvat/elektroniikka/mc34063/IEEEXplore.pdf
[24] http://www.linear.com/product/LT1160
[25] http://www.atmel.com/dyn/resources/prod_documents/doc8161.pdf
[26] www.arduino.cc
[27] http://www.dimec.unisa.it/leonardo_new/en/mppt.php
[28] http://www.st.com/internet/com/TECHNICAL_RESOURCES/TECHNICAL_LITERATURE/DATASHEET/CD00287506.pdf
[29] http://www.maxim-ic.com/app-notes/index.mvp/id/484
[30] Hohm, D. P.; Ropp, M. E. “Comparative Study of Maximum Power Point Tracking Algorithms.” *Progress in Photovoltaics: Research and Applications*, vol. 11, pp. 47–62, June 2002.
[31] http://powerelectronics.com/power_semiconductors/power_microinverters_computercontrolled_improve_0409/
[32] http://www.tech-faq.com/lcd.html
[33] http://www.altadox.com/lcd/knowledge/lcd_display_types.htm
[34] http://www.displayfuture.com/Display/Introduction.asp
[35] http://ftp1.digi.com/support/documentation/90000991_D.pdf
[36] http://www.digi.com/pdf/wp_zigbeevsdigimesh.pdf
[37] http://www.rovingnetworks.com/files/resources/WiFly-RN-XV-DS.pdf
[38] http://mosaic-industries.com/embedded-systems/05-app-notes/temperature-measurement/using-thermocouples
[39] http://www.designinfo.com/cornerstone/ref/negtemp.html
[40] http://datasheetreference.com/lm35-datasheet.html
[41] http://www.maxim-ic.com/datasheet/index.mvp/id/2738
[42] http://bama.ua.edu/~bwbuckley/projects/mppt.html
[43] http://www.sparkfun.com/products/8882
[44] http://www.analog.com/static/imported-files/data_sheets/AD8215.pdf
[45] http://www.ti.com/lit/ds/symlink/tsl235.pdf
[46] http://pdf1.alldatasheet.com/datasheet-pdf/view/143340/TI/TSL235.html

[47] http://batteryuniversity.com/
[48] http://www.windsun.com/Batteries/Battery_FAQ.htm
[49] http://www.powerbright.com/pw1500-12.html
[50] https://www.cobra.com/detail/cpi-880-800-watt-power-inverter.cfm
[51] https://www.cobra.com/detail/power-inverter-cable-kit.cfm
[52] http://www.littelfuse.com/searchresults.html?NttP=0297010.WXNV&Ntt=0297010.WXNV
[53] http://www.sunwize.com/info_center/pdf/SW%20OEM%20Manual-Eng-revK_5-08.pdf
[54] http://solarelectricityhandbook.com/solar-angle-calculator.html
[55] http://www.sunstore.co.uk/buy/universal-solar-panel-frame-mount-small_412975105.htm
[56] http://www.arduino.cc/en/Reference/SoftwareSerial
[57] http://www.mathworks.com/matlabcentral/answers/10924-pre-allocating-linked-arrays-for-live-plotting
[58] www.4pcb.com
[59] http://www.sunxtender.com/pdfs/Sun_Xtender_Battery_Technical_Manual.pdf
[60] http://www.datasheetcatalog.org/datasheet/philips/BYV42E_1.pdf
[61] http://www.abcsolar.com/pdf/sp75.pdf
[62] http://www.lakelandelectric.com/AboutUs/InsideLakelandElectric/MeettheExecutiveTeam/tabid/120/Default.aspx
[63] http://www.lakelandelectric.com/RenewableEnergy/tabid/379/Default.aspx
[64] Lohner, A.; Meyer, T.; Nagel, A. "A new panel-integratable inverter concept for grid-connected photovoltaic systems," *Industrial Electronics, 1996. ISIE '96., Proceedings of the IEEE International Symposium on* , vol.2, no., pp.827-831 vol.2, 17-20 June 1996.
[65] Woodward, S. W. “Maximum-Power-Point-Tracking Solar Battery Charger.” *Electronic Design*, pp.114-118, Sept. 1998.

Appendix B: Image Permissions

Sparkfun

http://www.sparkfun.com/static/contact

Product Photos: SparkFun product photos may be used without permission for educational purposes (research papers, school projects, etc.). However, permission must be granted for commercial use and proper credit to SparkFun must be given. For inquiries about the use of our product photos or permission to use them, please contact marketing@sparkfun.com.

Digi

Digi International- Contact Us Submission

Full view

Gumz, Carl Add to contacts
To 'skobosko@knights.ucf.edu'
12/07/11
Reply

We've added this sender to your safe list. That way you can always see what they've sent you.

Steven-

Thank you for your recent request on Digi.com, we appreciate your support.

You are free to use the diagrams from our site, and thank you for asking. We do ask that you use them solely in regards to your academic project and that you do not misrepresent Digi or Digi products/solutions.

That said, use anything you like, but please tell me more about what you are creating- how it works, what you're using etc!

Best Regards,

Carl Gumz
Associate Sales Representative
Digi International

Direct: 952 912 3277
Fax: 952 912 4966
Email: Carl.Gumz@digi.com

Battery University

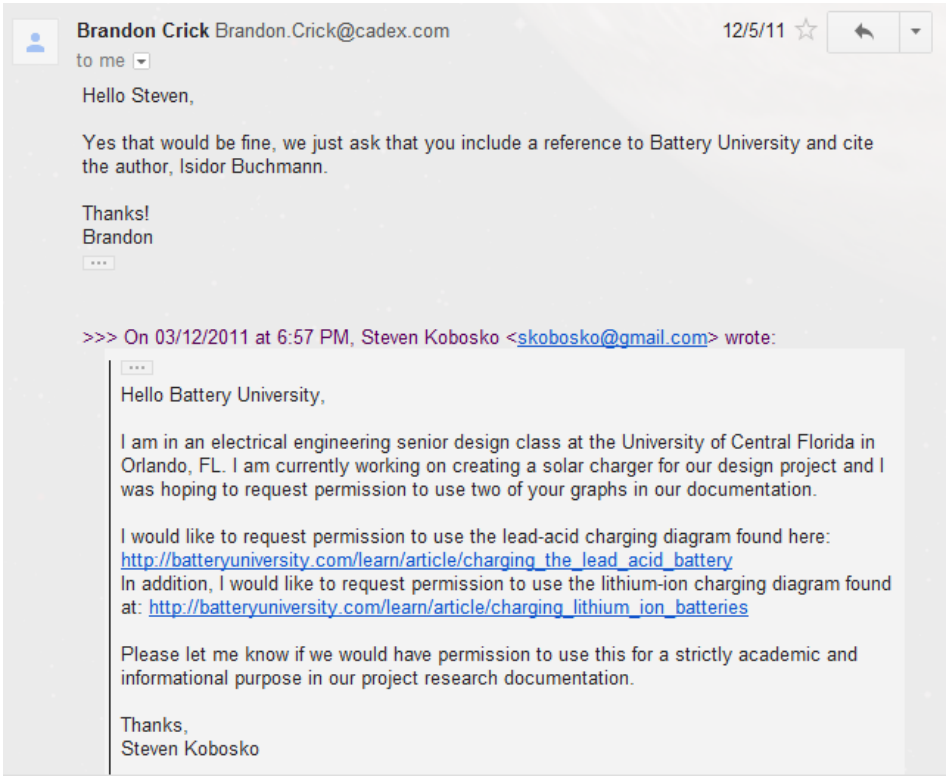

Brandon Crick Brandon.Crick@cadex.com 12/5/11

to me

Hello Steven,

Yes that would be fine, we just ask that you include a reference to Battery University and cite the author, Isidor Buchmann.

Thanks!
Brandon

>>> On 03/12/2011 at 6:57 PM, Steven Kobosko <skobosko@gmail.com> wrote:

Hello Battery University,

I am in an electrical engineering senior design class at the University of Central Florida in Orlando, FL. I am currently working on creating a solar charger for our design project and I was hoping to request permission to use two of your graphs in our documentation.

I would like to request permission to use the lead-acid charging diagram found here: http://batteryuniversity.com/learn/article/charging_the_lead_acid_battery
In addition, I would like to request permission to use the lithium-ion charging diagram found at: http://batteryuniversity.com/learn/article/charging_lithium_ion_batteries

Please let me know if we would have permission to use this for a strictly academic and informational purpose in our project research documentation.

Thanks,
Steven Kobosko

U.S. Energy Information Administration

Copyrights and Reuse

Public domain and use of EIA content

U.S. Government publications are in the public domain and are not subject to copyright protection. You may use and/or distribute any of our data, files, databases, reports, graphs, charts, and other information products that are on our website or that you receive through our email distribution service. However, if you use or reproduce any of our information products, you should use an acknowledgment, which includes the publication date, such as: "Source: U.S. Energy Information Administration (Oct 2008)."

Summary of Creative Commons License Attribution 3.0

http://creativecommons.org/licenses/by/3.0/

You are free:

- to Share — to copy, distribute and transmit the work
- to Remix — to adapt the work
- to make commercial use of the work

Under the following conditions: Attribution — You must attribute the work in the manner specified by the author or licensor (but not in any way that suggests that they endorse you or your use of the work).

NREL

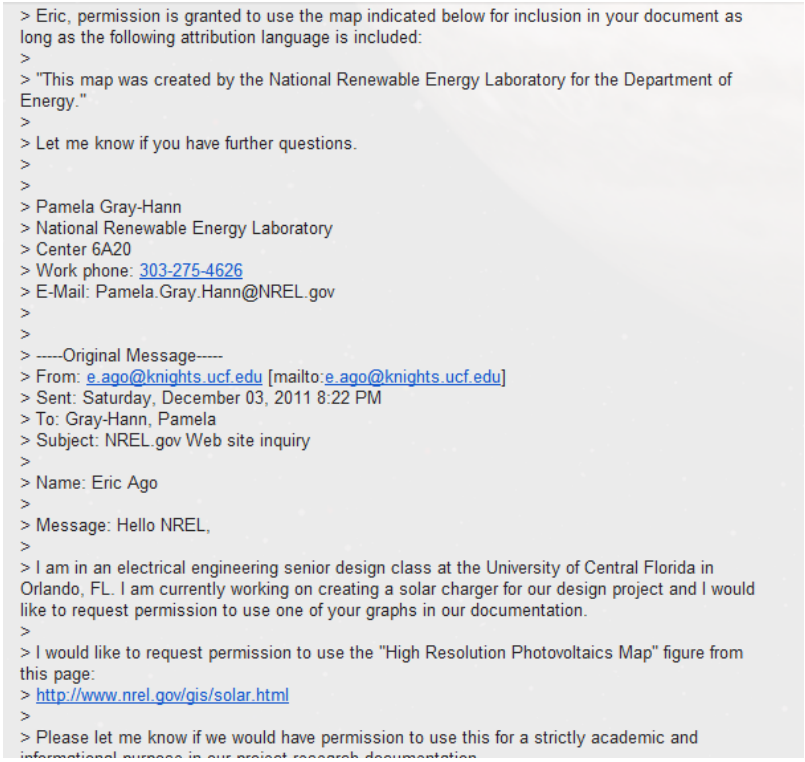

> Eric, permission is granted to use the map indicated below for inclusion in your document as long as the following attribution language is included:
>
> "This map was created by the National Renewable Energy Laboratory for the Department of Energy."
>
> Let me know if you have further questions.
>
>
> Pamela Gray-Hann
> National Renewable Energy Laboratory
> Center 6A20
> Work phone: 303-275-4626
> E-Mail: Pamela.Gray.Hann@NREL.gov
>
>
> -----Original Message-----
> From: e.ago@knights.ucf.edu [mailto:e.ago@knights.ucf.edu]
> Sent: Saturday, December 03, 2011 8:22 PM
> To: Gray-Hann, Pamela
> Subject: NREL.gov Web site inquiry
>
> Name: Eric Ago
>
> Message: Hello NREL,
>
> I am in an electrical engineering senior design class at the University of Central Florida in Orlando, FL. I am currently working on creating a solar charger for our design project and I would like to request permission to use one of your graphs in our documentation.
>
> I would like to request permission to use the "High Resolution Photovoltaics Map" figure from this page:
> http://www.nrel.gov/gis/solar.html
>
> Please let me know if we would have permission to use this for a strictly academic and

Texas Instruments

http://www.ti.com/corp/docs/legal/copyright.shtml?DCMP=TIFooterTracking&HQS=Other+OT+footer_copyright

"TI further grants permission to non-profit, educational institutions (specifically K-12, universities and community colleges) to download, reproduce, display and distribute the information on these pages solely for use in the classroom. This permission is conditioned on not modifying the information, retaining all copyright notices and including on all reproduced information the following credit line: "Courtesy of Texas Instruments". Please send us a note describing your use of this information under the permission granted in this paragraph. Send the note and describe the use according to the request for permission explained below"

Parallax

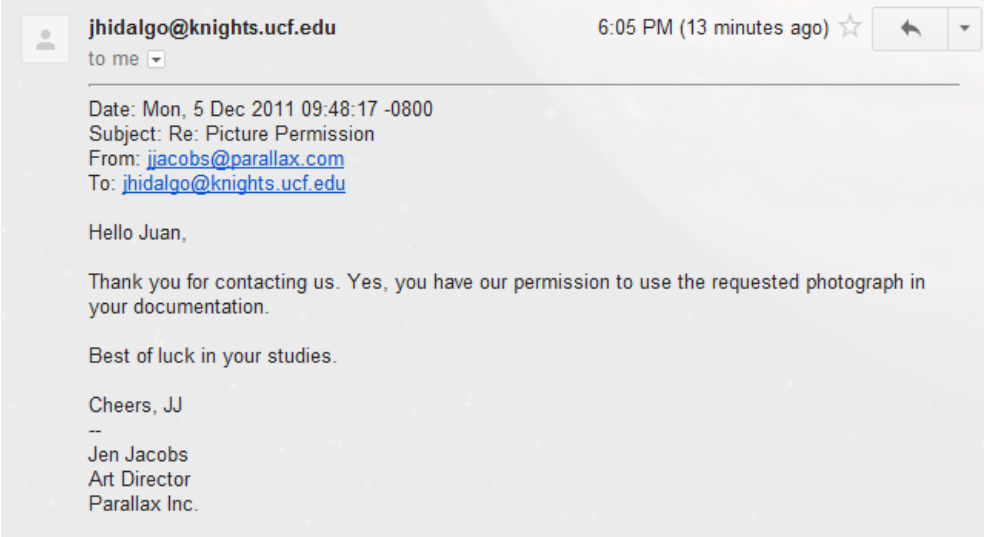

jhidalgo@knights.ucf.edu 6:05 PM (13 minutes ago)

to me

Date: Mon, 5 Dec 2011 09:48:17 -0800
Subject: Re: Picture Permission
From: jjacobs@parallax.com
To: jhidalgo@knights.ucf.edu

Hello Juan,

Thank you for contacting us. Yes, you have our permission to use the requested photograph in your documentation.

Best of luck in your studies.

Cheers, JJ
--
Jen Jacobs
Art Director
Parallax Inc.

PowerBright

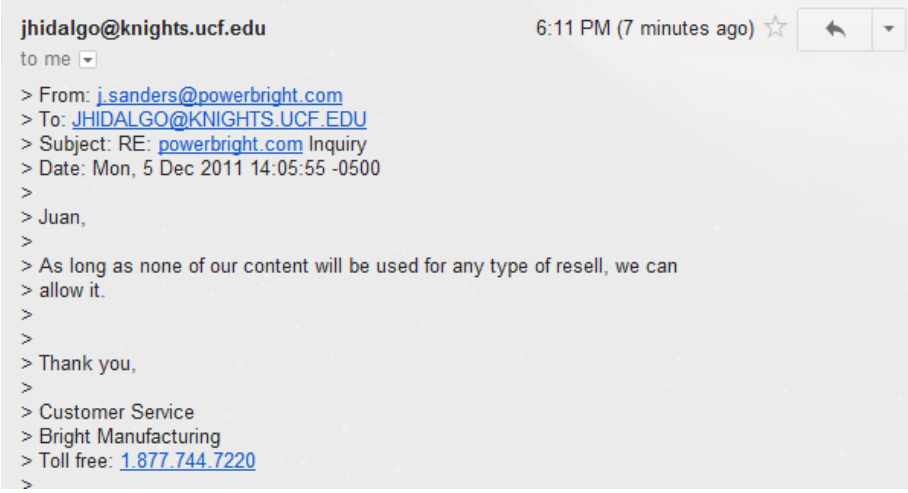

jhidalgo@knights.ucf.edu 6:11 PM (7 minutes ago)

to me

> From: j.sanders@powerbright.com
> To: JHIDALGO@KNIGHTS.UCF.EDU
> Subject: RE: powerbright.com Inquiry
> Date: Mon, 5 Dec 2011 14:05:55 -0500
>
> Juan,
>
> As long as none of our content will be used for any type of resell, we can
> allow it.
>
>
> Thank you,
>
> Customer Service
> Bright Manufacturing
> Toll free: 1.877.744.7220
>